

การเตรียมวัสดุเชิงประกอบพอลิเอไทรอินเทนแรงกระแทกสูง/คาร์บอนแบล็ก/เส้นใยมะพร้าว
เพื่อประยุกต์ในงานด้านบรรจุภัณฑ์สำหรับชิ้นส่วนอิเล็กทรอนิกส์




นางสาว วัชรภรณ์ พลแสน

วิทยานิพนธ์นี้เป็นส่วนหนึ่งของการศึกษาคณะศึกษาศาสตร์ปริญญาวิทยาศาสตรมหาบัณฑิต
สาขาวิชาวิทยาศาสตร์พอลิเมอร์ประยุกต์และเทคโนโลยีสิ่งทอ ภาควิชาวัสดุศาสตร์
คณะวิทยาศาสตร์ จุฬาลงกรณ์มหาวิทยาลัย
ปีการศึกษา 2549

ISBN 974-14-2050-1

ลิขสิทธิ์ของจุฬาลงกรณ์มหาวิทยาลัย

PREPARATION OF HIGH IMPACT POLYSTYRENE /CARBON BLACK/COIR FIBER
COMPOSITES FOR ELECTRONIC PACKAGING APPLICATIONS



Miss Wacharaporn Polsaen

A Thesis Submitted in Partial Fulfillment of the Requirements
for the Degree of Master of Applied Polymer Science and Textile Technology
Department of Materials Science

Faculty of Science
Chulalongkorn University

Academic Year 2006

ISBN 974-14-2050-1

Copyright of Chulalongkorn University

490273

วิทยากรณ์ พลแสน : การเตรียมวัสดุเชิงประกอบพอลิสไตรีนทนแรงกระแทกสูง/คาร์บอนแบล็ก/
เส้นใยมะพร้าวเพื่อประยุกต์ในงานด้านบรรจุภัณฑ์สำหรับชิ้นส่วนอิเล็กทรอนิกส์.

(PREPARATION OF HIGH IMPACT POLYSTYRENE/CARBON BLACK/COIR FIBER
COMPOSITES FOR ELECTRONIC PACKAGING APPLICATIONS) อ. ที่ปรึกษา :

ผศ. ดร. ดวงดาว อาจองค์, 113 หน้า. ISBN 974-14-2050-1.

งานวิจัยนี้เป็นการศึกษาการเตรียมวัสดุเชิงประกอบที่มีความสามารถในการนำไฟฟ้าเพื่อใช้ในงาน
ด้านบรรจุภัณฑ์สำหรับชิ้นส่วนอิเล็กทรอนิกส์ระหว่างผงเส้นใยมะพร้าวและพอลิสไตรีน ทนแรงกระแทกสูง
(HIPS)/ผงเขม่าดำ (CB) ที่มีปริมาณผงเส้นใยมะพร้าว 1-15 phr และผงเขม่าดำ 1-9 phr โดยการใช้เครื่อง
อัดรีดเกลียวหนอนคู่และเครื่องอัดแบบในการผสมและขึ้นรูปตามลำดับ จากผลการทดลองพบว่าสำหรับ
วัสดุเชิงประกอบของ HIPS/CB ที่มีปริมาณของ CB 5 phr เป็นปริมาณที่ต่ำที่สุดซึ่งสามารถเปลี่ยนสมบัติ
ความเป็นฉนวนของ HIPS ไปเป็นตัวนำไฟฟ้าซึ่งมีความต้านทานไฟฟ้าที่พื้นผิว (surface resistivity)
เท่ากับ 1.20×10^7 ohm/square โดยความสามารถในการนำไฟฟ้าของวัสดุเชิงประกอบนี้เป็นผลจากการ
รวมตัวกันของอนุภาค CB ในรูปของสายโซ่ (agglomerates และ aggregate chains) โดยแต่ละสายโซ่จะ
มาเชื่อมโยงซึ่งกันและกันเป็นโครงร่างตาข่าย (network structure) ในเนื้อพอลิเมอร์ ซึ่งโครงสร้างแบบโครง
ร่างตาข่ายจะช่วยให้อิเล็กตรอนสามารถเคลื่อนที่ได้อย่างทั่วถึงภายในเนื้อพอลิเมอร์ สำหรับสมบัติเชิงกล
พบว่า การเติม CB ส่งผลให้วัสดุเชิงประกอบมีค่ามอดูลัสและความทนแรงดึงและแรงดัดโค้งเพิ่มขึ้น
ในขณะที่ความทนแรงกระแทกลดลง ในกรณีของวัสดุเชิงประกอบของ HIPS/CB/ผงเส้นใยมะพร้าว พบว่า
การเติมผงเส้นใยมะพร้าวไม่ได้ทำให้ความต้านทานไฟฟ้าของวัสดุเชิงประกอบเพิ่มขึ้น ทั้งนี้เนื่องจากความ
มีขั้ว (polarity) ของผงเส้นใยมะพร้าวสามารถเหนี่ยวนำให้ CB มารวมตัวและเชื่อมโยงกันในรูปของโครง
ร่างตาข่ายบนพื้นผิวของอนุภาคเส้นใย แต่อย่างไรก็ตามพบว่า การเติมผงเส้นใยมะพร้าวในปริมาณ 5-9
phr ส่งผลให้วัสดุเชิงประกอบมีความต้านทานไฟฟ้าลดลงเล็กน้อย สำหรับสมบัติเชิงกลพบว่า การเติมผง
เส้นใยมะพร้าวส่งผลให้วัสดุเชิงประกอบมีค่ามอดูลัสเพิ่มขึ้น ในส่วนของความทนแรงดึงและแรงดัดโค้ง
พบว่า มีค่าใกล้เคียงกับวัสดุเชิงประกอบของ HIPS/CB (5 phr) ในขณะที่ความทนแรงกระแทกลดลง โดย
สรุปพบว่าวัสดุเชิงประกอบที่มีปริมาณของ CB 5 phr และผงเส้นใยมะพร้าว 9 phr มีสมบัติเชิงกลที่
เหมาะสมและมีความต้านทานไฟฟ้าต่ำที่สุด (4.15×10^5 ohm/square)

ภาควิชา วัสดุศาสตร์

สาขาวิชา วิทยาศาสตร์พอลิเมอร์ประยุกต์และเทคโนโลยีสิ่งทอ

ปีการศึกษา 2549

ลายมือชื่อนิสิต.....

ลายมือชื่ออาจารย์ที่ปรึกษา.....

4772464123 : MAJOR APPLIED POLYMER SCIENCE AND TEXTILE TECHNOLOGY

KEY WORD: HIPS / CARBON BLACK / COIR FILLER / POLARITY / SURFACE RESISTIVITY

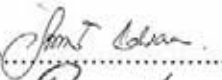
WACHARAPORN POLSAEN : PREPARATION OF HIGH IMPACT POLYSTYRENE /CARBON BLACK/COIR FIBER COMPOSITES FOR ELECTRONIC PACKAGING APPLICATIONS. THESIS ADVISOR : ASST. PROF. DUANGDAO AHT-ONG, 113 pp. ISBN 974-14-2050-1.

This research focused on the preparation of conductive composites for utilizing in the electronic packaging applications between coir fibers and high impact polystyrene (HIPS) /carbon black (CB) composites by varying contents of CB at 1-9 phr and coir filler at 1-15 phr. The composites were prepared by mixing the constituents and fabricating using a twin screw extruder and a compression molding, respectively. Experimental results reveal that for HIPS/CB composites, CB loading of 5 phr was the lowest amount which can change the conductive properties of the composite from an insulator to a conductor which had the surface resistivity equal to 1.20×10^7 ohm/square. The conductive properties of this composite resulted from the accumulation of CB particles in form of the CB agglomerates and aggregate chains that tended to flocculate and link together into network structure within the polymer matrix. The network structure facilitated movement of electrons through the polymer matrix. For mechanical properties, the addition of CB enhanced the modulus, tensile strength, and flexural strength of the composites whereas impact strength decreased. In case of HIPS/CB/coir filler composites, the addition of insulating coir filler did not cause an increase in the surface resistivity of the composites because of the polarity effect of coir filler that can induce the cluster of CB to form network structure on the fiber surface. In addition, the addition of coir filler loading, in particular at 5-9 phr, tended to decrease the surface resistivity of the composites gradually. For mechanical properties, the addition of coir filler enhanced the modulus of the composites, while the tensile strength and flexural strength were closed to HIPS/5CB composite and the impact strength decreased. In conclusion, the HIPS/CB (5phr)/coir filler (9 phr) composite showed suitable mechanical properties and had the lowest resistivity (4.15×10^5 ohm/square).

Department Materials Science

Field of Study Applied Polymer Science and Textile Technology

Academic Year 2006

Student's Signature.....

Advisor's Signature.....

ACKNOWLEDGMENTS

The author would like to take this opportunity to express sincere thanks to her teachers and people who gave useful advice and full support for this research.

The author wishes to express her gratitude to Asst. Prof. Dr. Duangdao Aht-Ong, her adviser, for her valuable guidance and attention throughout this research. It goes without saying to the thesis committee, Assoc. Prof. Saowaroj Chuayjuljit, Assoc. Prof. Paiparn Santisuk, Assoc. Prof. Onusa Saravari, and Assoc. Prof. Dr. Pranut Potiyaraj, for reading and criticizing the manuscript.

She appreciates all the teachers who have invaluable knowledge while studying in the Department of Materials Science, Faculty of Science, Chulalongkorn University.

She thanks to Dow Chemical Co., LTD. for providing high impact polystyrene and the National Metal and Materials Technology Center (MTEC) for instrument analysis.

She also would like to give the special thanks to all of her friends at the Department of Materials Science who have been helping and encouraging her while studying at Chulalongkorn University.

Last, the author would like to express her appreciation to her mother for care and encouragement.

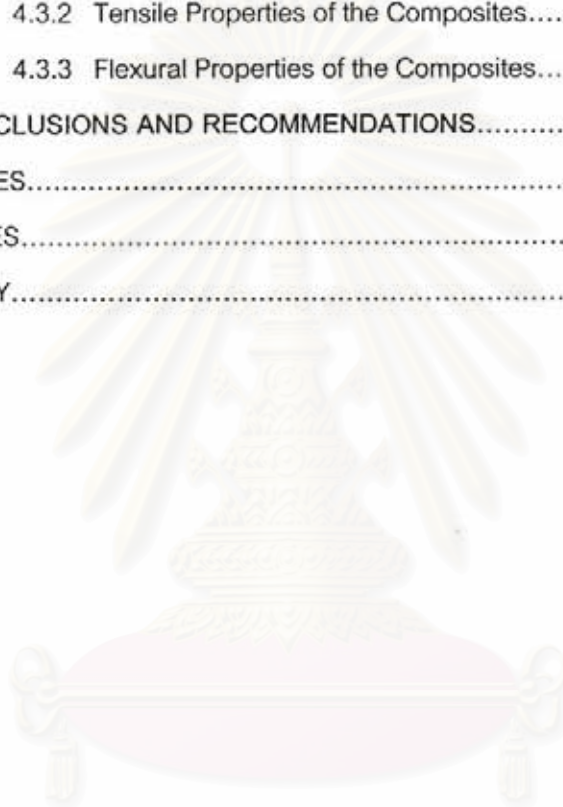
สถาบันวิทยบริการ
จุฬาลงกรณ์มหาวิทยาลัย

CONTENTS

	Page
Abstract (Thai).....	iv
Abstract (English).....	v
Acknowledgements.....	vi
Contents.....	vii
List of Tables.....	x
List of Figures.....	xii
CHAPTER	
I INTRODUCTION.....	1
II LITERATURE SURVEY.....	6
2.1 Conductive Plastics.....	6
2.1.1 Background.....	6
2.2.2 Classification of Conductive Compounds.....	6
2.2 Carbon Black Containing Thermoplastic Compounds.....	7
2.2.1 The Electrical Conductivity and the Percolation Threshold.....	8
of CB Containing Thermoplastic Compounds	
2.2.2 Factors affecting the Electrical Conductivity.....	10
And the Percolation Threshold of CB containing Thermoplastic	
Compounds	
2.3 Carbon Black Containing Polymer Blends.....	16
2.3.1 The Electrical Conductivity and the Percolation Threshold.....	16
of CB containing Immiscible Blends	
2.3.2 Factors affecting the Electrical Conductivity.....	18
and the Percolation Threshold of CB containing Immiscible Blends	
2.3.3 Literature Reviews of CB containing Immiscible Blends.....	20
2.4 Using Conductive Plastics in Electronic Packaging Applications.....	23
2.5 Materials, Equipments, and Test Methods.....	25
2.5.1 Materials.....	25
2.5.2 Processing Equipments.....	29

CHAPTER	Page
2.5.3 Surface Resistivity Measurement	31
2.5.4 Particle Size Distribution Analysis.....	33
(Low Angle Laser Light Scattering (LALLS) Technique)	
III EXPERIMENTS.....	34
3.1 Materials.....	34
3.1.1 High Impact Polystyrene.....	34
3.1.2 Carbon Black.....	34
3.1.3 Coir Fibers.....	34
3.2 Equipments.....	34
3.2.1 Attritor.....	34
3.2.2 Ball Mill.....	35
3.2.3 Particle Size Distribution Analyzer.....	35
3.2.4 Twin Screw Extruder.....	36
3.2.5 Compression Molding.....	36
3.2.6 Electrometer.....	37
3.2.7 Tensile Testing Machine.....	37
3.2.8 Flexural Testing Machine.....	38
3.2.9 Impact Tester.....	38
3.2.10 Thermo Gravimetric Analyzer (TGA).....	39
3.2.11 Scanning Electron Microscope.....	39
3.3 Methodology.....	39
3.3.1 Preparation of Filler from Coir Fibers.....	41
3.3.2 Preparation of the Composites.....	41
3.3.3 Characterization of Coir Fiber, Coir Filler, and Carbon Black.....	43
3.3.4 Characterization of the Composites.....	44
IV RESULTS AND DISCUSSION.....	45
4.1 Characterization of Raw Materials.....	45
4.1.1 Morphology Studies of Coir Fiber, Coir Filler, and Carbon Black....	45
4.1.2 Particle Size Distribution of Coir Filler and Carbon Black.....	50

CHAPTER	Page
4.1.3 Thermal Properties of Coir Fiber.....	51
4.2 Surface Resistivity and Morphology of the Composites.....	53
4.2.1 Surface Resistivity of the Composites.....	53
4.2.2 Morphology of the Composites.....	56
4.3 Mechanical Properties of the Composites.....	65
4.3.1 Notched Izod Impact Strength of the Composites.....	66
4.3.2 Tensile Properties of the Composites.....	73
4.3.3 Flexural Properties of the Composites.....	81
V CONCLUSIONS AND RECOMMENDATIONS.....	85
REFERENCES.....	88
APPENDICES.....	92
BIOGRAPHY.....	113



สถาบันวิทยบริการ
จุฬาลงกรณ์มหาวิทยาลัย

LIST OF TABLES

Table	Page
2.1 Definition of the Types of the Packaging.....	23
2.2 Definition of the Packaging Materials Types.....	24
2.3 Summarizes the physical properties of HIPS.....	26
2.4 Chemical Compositions of Coir Fiber.....	27
2.5 Properties of some representative conducting carbon blacks.....	29
2.6 Classification of materials based on surface resistivity (Ohm/Square).....	32
3.1 Formula (phr) of the Composites.....	42



สถาบันวิทยบริการ
จุฬาลงกรณ์มหาวิทยาลัย

LIST OF FIGURES

Figure	Page
2.1 Structure of carbon black in the polymer matrix.....	9
2.2 Schematic of CB containing immiscible blend structure at different blend ratio..	18
2.3 Chemical structure of high impact polystyrene.....	26
2.4 Steps of coconut husk to coir fiber.....	27
2.5 Chemical structure of carbon black.....	28
2.6 Intermeshing twin screw extruder.....	30
2.7 Compression molding process.....	30
2.8 Surface resistivity measurement technique.....	31
2.9 Circular electrode dimensions.....	32
2.10 Schematic of LALLS technique.....	33
3.1 FRISCH attritor model FR150.....	34
3.2 Ball Mill.....	35
3.3 Mastersizer S long Bed Version 2.11.....	35
3.4 Thermo PRISM co-rotating twin screw extruder model TSE-16-TC.....	36
3.5 Lab Tech model LP-S-50.....	36
3.6 Keithley Electrometer 617 based on contacts.....	37
in sandwich configuration	
3.7 LLOYD Universal Testing Machine model LR 100K plus	37
3.8 LLOYD Universal Testing Machine model LR10K.....	38
3.9 Zwick 5102 Pendulum Impact Tester.....	38
3.10 METTLER TOLED model TGA/SDTA 851 ^e	39
3.11 Jeol JSM-5410LV scanning electron microscope.....	39
3.12 Flowchart of the manufacturing process.....	40
4.1 SEM micrographs of (a) lengthwise section of coir fiber at low magnification (magnification : 200 x, scale bar 100 μm); (b) lengthwise section of coir fiber at high magnification (magnification : 2,000 x, scale bar 10 μm); (c) fractured surface of coir fiber at low magnification (magnification : 200 x, scale bar 100 μm); and (d) fractured surface of coir fiber at high magnification (magnification	

Figure	Page
: 2,000 x, scale bar 10 μm).....	46
4.2 SEM micrographs of (a) coir filler (magnification : 200 x, scale bar 100 μm); (b) a lava-like structure of fiber particle (magnification : 350 x, scale bar 50 μm); (c) surface of the lava-like structure particle (magnification : 10,000 x, scale bar 1 μm); (d) a particulate shape of fiber particle (magnification : 350 x, scale bar 50 μm); and (e) surface of the particulate particle (magnification : 10,000 x, scale bar 1 μm).....	47
4.3 SEM micrographs of (a) carbon black pellet (magnification : 75 x, scale bar 200 μm) and (b) carbon black agglomerates at low magnification (magnification : 350 x, scale bar 50 μm); and (c) carbon black agglomerates at high magnification (magnification : 10,000 x, scale bar 1 μm).....	49
4.4 Volume percentages of coir filler and carbon black.....	51
4.5 TGA thermogram of coir filler.....	52
4.6 Logarithm of surface resistivity of (a) HIPS/CB composites as a function of CB content; and (b) HIPS/5CB, HIPS/coir filler, and HIPS/5CB/coir filler composites as a function of coir filler content.....	55
4.7 SEM micrographs of (a) HIPS at low magnification (magnification : 1,000 x, scale bar 10 μm); (b) HIPS at high magnification (magnification : 10,000 x, scale bar 1 μm); (c) HIPS/3CB composite at low magnification; (d) HIPS/3CB composite at high magnification; (e) HIPS/5CB composite at low magnification; and (f) HIPS/3CB composite at high magnification.....	58
4.8 SEM micrographs of (a) HIPS/5CB/3coir filler composite (magnification : 200 x, scale bar 100 μm); (b) fiber particle at low magnification (magnification : 1,000 x, scale bar 10 μm); and (c) fiber particle at high magnification (magnification : 10,000 x, scale bar 1 μm).....	60
4.9 SEM micrographs of (a) HIPS/5CB/5coir filler composite (magnification : 200 x, scale bar 100 μm); (b) fiber particle at low magnification (magnification : 1,000 x, scale bar 10 μm); and (c,d) fiber particle at high magnification (magnification : 10,000 x, scale bar 1 μm).....	62
4.10 SEM micrographs of (a) HIPS/5CB/9coir filler composite (magnification	

Figure	Page
: 200 x, scale bar 100 μm); (b,d) fiber particle at low magnification (magnification : 1,000 x, scale bar 10 μm); and (c,e) fiber particle at high magnification (magnification : 10,000 x, scale bar 1 μm).....	64
4.11 Notched Izod impact strength of HIPS/CB composites as a function of CB content.....	67
4.12 Impact strength of the composites as a function of coir filler content.....	68
4.13 SEM micrograph of (a) crack growth region of HIPS/7coir filler composite (magnification : 150 x, scale bar 100 μm); (b) micro-cracks and debonding of HIPS/7coir filler composite (magnification : 500 x, scale bar 10 μm); (c) crack growth region of HIPS/15coir filler composite (magnification : 200 x, scale bar 100 μm); and (d) micro-cracks of HIPS/7coir filler composite (magnification : 1000 x, scale bar 10 μm) under impact loading.....	69
4.14 Crack growth region of HIPS/5carbon black/7coir filler composite under impact loading.....	72
4.15 Crack growth region of pure HIPS under impact loading.....	72
4.16 Load-extension curve of the composites.....	74
4.17 The effect of CB content on (a) tensile modulus, (b) tensile strength, and (c) elongation at break of HIPS/CB composites.....	77
4.18 The effect of coir filler content on (a) tensile modulus, (b) tensile strength, and (c) elongation at break of the composites.....	79
4.19 Flexural modulus (a) and flexural strength (b) of HIPS/CB composites.....	82
4.20 Flexural modulus (a) and flexural strength (b) of the composites as a function of coir filler content.....	83



CHAPTER I INTRODUCTION

Up to the present time, electronics industry that becomes the greatest industry in the world has encountered a serious problem associated with electrostatic discharge (ESD). Industry experts have reported that approximately 8 to 33 % of electronic devices are destroyed by ESD. Moreover, they have found that the cost of ESD damage to the electronics industry is the billion of dollars annually. [1]

ESD is mostly created by the contact and separation of two materials. When the two materials are come in contact and then separate, electron is transferred between the two materials. One of the materials that losses electron results in a positive charge on its surface and the other that gains electron, a negative charge. As a result, electric potentials of the two materials are different expressing as electrostatic voltage. Level of the electrostatic voltage depends on material type, speed of contact and separation, humidity, and several other factors. To eliminate the electrostatic voltage, the positive charge is transferred to the negative charge at the different electrical potentials. This charge transfer is known as ESD. [1] However, if the level of electrostatic voltage is high enough, a great many charges carrying energy is rapidly transferred to the sensitive material. Hence, the sensitive material is suddenly destroyed by ESD attack. [2]

In the electronics industry, ESD can be occurred on the devices throughout touch of charged human bodies to the devices, move of devices across machine surfaces, slide of devices in packages, or induction of electrostatic fields, etc. [1] Occurred ESD can easily damage the sensitive devices in the form of an arc or spark at the sufficiently different electrical potentials. Accordingly, the sensitive devices fail immediately or loss their electrical characteristics. Furthermore, reduction of device sizes to increase speed and decrease power consumption today cause increment of their sensitivity to ESD damage at very low electrostatic voltages. [1,2] Consequently, static safe techniques such as grounding, ionization, and the use of conductive packaging materials have been developed to protect products from ESD. [1]

One of the static safe techniques that can directly protect the devices from ESD damage is the use of conductive packaging materials. When surface of the conductive packaging becomes charged by rubbing between the device and the packaging, the charges are allowed to dissipate across its surface or through its volume and then transfer to ground or another nearby conductive object in order to reduce the electrostatic voltage to the low level. As a result, ESD event is not violent enough to damage the device. Accordingly, the conductive packaging materials can safely protect the devices from ESD event by limiting the passage of ESD current and reducing the energy that causes from ESD. Moreover, they can shield the electrostatic fields which induce charges to accumulate on the devices and create ESD. Typically, the material's ability to prevent ESD damage is measured by surface resistivity. Conductive compounds which have surface resistivity values in a range of 10^5 - 10^9 ohm/square can be used to directly protect products from ESD event. [1,2]

Electronic packaging materials are most commonly made from conductive compounds which compose of thermoplastic resins and conductive fillers, in particular, carbon black (CB). [2] In principle, the incorporation of conductive filler into the nonconductive polymer matrix causes a sharp transition from insulator to conductor system at a critical concentration of the filler. This critical concentration is called the percolation threshold. [3] At the percolation threshold of CB-containing polymer systems, CB particles tend to coagulate and form flocculate chains which link together in network structures. These network structures facilitate movement of electrons through the polymer matrices so the surface resistivity of compounds can be decreased dramatically. [4] In general, the percolation threshold of CB-filled single polymer systems varies from polymer to polymer as a consequence of different polymer properties such as viscosity, surface tension, polarity, and degree of crystallinity. [5,6] These polymer properties affect on characteristics of CB distribution. The characteristics of CB distribution in the polymer matrices lead to increase or decrease the percolation threshold and the electrical conductivity of CB filled single polymer systems. If CB particles tend to distribute uniformly in the polymer matrix, system

requires high CB loadings to form network structures. Thus, the percolation threshold of the system is increased. In contrast, if the CB particles tend to coagulate or distribute non-uniformly in the polymer matrix, network patterns are formed at low CB contents so the percolation threshold and the surface resistivity of the system are decreased. [5]

Nevertheless, many CB-filled single polymer compounds produced in compound industry often show non-uniform surface resistivity due to loss of electron paths in some positions of their surface. [7] These positions indicate uniform distribution of CB particles in the polymer matrices. Hence, when the devices vibrate in the non-uniform conductive packaging, accumulative charges on surface of the packaging can not dissipate across its surface due to insulating area of the surface creating high level of electrostatic voltage. Therefore, occurred ESD is violent enough to damage the devices. Moreover, it has been found that these CB-filled single polymer compounds normally require high CB loading (~10-20 wt %) to reach the percolation threshold. [6] It is well known that disadvantages of using high content of carbon black are relatively high cost, difficult processing, sloughing (peeling off of CB from product surfaces), and inferior mechanical properties. [8] Thus, several authors have been studying to enhance the electrical conductivity and reduce the critical CB content in CB filled single polymer system through studying the effect of processing conditions, such as processing temperature and mixing speed. It has been noted that increasing processing temperature or decreasing mixing speed in mixing process of CB filled single polymer systems can reduce the surface resistivity and the percolation threshold of the system because both of them promote the enhancement of network quality in the CB filled single polymer systems. [7,9]

Even if decrement of the surface resistivity and the critical CB content in one component matrices are attained by using preferable processing parameters, many researchers have been trying to obtain lower values of the percolation threshold via applying immiscible polymer blend systems. [5,6,8] Utilizing an immiscible multi-component matrix in place of a single polymer presents more favorably answer namely lower CB contents and superior electrical conductivity as a result of the support of blend

properties and blends morphology to provide CB accumulation at preferential locations and form highly network patterns. [5,8,10] There are two types of CB locations for enhancement of the electrical conductivity. One is a non-uniform distribution of CB at the interface of blend and the other is a non-uniform distribution of CB within one polymer phase. Moreover, observed co-continuous structure of blend at the critical component ratio serves CB accumulate in the form of continuous structure that locates at the interface of continuous matrix or within continuous matrix. Thus, double percolation is achieved. [5,8,10] However, obtaining the structures depends upon a balance between viscosity effects, CB-polymer interactions, CB contents, and processing conditions. [5,10]

As noted earlier, it was demonstrated that both of CB-filled single polymer systems produced from preferable processing conditions and CB-filled immiscible polymer blend systems efficiently promote the enhancement of the electrical conductivity and the decrement of the critical CB content. However, the reduction in the usage of the plastics made from petroleum oil is high necessary at the present time because critical concern on energy crisis and ecological and environmental problems. [11] For this purpose, the cellulose fiber- filled conductive composites become interesting choice for utilizing in the electronic packaging applications. It is well known that advantages of cellulose fiber are low cost, light weight, renewable, high specific mechanical performance, enhanced energy recovery, and biodegradability. [12] In addition, it has been reported that the polarity of polymer disperse phase in system of CB filled immiscible blend is significant factor that leads to enhance network quality of CB. Since the polarity of the disperse phase can induce CB to flocculate at its surface or within it, CB has less opportunity to distribute uniformly in the continuous phase of the blend. As a result, the surface resistivity and the percolation threshold of CB filled multiphase components are efficiently reduced by the polarity of the polymer disperse phase. [6,10] With regard to cellulose fiber, it is well known that cellulose fiber is polarity in nature. [13] Thus, the incorporation of cellulose fiber in the polymer matrix may induce CB to accumulate on its surface; as a result, the surface resistivity and the critical CB

content of cellulose fiber filled-conductive composite may be reduced due to the polarity of cellulose fiber. Consequently, the cellulose fiber- filled conductive composites may maintain the balance between conductive composite properties, cost effectiveness, and environmental issues for electronic packaging industrial applications. Nevertheless, the study of the cellulose fiber- filled conductive composites has been limited. In addition, the study of utilizing cellulose fiber for reducing cost and decreasing plastic loadings including the investigation of the cellulose fiber on the electrical conductivity of conductive composites have never been carried out before.

In many countries coir fiber, one of the components found in the husk of coconut *Cocos nucifera* L. fruit, is most widely used for manufacturing ropes, matting, basket liners, and many other products. When coir fibers are separated from the husk, long fibers are removed to use for industrial applications. As a result, short to medium length fibers still remain as a waste product that are usually incinerated or dumped without control. [14] Hence, bringing these waste fibers to apply as a filler in conductive composites is another interesting way to solve waste problems and provide cost effectiveness for conductive composites.

Accordingly, this research is focused on the study of using waste coir fibers as a filler in high impact polystyrene (HIPS) /carbon black (CB) composites, which is used mainly for IC shipping tray and packaging for electronic parts. [7] The objectives of this study are to investigate the effects of fiber loadings on mechanical performance and electrical conductivity of prepared composites, to find the suitable mixing and processing methods for providing uniform distribution of coir fibers and network structures of CB in HIPS, and to find the suitable ratio between HIPS, CB, and coir fibers. All of the composites are prepared by premixing the components in ball mill and subsequently mixing in a twin screw extruder. After compounding, the compounds are moulded into sheets via a compression moulding. Finally, the composite sheets are used for surface resistivity measurement by an electrometer and mechanical properties testing. Morphology of the composites is investigated through scanning electron microscope (SEM).

CHAPTER II

LITERATURE SURVEY

2.1 Conductive Plastics

This topic relates to the background of conductive plastics and their classifications. The details are as follows:

2.1.1 Background

Conductive plastics are molding materials which compose of thermoplastic resins and conductive fillers such as aluminum flakes, metal powder, carbon black, and carbon fiber, etc. It is known that most of thermoplastic resins are electrical insulators but incorporation of conductive fillers can dramatically change their non-conductive properties into conductive properties at the critical concentration of fillers so called the percolation threshold. Since conductive plastics can be more cost effective, more design capability, and better mechanical performance such as superior impact resistance as compared to metals, they are used widely in some applications requiring electrical conductivity or ESD protection. In compound industry, carbon black (CB) is usually used as conductive filler in thermoplastic resins as a consequence of its lightweight and its permanent conductivity. In general, CB filled thermoplastic compounds are utilized for a variety of conductive material applications such as liquid or chemical vapor sensors, positive temperature coefficient materials, and electronic packaging materials. [2,6]

2.1.2 Classification of Conductive Compounds

According to the U.S. Department of Defense's Handbook 263 (DOD-HDISK-263), plastic composites for using in ESD protection can be classified into three categories according to their surface resistivity. In other words, surface resistivity is measured to indicate the conductivity of materials. [2]

1. Antistatic Composites

Antistatic composites are defined as having a surface resistivity of greater than 10^9 and less than 10^{14} ohms-square. Commercial grades of compounds that fall into this category allow electrons to flow across its surface slowly. Therefore, they are normally used as the barrier materials to avoid the direct contact between the sensitive components and the conductive materials.

2. Static Dissipative Composites

Static dissipate composites have a surface resistivity of greater than 10^5 and less than 10^9 ohms-square. In this category, flow of electrons is significantly faster than from antistatic composites and slower than from conductive composites. Because speeds of charge transfer in static dissipative materials are in safe levels, they can be used for dissipating charges that cause ESD event by direct contact with the sensitive components.

3. Conductive Composites

Conductive composites are the most highly conductive category. These materials are defined as having a surface resistivity of less than 10^5 ohms-square. They can rapidly dissipate charges and shield the sensitive components from electrostatic fields because electrons are allowed to flow across their surface quickly. Thus, they are normally used in applications requiring electrostatic shields. However, the sensitive components would have to be isolated from direct contact with conductive composites by using antistatic composites as barrier materials since the direct contact may result in a rapid charge transfer which can immediately damage the sensitive components.

2.2 Carbon Black Containing Thermoplastic Compounds

As described earlier, conductive materials are most commonly made from carbon black (CB) filled thermoplastic compounds. However, the electrical conductivity and the percolation threshold of conductive compounds are not preferable at present.

[15] Thus, there is a great need to produce polymeric materials with relatively higher conductivity and lower critical CB content than they are currently available. To achieve the goals, it is necessary to know about the electrical conduction and the percolation threshold of CB filled polymer systems and factors affecting on their electrical conduction and the percolation threshold. These are explained as follows:

2.2.1 The Electrical Conductivity and the Percolation Threshold of CB Containing Thermoplastic Compounds

In conductive filler filled polymer system, incorporation of the critical filler content in the insulating polymer matrix results in a drastic transition from insulator to conductor system. The critical filler content is called the percolation threshold. At the percolation threshold of conductive compounds, the electrical conductivity is dramatically enhanced. [3] Likewise, at the percolation threshold of CB filled polymer systems, the electrical conductivity is sharply increased due to the appearance of the CB network structures in the polymer matrices. [15] Typically, the electrical conductivity and the percolation threshold of CB filled single polymer compounds vary from polymer to polymer due to the difference of polymer properties and mixing conditions. [5,6] Polymer properties such as viscosity, surface tension or polarity, and degree of crystallinity and processing conditions also affect on characteristics of CB distribution in the polymer matrices. [5,7,10] The characteristics of CB distribution in the polymer matrices indicate network quality of systems. [5] If CB tends to flocculate in the polymer matrices, higher network quality is found in comparison to uniform distribution of the CB particles. Higher network quality of CB filled single polymer systems promotes the higher electrical conductivity and the lower CB content to percolation. [5,10] Next detail describes distribution of CB at the percolation threshold of common CB filled one component systems.

Generally, as received CB is in the form of chain-like aggregates of the CB particles. Addition of the critical CB loading in the polymer matrix results in larger aggregates of the CB particles. The larger aggregates are called agglomerates. Under interactions of CB-CB and of CB-melting polymer and mixing conditions, some CB

agglomerates may be come to coalesce in larger agglomerates while the others may be reduced to primary aggregates during mixing. Both of the agglomerates and the primary aggregates that tend to flocculate and link together in a network pattern results in a sharp transition from the insulating system into the conducting system. The network structures cause in the sharp enhancement of the electrical conductivity in CB filled polymer compounds. [7,15] The structure of carbon black in the polymer matrix is shown in Figure 2.1. [16]

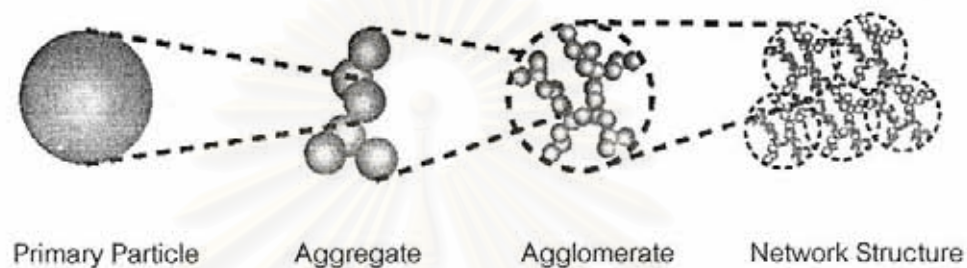


Figure 2.1 Structure of carbon black in the polymer matrix.

As noted earlier, at the percolation threshold of CB filled single polymer systems, network structures of CB are created to support electrical conduction of the systems. Nevertheless, the improvement of network quality can enhance the electrical conductivity and reduce the percolation threshold in CB filled one component systems. [5] Seemingly, obtaining the CB primary aggregates becomes important in the improvement of network quality of CB filled polymer compounds. [5,7] In theory, an ideal structure of CB filled polymer systems which can increase the electrical conductivity and decrease the percolation threshold is a structure that the CB primary aggregates disperse with two features of branching aggregates and of the shortest possible inter-aggregate distances in the polymer matrices. [7] It was demonstrated that compound formulation and mixing parameters affect on network quality of CB in the polymer matrices. [5-7] Thus, optimum design of compound formulation and mixing parameters can develop network quality by inducing rupture of the CB agglomerates and reduce them to the primary aggregates. [5]

2.2.2 Factors Affecting the Electrical Conductivity and the Percolation Threshold of CB Containing Thermoplastic Compounds

In this topic, effects of CB contents, polymer properties, and processing parameters on the electrical conductivity and the percolation threshold of the CB filled single polymer systems are described as follows:

2.2.2.1 CB Contents

It was demonstrated that the electrical conductivity and the percolation threshold of CB containing thermoplastic resins depend on the modes of filler distribution. Because addition of different CB loadings in the polymer matrices causes difference in their distribution, the electrical conductivity and the percolation threshold of conductive compounds are related to CB contents. [15]

At low CB content, small CB particles (aggregates or agglomerate) are distributed homogeneously in the polymer matrix since the distances between the CB particles in the polymer matrix are far apart. Thus, the less amount of CB can not increase the electrical conductivity of the insulating matrix as electron paths are not created to facilitate the electrical conduction through the polymer matrix.

Increasing CB content in the polymer matrix results in larger agglomerates of the CB particles because the CB particles tend to contact together at higher CB content. Hence, the electrical conductivity of system can be increased slightly.

At a certain critical CB content (the percolation threshold), the growing agglomerates reach a size that makes large scale of contact to form a compact one, two, or three-dimensional network of the conducting phase within the polymer matrix. The first appearance of the networks results in a drastic transition from insulator to conductor system. The drastic transition causes a sharp enhancement in the electrical conductivity of system.

2.2.2.2 Polymer Properties

This topic describes influence of polymer properties such as viscosity, surface tension or polarity, and degree of crystallinity on the percolation threshold of the CB filled one component systems. The details are explained as follows:

1. Viscosity

In mixing process, polymer viscosity plays an important role in the dispersion of particles including agglomerate rupture, re-agglomeration, and flocculation. [5] With regard to common system of suspending liquid, since the viscosity of the liquid exerts hydrodynamic forces to compete with the cohesive forces of the agglomerates, a high viscosity liquid may induce agglomerate rupture while a low viscosity liquid provides the opposed effect of particle flocculation. [5] Similarly, in mixing process of CB filled polymer matrix system, matrix of lower viscosity serves the lower critical CB content in as much as it exerts lower shear stresses on the agglomerates. Lower shear stresses which are exerted from lower polymer viscosity provide less agglomerate rupture. In addition, lower shear stresses of lower polymer viscosity promote more opportunity of the isolated agglomerates to return in approach one another during mixing because lower shear stresses exert less resistance to re-agglomeration. The return to flocculation of the isolated agglomerates is known as re-agglomeration. Therefore, the CB aggregates tend to approach one another more easily and form conductive networks in lower polymer viscosity. In contrast, higher shear stresses of higher polymer viscosity can break up the agglomerates more easily. In addition, higher shear stresses show higher resistance to inhibit re-agglomeration of the isolated agglomerates. Thus, matrix of higher viscosity serves the higher percolation threshold as compared to matrix of lower viscosity. [5]

O. Breuer et al. [5] have investigated the effect of polymer viscosity on the percolation threshold via studying two LLDPE grades which are different in their melt flow index. In this study, they have found that CB filled lower viscosity LLDPE system has the percolation threshold less than system of CB filled higher viscosity LLDPE. In

the lower viscosity grade, they have reported that CB tends to flocculate more easily and form flocculate chains or network-like structure because the lower viscosity LLDPE exerts lower shear stresses on the agglomerates. Accordingly, lower shear stresses cause less agglomerate fracture and less re-agglomerate resistance. On the contrary, CB disperses more uniformly in the higher viscosity grade exerting higher hydrodynamic forces to reduce particle size and inhibit particle flocculation. Thus, the lower viscosity LLDPE serves the lower critical CB content while the higher viscosity LLDPE provides the higher percolation threshold.

2. Surface Tension or Polarity

It was indicated that the critical CB content for percolation may relate to the surface tension or polarity of the polymer matrices. Based on several researches, it was found that the system of CB filled the polymer matrix with intermediate surface tension or polarity shows the lowest percolation threshold as compared to the system of CB filled the polymer matrix with low surface tension or non-polarity and the system of CB filled the polymer matrix with very high surface tension or polarity, respectively. This indicates that the different levels of surface tension or polarity of the polymer matrices may result in the different characteristics of distribution of CB in the polymer matrices. In the system of CB filled the polymer matrix, a very high surface tension or polarity of the polymer matrix can completely wet CB to disperse uniformly in the polymer matrix with very high surface tension or polarity so this system requires the high critical CB content to percolation. With regard to the system of CB filled the polymer matrix with low surface tension or non-polarity, the polymer matrix has low interaction with CB that has relatively high surface tension or polarity on its surface; as a result, CB tends to cluster and form conductive networks in the polymer matrix so the lower percolation threshold of this system is obtained as compared to the system of CB filled the polymer matrix with very high surface tension or polarity. In system of CB filled the polymer matrix with intermediate surface tension or polarity, the polymer matrix has better interaction with CB in comparison to the polymer matrix with low surface tension or non-polarity. In other words, intermediate surface tension or polarity of the polymer matrix can break up some

CB particles and reduce them to primary aggregates without completely uniform dispersion of CB in the polymer matrix; as a result, the amount of conductive bridges in this system is higher than the system of CB filled the polymer matrix with low surface tension or non-polarity at the same CB content. Therefore, the percolation threshold of this system is lower than the percolation threshold of the system of CB filled the polymer matrix with low surface tension or non-polarity. Accordingly, it can be concluded that the system of CB filled the polymer matrix with intermediate surface tension or polarity has the lowest percolation threshold as compared to the system of CB filled the polymer matrix with low surface tension or non-polarity and the system of CB filled the polymer matrix with very high surface tension or polarity, respectively. [5-6,10,15]

O. Breuer et al. [5] have described the influence of surface tension or polarity on the percolation threshold through using HIPS with intermediate surface tension or polarity and LLDPE with low surface tension or non-polarity as polymer matrices. HIPS has higher surface tension than LLDPE (~ 41, 36 dyne/cm at 20°C, respectively). In addition, HIPS also has higher polarity (0.168) as opposed to LLDPE (0.0). From this research, it was found that CB filled HIPS system has the lower critical CB content for percolation as compared to CB filled LLDPE system. Based on these results, they suggested that intermediate surface tension or polarity of HIPS could enhance some particle breakage to primary aggregates which is sufficient to provide conductive bridges without completely uniform dispersion of CB in HIPS matrix.

R. Tchoudakov et al. [15] have studied the effect of a very high surface tension or polarity of the polymer matrix on the percolation threshold. In this research, they used nylon (NY) which has a very high surface tension or polarity resulting from the NY amide groups in comparison to PP which has a low surface tension or non-polarity. They have reported that CB filled NY system requires very high CB content to reach the percolation threshold while system of CB filled PP needs low CB content to percolation. At the same CB content, it was observed that CB particles flocculate in the form of a chain-like structure in PP matrix as opposed to CB filled NY matrix system which is clearly observed a more uniform of CB distribution. Consequently, it can be concluded

that a very high surface tension or polarity of NY can readily wet some CB particles to completely disperse in the matrix. Hence, higher concentrations are needed to achieve the state of network formation in NY matrix.

3. Degree of Crystallinity

An additional factor to be considered is the degree of crystallinity. Since CB tends to accumulate within the amorphous regions of the polymer, the effective CB content within these regions increases and form conductive paths. Thus, the critical CB contents for percolation in the polymer matrices having low degree of crystallinity are reduced. [10]

2.2.2.3 Processing Parameters

Efficient mixing process by preferable mixing parameters such as mixing speed, mixing equipment design, and processing temperature can also enhance the percolation threshold and the electrical conductivity of CB filled one component systems. [7,9] The details are described as follows:

1. Mixing Speed

Understandably, in mixing process of polymer compounds, higher mixing speed promotes less mixing efficiency as compared to lower mixing speed. It is known that higher mixing speed produced shorter mixing time in mixing process. In mixing process of CB filled single polymer systems, shorter mixing time of higher mixing speed results in less dispersion of CB. Less dispersion of CB by higher mixing speed causes less number of the CB primary aggregates to flocculate and form network structures. [7,10] With regard to the effect of shear rate which relates to mixing speed, it was noted that shear force applied on fluid causes alteration in flow velocity of the fluid. Rate of change in velocity of the fluid under applied shear force through the depth of the fluid is determined as shear rate. [17] Likewise, in mixing process of polymer systems, the mixing speed exerts shear stresses on the melting polymer undergoing mixing. As a result, shear rate is promoted under applying shear stresses of mixing speed on the melting polymer. At higher mixing speed, higher shear rate is promoted. [10] In mixing

process of CB filled single polymer systems, higher shear rate of higher mixing speed breaks up the agglomerates to isolate from one another more easily and exerts higher resistance to inhibit re-agglomeration. Hence, conductive bridges are less created in the polymer matrices with higher mixing speed. [10] For these reasons, the percolation threshold and the surface resistivity of CB filled single polymer systems are increased at higher mixing speed. [7,10]

S. Phiboonkulsumrit et al. [7] have researched the effects of screw speeds on the percolation threshold and surface resistivity of CB/HIPS compounds by using twin screw extruder technique. In this research, it was found that lower speed of mixing provides the lower critical CB content and the higher electrical conductivity in CB filled HIPS system. Based on these results, they concluded that higher mixing time of lower mixing speed serves higher mixing energy to increase mixing efficiency of CB/HIPS compounds. In higher mixing time of lower mixing speed, CB becomes better dispersed in HIPS matrix so the amount of CB primary aggregates are higher to form conductive networks. In addition, lower shear rate of lower mixing speed exerts less resistance to reduce re-agglomeration of the dispersed CB. Accordingly, CB filled HIPS system produced by using lower mixing speed has the lower critical CB content to percolation and the higher electrical conductivity.

2. Mixing Equipment Design

In view of mixing equipment design, S. Phiboonkulsumrit et al. [7] have studied the effects of screw design to the percolation threshold and surface resistivity of CB /HIPS compounds by using twin screw extruder technique. Two configurations of screw designs were used and compared in their experiments. The first design has one kneading disc (Type I), while the other one has two kneading discs (Type II). It is known that kneading blocks are segments adding to screws for improving mixing efficiency by increasing dispersion of the particles in twin screw extruders. In this study, they have found that CB/HIPS compounds produced by screw type II showed a much lower surface resistivity and the lower percolation threshold in comparison to CB/HIPS compounds produced by using screw configuration type I. From the results, they have

described that screw type II having two kneading zones can provide higher dispersion and/or distribution of CB in HIPS matrix to create a desirable network like structure of CB primary aggregates.

3. Processing Temperature

In CB filled one component systems, increasing mixing temperature can enhance the electrical conductivity of the system. As higher mixing temperature serves higher mobility of the polymer molecules, the CB particles can penetrate into the polymer matrix and tend to flocculate in the form of network structures. In addition, higher processing temperature increases the time that allows flocculation of the CB aggregates to create higher amount of electron paths in the polymer matrix after the material has left the die into ambient air. [9]

2.3 Carbon Black Containing Immiscible Polymer Blends

It was demonstrated that immiscible polymer blends are interesting host matrices for the incorporation of CB. [5,6] Namely, the multiphase nature of these systems provides an opportunity for CB to distribute non-uniformly in the immiscible blend matrices. As a result, the lower critical CB contents and superior electrical conductivity of CB filled immiscible blend systems are obtained in comparison with systems of CB filled one component. [10]

2.3.1 The Electrical Conductivity and the Percolation Threshold of CB Containing Immiscible Blends

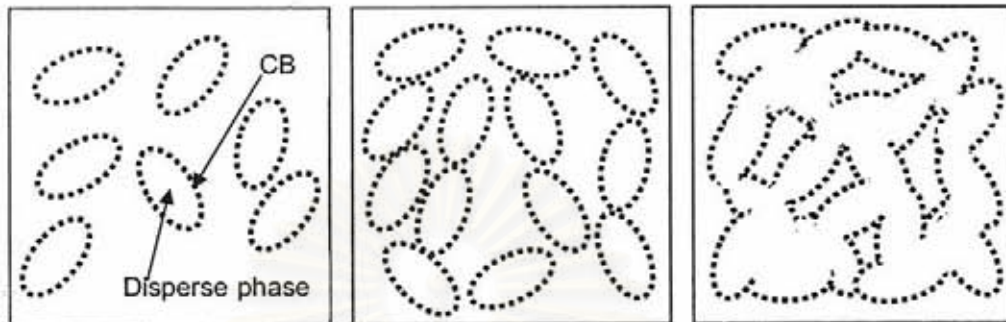
It has been established that the electrical conductivity and the percolation threshold of CB filled immiscible polymer blends depend on morphologies of the conductive blends and content of CB. [5,8,10] To understand the electrical conductivity and the percolation threshold of CB filled immiscible polymer blends, simple morphologies of neat blends and of CB filled immiscible blends are described as follows:

In view of the morphology of the immiscible blend, it has been observed that low content of the polymer disperse phase presents a very small of the disperse phase size which is a spherical shape in the polymer continuous phase. At higher content of the disperse phase, lower amount of the spherical shape and higher amount of elongation shape are appeared in the continuous phase. When the disperse phase reaches certain content in the continuous phase, the co-continuous structure is obtained in the blend. [5,10,15]

Incorporation of CB in different ratio of the blend components causes the alteration in size and shape of the polymer disperse phase. Namely, the disperse phase size becomes smaller and the shape of the disperse phase becomes more elongate structure in the continuous phase when CB is incorporated in the blends as compared to the neat blends. The alteration in both of the size and the shape of the disperse phase due to the addition of CB in the blends caused by the friction between the CB coated disperse particles and the continuous phase. More elongate structures of the polymer disperse phase result in decreasing the electrical resistivity and the percolation threshold of CB filled immiscible blends. [5,10]

Nevertheless, at low content of CB in the blend, CB does not percolate in the disperse phase. As a result, the high resistivity is obtained. Increasing the CB content causes the slight declination of the resistivity of the system due to the increased CB concentration in the disperse phase. When CB reaches a higher certain content in the blend, CB can percolate in the disperse phase. Thus, the enhancement in electrical conductivity of the system is achieved and the percolation threshold of the system is achieved due to the effective CB in the disperse phase. [5-6,10] When the high enough content of CB is added in the co-continuous matrix, CB accumulates in the form of continuous structure that locates at the interface of continuous matrix or within continuous matrix. The continuous structure or honey comb-like structure of CB in the co-continuous matrix results in achieving the double percolation threshold of the blend. Accordingly, the co-continuous structure of the blend is exceptional structure that enhances the electrical conductivity and reduces the critical CB contents for percolation

so that percolation may be obtained at exceptionally low CB contents with low resistivity values. [5-6,8] Schematic of CB containing immiscible blend structures and CB containing co-continuous structure of immiscible blend is shown in Figure 2.2. [8]



(a) low disperse phase ratio (b) high disperse phase ratio (c) co-continuous structure

Figure 2.2 Schematic of CB containing immiscible blend structures at different blend ratio.

2.3.2 Factors Affecting the Electrical Conductivity and the Percolation Threshold of CB Containing Immiscible Blends

As noted earlier, the electrical conductivity and the percolation threshold of CB filled immiscible blend are controlled by morphology of the blend and content of CB in the blend. [5-6,10] However, it was demonstrated that location of CB in the blend is another significant factor that directly influences on the electrical conductivity and the percolation threshold of CB filled immiscible blends. [5-6,10] Since the effects of the morphology of the blend and the content of CB on the electrical conductivity and the percolation threshold of CB filled immiscible blends are simply depicted in the above topic. Thus, this topic is exceptionally described about the effect of the location of CB that relates to properties of the blend components such as viscosity and surface tension or polarity and processing parameters.

In view of the location of CB in the blend, the preferential locations of CB to enhance the electrical conductivity in the blend are the location of CB at the interface of

the blend or within the polymer disperse phase. [5-6,10] It was demonstrated that properties of the blend constituents such as viscosity and surface tension or polarity as well as processing parameters are significant factors to determine the preferential location of CB within the blend and also include distribution and/or dispersion of CB in the blend. Thus, suitable selection of the blend constituents may provide the preferential location of CB in the blend to enhance the electrical conductivity and reduced the critical CB content of CB filled immiscible polymer blend system. [5-6,10]

Based on several researches, it was suggested that the polymer disperse phase should has good affinity with CB while the affinity between CB and the continuous phase should be poor interactions to provide the preferential location of CB in the blend. If CB has good affinity with the continuous phase, CB tends to locate in the continuous phase by uniformly distribution. As a result, the percolation threshold and surface resistivity value of the system are increased. In contrast, if the affinity between CB and the disperse phase is better than the affinity between CB and the continuous phase, CB tends to locate at interface of the blend or within the polymer disperse phase. The locations of CB at the interface of the blend or within the disperse phase lead to improve network quality so the critical CB content and the surface resistivity values of CB filled multiphase components are reduced. [5-6,10]

It has been reported that a polymer which has lower viscosity, higher polarity or surface tension, and/or higher percolation threshold (percolation of CB in individual polymer) has better affinity with CB. Hence, the polymer disperse phase with lower viscosity, higher polarity or surface tension, and/or higher percolation threshold as compared to the continuous phase should be selected for providing the preferential location of CB in the blend to enhance the electrical conductivity and reduce the percolation threshold of the system due to the better affinity between CB and the disperse phase that has these properties. [5,6]

For distribution of CB locating at the surface of the disperse phase or within the disperse phase, it mainly depends on viscosity of the polymer disperse phase whereas

the continuous phase is higher viscosity than the disperse phase. [5,6] If the viscosity of polymer disperse phase is low enough, CB can penetrate within the disperse phase. In contrast, CB tends to locate at the surface of the polymer disperse phase (location of CB at the interface of the blend) when CB can not penetrate within the disperse phase with higher viscosity than critical value. While suitable surface tension or polarity of the polymer disperse phase is a significant factor to break up some CB particles locating at the interface of the blend or within the disperse phase and reduce them to primary aggregates which enhance the electrical conductivity of CB filled immiscible blend system. [6,10,15]

With regard to processing parameters such as shear rate and processing temperatures, it has been found that level of shear rate is additional factor that influences on the location of CB in the blend. [5,15] Increasing shear rate can promote migration of CB particles to the interface of the blend or within the disperse phase since higher shear rate causes the decrement of viscosity ratio of the blend leading to enhance the electrical conductivity. However, increment of shear rate in some systems of CB filled immiscible blend can enhance the uniform distribution of CB by increasing gaps between the CB particles locating at the interface of the blend or within the disperse phase, thus the electrical conductivity of this system is decreased. In view of processing temperature, it has been reported that an increase of blending temperature can enhance the electrical conductivity of CB filled immiscible blend system by facilitating CB to penetrate at the surface of the disperse phase or within the disperse phase as same as increasing shear rate. In addition, higher temperature increases the time that allows flocculation of the CB aggregates at the interface of the blend or within the disperse phase to create higher amount of electron paths after the material has left the die into ambient air. [9]

2.3.3 Literature Reviews of CB Containing Immiscible Blends

There are many reports attempting to describe the electrical conductivity and the percolation threshold of CB filled immiscible blends. [3-6,7-10] Based on these studies, it was demonstrated that utilizing an immiscible multi-component matrices in place of

single polymers presents more favorably answer namely lower CB contents and superior electrical conductivity. [7-10] However, obtaining the double percolation threshold seems hardly to achieve in several systems of CB filled immiscible blends due to the complication of a balance between the morphology of the blend, the content of CB, and the level of shear rate. [5-6,10,15] Examples of some literature reviews are described as follows:

In 1997, O. Breuer et al. [5] studied the electrical conductivity of the systems containing CB filled immiscible HIPS/LLDPE blends. They have found that most of CB tends to locate at the interface of the blend more than distribution in HIPS matrix. This result suggests the better affinity between CB and LLDPE (disperse phase) in comparison with the affinity between CB and HIPS (continuous phase) due to the lower viscosity of LLDPE and the higher percolation threshold of CB in LLDPE system. With regard to the percolation threshold of CB filled HIPS/LLDPE blends, the results show that 85/15 blend exhibits the lowest content of CB to percolation as compared to the percolation threshold of CB filled HIPS, CB filled LLDPE, and CB filled all blend ratios due to the elongate structure of LLDPE phase at 85/15 blend. Although the co-continuous structure of 70/30 blend is obtained, the 70/30 blend requires higher content of CB to percolation in comparison with the critical content of CB in HIPS system and the critical content of CB in 85/15 blend. This is due to the fact that higher LLDPE requires higher effective CB content to percolate at the interface of the co-continuous blend. Thus, the double percolation threshold is not achieved in CB containing immiscible HIPS/LLDPE blends.

Two years later, O. Breuer et al. [10] have found that level of shear rate influenced on the morphology of CB filled immiscible HIPS/EVA blends. For this system, the results revealed that CB tends to locate within the disperse phase of EVA in HIPS matrix due to lower viscosity and higher polarity of EVA and higher content of CB to percolation in EVA in comparison with HIPS. Using high level of shear rate in this system can increase uniform dispersion of the EVA phase that contains CB within it in the HIPS matrix and enhance the uniform dispersion of CB locating within the EVA

phase. As a result, the lower electrical conductivity and the higher percolation threshold are obtained in CB filled immiscible HIPS/EVA blends with high level of shear rate. Moreover, the double percolation threshold of the co-continuous HIPS/EVA blend is not achieved at high level of shear rate. Although high level of shear rate can not change the co-continuous structure of the blend, high level of shear rate can increase the uniform dispersion of CB in the co-continuous blend. In contrast, at low level of shear rate, the CB containing EVA component assumes random positions, enabling contact between them. Thus, the electrical resistivity and the percolation threshold of CB filled HIPS/EVA blends with low level of shear rate are lower than the electrical resistivity and the percolation threshold of CB filled HIPS/EVA blends with high level of shear rate. Furthermore, the double percolation threshold of CB filled co-continuous HIPS/EVA blend is achieved at the low level of shear rate due to less uniform dispersion of CB within the co-continuous blend.

In 2005, Y. Li et al. [6] investigated system of CB filled PP/epoxy/glass fiber composites. In this system, the double percolation threshold is achieved due to the complete continuity of the epoxy phase. Namely, using glass fibers which have high polarity and elongate structure can induce epoxy with high polarity to accumulate around their surface. At high enough content of the glass fibers, the interconnection between them is observed. The interconnection of the glass fibers can provide epoxy to accumulate in the form of continuous structure. As a result, CB comes to flocculate in the form of continuous structure within the continuous structure of epoxy coated the glass fibers in the PP matrix so the double percolation threshold can be achieved in this system.

After that, in 2006 Y. Li et al. [18] studied CB filled immiscible PP/epoxy blends. They have found that CB tends to locate within the disperse phase of epoxy in PP matrix due to higher polarity of epoxy and higher content of CB to percolation in epoxy in comparison with PP. As a result, the electrical conductivity can be increased with increasing the epoxy content. However, the double percolation threshold is not

obtained in this system due to the incomplete continuity of the epoxy phase in the PP matrix.

2.4 Using Conductive Plastics in Electronic Packaging Applications

Up to now, the critical problem in the electronics industry is the damage of electronic devices by electrostatic discharge (ESD). [1] In the electronics industry, ESD can be occurred throughout the manufacturing, testing, shipping, or handling. [1] Since several types of the electronic devices are sensitive to destroy by ESD, a variety of static safe techniques such as grounding, ionization, and the use of conductive packaging materials have been developed to protect products from ESD. [2,7] In view of the conductive packaging materials, it has been noted that the conductive packaging materials can safely protect the devices from ESD event by limiting the passage of ESD current, reducing the energy that causes from ESD, and shielding the electrostatic fields from the devices. [1] However, use of the non- suitable conductivity of the packaging to contain the devices results in ESD damage so it is necessary to select the suitable conductivity of the packaging for efficiently preventing ESD damage with the devices. [1] According to EOS/ESD 61340-5-1, the types of the packaging are defined in three categories namely, intimate, proximity, and secondary packaging. [19] Definition of the types of the packaging is shown in Table 2.1. In EOS/ESD 61340-5-1 & 2, the classes of the packaging materials that are used as intimate and proximity packaging to contain electrostatic discharge sensitive device (ESDS) outside ESD protected area (EPA) are classified into four categories. [19] These classes of the packaging materials are presented in Table 2.2.

Table 2.1 Definition of the types of the packaging [19]

Term	Definition
Intimate packaging	Packaging that makes contact with electrostatic discharge sensitive device (ESDS), for example the inner surface of an ESD protective bag.

Table 2.1 (Contd)

Term	Definition
Proximity packaging	Material that is used to enclose one or more devices but not making contact with ESDS. For example the outer surface of an ESD protective bag, or ESD packaging used to contain ESDS already within other packaging.
Secondary packaging	Material that is used primarily to give additional physical protection to the outside of a proximity package. E.g. cardboard boxes, padded bags, polyethylene wrap.

Table 2.2 Definition of the packaging material types [19]

Packaging material	Definition
Low charging	Packaging which has a surface resistance more than 10^6 ohm-square and can be used as intimate packaging for powered ESDS (high ESD sensitive device) and non-powered ESDS (low ESD sensitive device).
Shielding	Packaging which has a surface resistance less than 10^3 ohm-square and can be used as proximity packaging for powered ESDS and non powered ESDS.

Table 2.2 (Contd)

Packaging material	Definition
Conductive	Packaging which has a surface resistance between 10^2 ohm-square and 10^5 ohm-square and can be used as intimate packaging with low charging material for non-powered ESDS.
Dissipative	Packaging which has a surface resistance between 10^5 ohm-square and 10^{11} ohm-square and can be used as intimate packaging for non-powered ESDS or must be used with low charging material for powered ESD.

2.5 Materials, Equipments, and Test Methods

This topic relates to the basic details of the materials that were used in this experiments namely high impact polystyrene (HIPS), coir fiber, and carbon black (CB) along with processing equipments, surface resistivity measurement, and particle size distribution analysis. The details are as follows:

2.5.1 Materials

1. High Impact Polystyrene (HIPS)

High impact polystyrene (HIPS) is synthesized from emulsion polymerization process through grafting polystyrene on polybutadiene or styrene-butadiene rubber for enhancing impact strength in polystyrene. [20] Chemical structure of HIPS is shown in Figure 2.3. [20] HIPS is mainly used for food or electronic

packaging, toys, and housewares due to its high dimensional stability and its excellent abrasive resistance. Physical properties of HIPS are summarized in Table 2.3. [21]

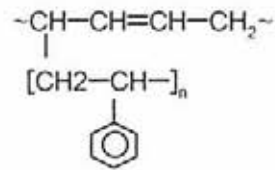


Figure 2.3 Chemical structure of high impact polystyrene.

Table 2.3 Summarizes the physical properties of HIPS

Physical properties	
Tensile modulus (ASTM D638)	270 MPa
Ultimate tensile strength (ASTM D638)	2.76 MPa
Notched Izod impact strength (ASTM D256)	1.61 ft-lb/in
Processing temperature, T_p	180-190°C
Glass Transition Temperature, T_g	93-100°C

2. Coir Fiber

Coir fiber is a hard fiber obtained from the husk of coconut *Cocos nucifera* L. fruit. The coir fiber is one of the hardest natural fibers because of its high content of lignin so coir fiber is applied in different applications such as ropes, matting, basket liners, and many other products. [22] In coir industry, processing steps from husk to coir fiber are shown in Figure 2.4. [23] Chemical compositions of coir fiber are presented in Table 2.1. [22]

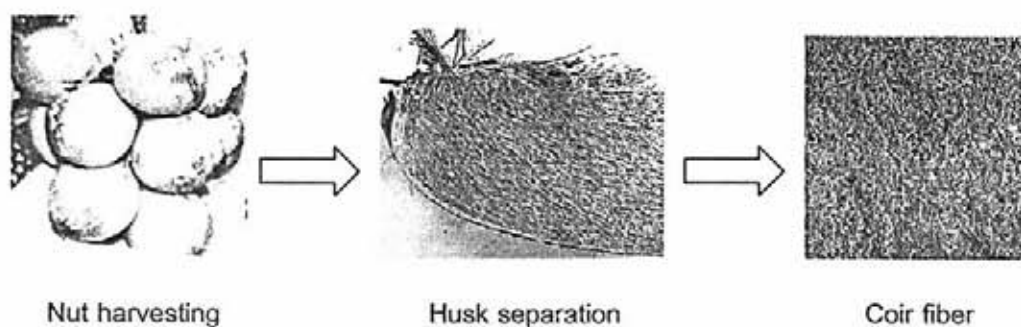


Figure 2.4 Manufacturing steps from coconut husk to coir fiber.

Table 2.4 Chemical compositions of coir fiber

Composition	Weight percentage
Lignin	45.84
Cellulose	43.44
Hemi-Cellulose	0.25
Pectin	3.00
Water soluble	5.25
Ash	2.22

3. Carbon Black (CB)

Carbon black is a black powder or granular substance made by burning hydrocarbons in a limited supply of air. Typically, carbon black is composed of 90-99% of carbon, 0.1-10% of oxygen, 0.2-1% of hydrogen, and less amount of sulfur and ash. [24] Chemical structure of carbon black is shown in Figure 2.5. [25] Carbon black is widely used in the manufacture of automotive tires, color printing ink, painting, and paper; moreover, it is favorably used as conductive filler in rubber and plastic due to its light weight and its permanent conductivity. [2] Properties of some representative conducting carbon blacks are shown in Table 2.5. [2]



Figure 2.5 Chemical structure of carbon black.

Table 2.5 Properties of some representative conducting carbon blacks

Properties	SCF	CF	XCF	Acetylene black
% Volatile	1.6	1.9	1.8	1.1
Bulk density (kg/m ³)	350	340	240	190
Mean particle diameter (nm)	21	23	30	48
N ₂ surface area [k(m ² /kg)]	200	140	250	58
DBP adsorption (cm ³ /100g)	107	100	200	145
Electrical resistivity (Ωm) with 50 phr black in NR	0.24	0.40	0.14	0.40

(SCF= Super Conductive Furnace Black, CF = Conductive Furnace Black, XCF = Extra Conductive Furnace Black)

2.5.2 Processing Equipments

1. Ball Mill

A ball mill, a type of crusher, is a cylindrical device used to grind or mix materials like ores, chemicals, ceramics, and paints. Ball mill rotates around a horizontal axis, partially filled with the material to be ground plus the grinding medium. Different materials are used for media, including ceramic balls, flint pebbles, and stainless steel balls. An internal cascading effect reduces the material to a fine powder. Good ball mill can grind mixture as small as 0.0001 mm. [26]

2. Twin Screw Extruder

Twin screw extruder (TSE) is one of the most important equipments for polymer processing, which is used mainly for blending and compounding operations. The equipment utilized in the TSE process basically consists of an extruder with two screws, typically fully intermeshing (Figure 2.6). Feeder is attached to the barrels for accurately controlling the addition of liquid or solid ingredients to the process. Proper configuration of screw elements can result in higher homogeneous of mixing compound. [27]

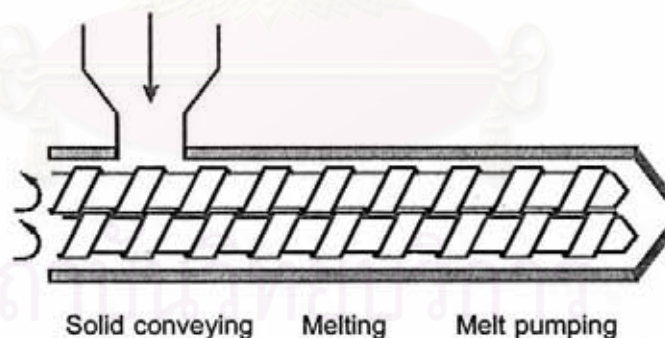


Figure 2.6 Intermeshing twin screw extruder.

3. Compression Molding

Compression molding is a process of applying heat and pressure to a plastic resin in matched dies. The resin melts due to the heat and then the pressure causes it to form into a desired shape. This is done in a compression molding press. Mainly application of compression molding is used for molding thermoset materials; however, thermoplastic materials can also be used in the compression molding process. The compression molding process is shown in Figure 2.7. [28]



Figure 2.7 Compression molding process.

2.5.3 Surface Resistivity Measurement

Surface resistivity is defined as the electrical resistance of the surface of an insulator material. It is measured from electrode to electrode along the surface of the insulator sample. Since the surface length is fixed, the measurement is independent of the physical dimensions (i.e., thickness and diameter) of the insulator sample. [29]

Electrometer is the equipment to determine surface resistivity of the insulator. Surface resistivity is measured by applying a voltage potential across the surface of the insulator sample and measuring the resultant current as shown in Figure 2.8. [29]

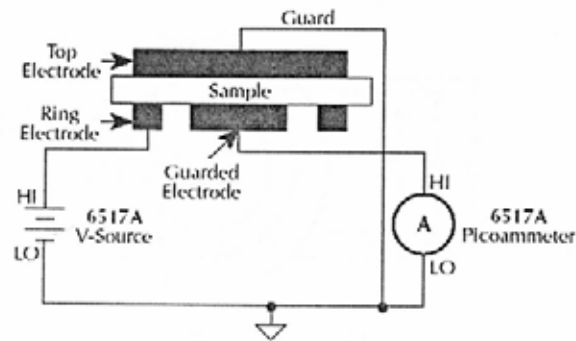


Figure 2.8 Surface resistivity measurement technique.

The following calculation of the surface resistivity that is automatically performed from the electrometer is displayed as follows:

$$\rho_s = K_s R \quad \text{-----} \quad (2.1)$$

ρ_s = surface resistivity (ohm per square)

R = measured resistance in ohms (V/I)

$K_s = P/g$

Where:

P = the effective perimeter of the guarded electrode (mm)

g = distance between the guarded electrode and the ring electrode (mm). Refer to Figure 2.9 to determine dimension g .

For circular electrodes:

$$P = \pi D_o \quad \text{-----} \quad (2.2)$$

$$D_o = D1 + g \text{ (refer to Figure 2.9 to determine dimension } D_o\text{)}. \quad \text{---} \quad (2.3)$$

สถาบันวิทยบริการ
จุฬาลงกรณ์มหาวิทยาลัย

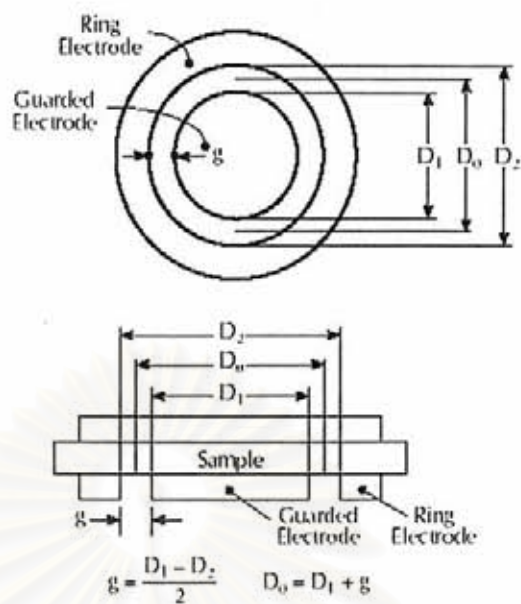


Figure 2.9 Circular electrode dimensions.

Classification of materials based on surface resistivity (Ohm/Square) is shown in Table 2.6. [7]

Table 2.6 Classification of materials based on surface resistivity (Ohm/Square)

Material	Surface Resistivity
Metal	$< 10^{-4}$
Pure compressed carbon black	$10^{-4} - 10^0$
Conductive composite	$10^0 - 10^5$
Static dissipative	$10^5 - 10^9$
Antistatic	$10^9 - 10^{12}$
Plastics (Insulators)	$10^{12} - 10^{18}$

2.5.4 Particle Size Distribution Analysis (Low Angle Laser Light Scattering (LALLS) Technique) [30]

Particle size distribution analysis using low angle laser light scattering (LALLS) technique can determine particle size distribution information between 0.05-3480 μm . The LALLS technique can analyze particle size distribution of samples in powder, liquid, emulsion, suspension, and aerosol forms. This technique is passing He-Ne laser beam through sample and detecting light intensity that scatters from particle at low angle (comparison with line of laser beam). The light that scatters from particles with different sizes has a variety of angles. Measurement and calculation of light intensity to class size of particle at different angles are determined by using Mie theory. Schematic of LALLS technique is illustrated in Figure 2.8

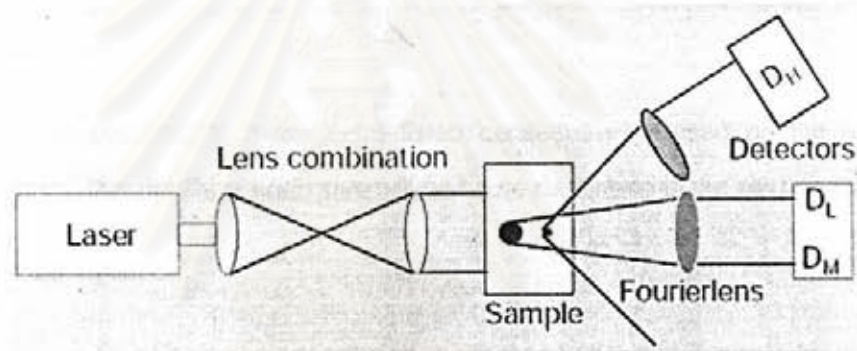


Figure 2.8 Schematic of LALLS technique.

สถาบันวิทยบริการ
จุฬาลงกรณ์มหาวิทยาลัย

CHAPTER III EXPERIMENTS

3.1 Materials

3.1.1 High impact polystyrene (HIPS) was used as a matrix. It was provided by Dow Chemical Thailand Ltd., under the trade name of Styron 486M. Its melt flow index and density were 3 g/10 min and 1.04 g/cm³, respectively.

3.1.2 Carbon black (CB) was used as a conductive filler to enhance the electrical conductivity of polymer composites. It was supplied by JJ-Degussa Chemicals (T) Ltd., under the trade name of Printex XE 2B. Its DBP (dibutylphthalate) absorption and its BET (Brunauer, Emmett, and Teller) were 380 ml/100 g and 95 m²/g, respectively.

3.1.3 Coir fibers were used as a filler and purchased from Jatujuk Market.

3.2 Equipments

The equipments below were listed consecutively based on the experimental procedure. The details of each step will be future described in the next section.

3.2.1 Attritor

Coir fibers were grinded in an attritor as shown in Figure 3.1.



Figure 3.1 Attritor.

3.2.2 Ball Mill

The premixing of the components of the composites was done in a ball mill presented in Figure 3.2.

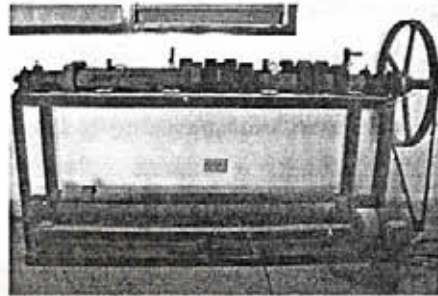


Figure 3.2 Ball Mill.

3.2.3 Particle Size Distribution Analyzer

A Mastersizer S long Bed Version 2.11 (Figure 3.3) was used to measure particle size distribution of ground coir fiber after passing through a 50 mesh sieve (coir filler) and carbon black separated from the premix (HIPS/5CB) after premixing with in a ball mill.



Figure 3.3 Mastersizer S long Bed Version 2.11.

สถาบันวิจัยและพัฒนา
จุฬาลงกรณ์มหาวิทยาลัย

3.2.4 Twin Screw Extruder

After premixing, the composites were compounded, extruded, and pelletized by a Thermo PRISM co-rotating twin screw extruder model TSE-16-TC (Figure 3.4).



Figure 3.4 Thermo PRISM co-rotating twin screw extruder model TSE-16-TC.

3.2.5 Compression Molding

The compounded pellets were pressed by a Lab Tech model LP-S-50 (Figure 3.5).



Figure 3.5 Lab Tech model LP-S-50.

3.2.6 Electrometer

A Keithley Electrometer 617 based on contacts in sandwich configuration (Figure 3.6) was utilized for measuring the electrical surface resistivity of all composites.



Figure 3.6 Keithley Electrometer 617 based on contacts in sandwich configuration.

3.2.7 Tensile Testing Machine

Tensile properties of the composite samples were measured by a LLOYD Universal Testing Machine model LR 100K plus (Figure 3.7), according to the ASTM D638.

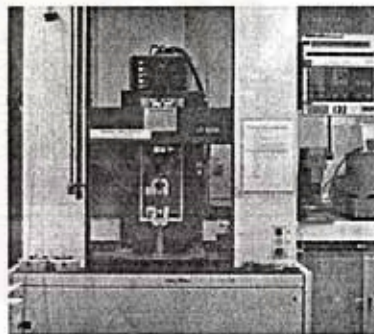


Figure 3.7 LLOYD Universal Testing Machine model LR 100K plus.

สถาบันวิทยบริการ
จุฬาลงกรณ์มหาวิทยาลัย

3.2.8 Flexural Testing Machine

Flexural properties of the composite samples were carried out by a LLOYD Universal Testing Machine model LR10K (Figure 3.8), according to the ASTM D790.



Figure 3.8 LLOYD Universal Testing Machine model LR10K.

3.2.9 Impact Tester

Impact tests of the composite samples were performed by a Zwick 5102 Pendulum Impact tester (Figure 3.9), according to the ASTM D256.



Figure 3.9 Zwick 5102 Pendulum Impact tester.

สถาบันวิศวกรรม
จุฬาลงกรณ์มหาวิทยาลัย

3.2.10 Thermogravimetric Analyzer (TGA)

Thermal degradation temperature (T_d) of coir filler was determined by a METTLER TOLED model TGA/SDTA 851[®] (Figure 3.10) under nitrogen atmosphere.



Figure 3.10 METTLER TOLED model TGA/SDTA 851[®].

3.2.11 Scanning Electron Microscope (SEM)

Fractured surfaces of the impact test specimens and the morphology of the coir filler and carbon black were observed with a Jeol JSM – 5410LV scanning electron microscope (Figure 3.11) at acceleration voltage of 15 KV. In addition, the morphology of the composites specimens before mechanical testing and of the coir fiber before grinding were also investigated by fracturing the specimens after 40 min and 10 min of immersion in liquid nitrogen, respectively. All the specimens were sputter-coated with gold prior to being examined.



Figure 3.11 Jeol JSM – 5410LV scanning electron microscope.

3.3 Methodology

Flow chart of the entire manufacturing process is shown below in Figure 3.12.

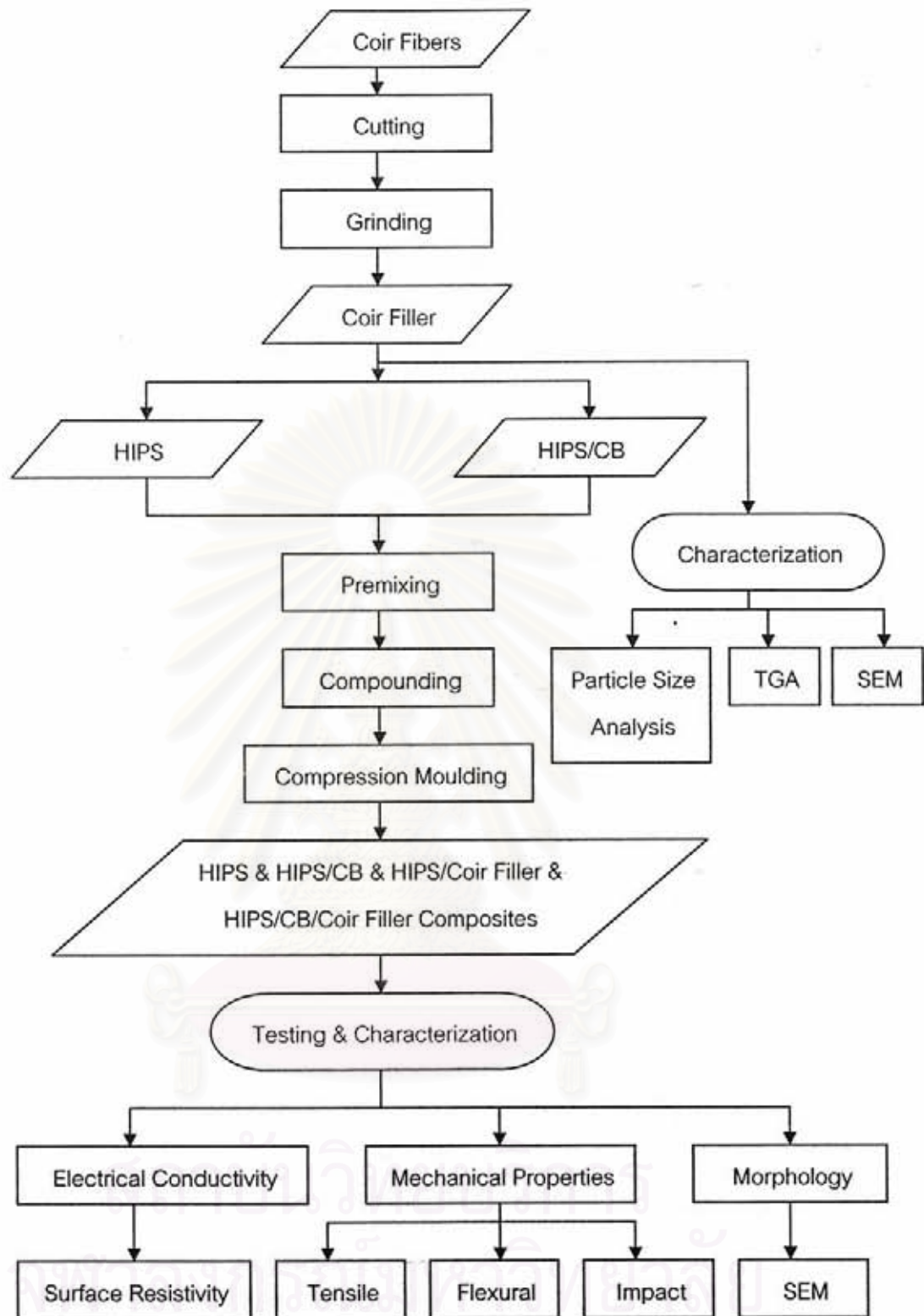


Figure 3.12 Flow chart of the manufacturing process.

3.3.1 Preparation of Filler from Coir Fibers

The first step was to remove moisture from raw material by placing coir fibers under sunlight for 2-3 days. After that the coir fibers were cut into small pieces with approximate length of 2-3 mm. Then, small pieces of coir fibers were oven-dried at 70°C for 24 h. Next, the dried coir fibers were ground by an attritor for 3 min per 2.5 g of the dried coir fibers. After grinding, the ground coir fibers were screened to remove excess particles or fibers through sieve number 50 mesh. Finally, the samples (coir filler) were kept in an electric desiccator prior to being used.

3.3.2 Preparation of the Composites

All of the composites (high impact polystyrene/ carbon black, high impact polystyrene/coir filler, and high impact polystyrene/carbon black/coir filler composites) were prepared by premixing the components of each composite in a ball mill containing alumina ball (diameter 10 mm) for 1 h. After that, the composites were oven-dried at 70°C overnight prior to mixing in a twin screw extruder. Formula of the composites are tabulated in Table 3.1.

In mixing process, the premix was proceeded on a twin screw extruder with the rotor speed of 20 rpm. The processing temperatures were 160, 190, 195, 200, and 205°C according to 5 zones of the extruder, respectively. After mixing, the extrudate was cooled in water, palletized, and dried.

Finally, the compounded pellets were molded into sheets by a compression moulding after drying in an oven at 70°C overnight. The molding temperature and pressure were set at about 205°C and 10 tons, respectively. The compounded pellets were preheated for 5 min and then pressed for 5 min before cooled down to 40°C. The composite sheets were used for surface resistivity measurement, mechanical properties testing, and morphological investigation.

Table 3.1 Formula (phr) of the composites

Batch	HIPS	Carbon Black	Coir Filler
1.	100	-	-
2.	100	1	-
3.	100	3	-
4.	100	5	-
5.	100	7	-
6.	100	9	-
7.	100	-	1
8.	100	-	3
9.	100	-	5
10.	100	-	7
11.	100	-	9
12.	100	-	11
13.	100	-	13
14.	100	-	15
15.	100	5	1
16.	100	5	3
17.	100	5	5
18.	100	5	7
19.	100	5	9
20.	100	5	11
21.	100	5	13
22.	100	5	15

3.3.3 Characterization of Coir Fiber, Coir Filler, and Carbon Black

3.3.3.1 Morphological Studies

The morphology of the coir filler and carbon black were investigated with a Jeol JSM – 5410LV scanning electron microscope at acceleration voltage of 15 KV in order to study shape and size of the coir filler and carbon black. In addition, the morphology of the coir fiber before grinding was also investigated by fracturing the fiber after 10 min of immersion in liquid nitrogen. All the specimens were sputter-coated with gold prior to being examined.

3.3.3.2 Particle Size Distribution Analysis (Low Angle Laser Light Scattering (LALLS) Technique)

Particle size distribution analyzer using He-Ne laser and Low Angle Laser Light Scattering (LALLS) technique for determining particle size distribution information between 0.05-3480 μm was used to measure particle size distribution of the coir filler and carbon black. For particle size distribution measurement of the coir filler, few amount of surfactant was dropped on coir filler before testing to decrease surface tension of the filler. After that, the coir filler was incorporated into 150 ml of toluene which was used as a dispersing medium, and then the suspension was stirred to facilitate wettability of the coir filler in the medium. Finally, He-Ne gas laser was projected through the suspension and the particle size was analyzed. Likewise, particle size distribution of carbon black was determined through the same method while using water as a dispersing medium. In these tests, the particle size distribution measurement of both coir filler and carbon black was reproduced three times and the results were then reported as an average value determining from these 3 measurements.

3.3.3.3 Thermal Properties

Thermogravimetric analyzer (TGA) was used to examine thermal degradation temperature (T_d) of coir filler. Coir filler of approximately 3.34 mg was heated with a heating rate of 10°C/min from 50°C to 900°C under nitrogen atmosphere.

3.3.4 Characterization of the Composites

3.3.4.1 Electrical Properties

Surface resistivity measurements, using silver paint electrode, were performed, according to the ASTM D 257. Square test specimens with dimensions of 3 inch wide, 3 inch long, and 3.2 mm thick were tested using a constant voltage of 500 V. One specimen of each sample was tested by measuring at five times and the results were averaged from five values to obtain a mean value. The specimens were left at the temperature 23°C and 50 % relatively humidity for 48 hrs before tests.

3.3.4.2 Mechanical Properties

Tensile tests of dumbbell shaped specimens were conducted using a crosshead speed of 50 mm/min and a gauge length of 65 mm, according to the ASTM D638. Flexural tests were performed by using three point bending mode according to the ASTM D790. Rectangular test specimens with dimensions of 25 wide, 80 mm long, and 3.2 mm thick were tested using a crosshead speed of 10 mm/min and a span length of 50 mm. Impact tests were performed according to the ASTM D256 test method by izod pendulum. The specimens with dimensions of 12.70 mm wide, 60.30 mm long, and 3.2 mm thick were notched. All tests were carried out at 25°C. At least five specimens of each composites were tested and the results were averaged to obtain a mean value.

3.3.4.3 Morphological Studies

Scanning electron microscope (SEM) at acceleration voltage of 15 KV was used to study the fractured surfaces of the specimens in order to understand the electrical conductivity of the composites. The fractured surfaces of the specimens were prepared by fracturing in liquid nitrogen after 40 min of immersion in liquid nitrogen and then coated with gold before being scanned. In addition, the fractured surfaces of the composites after impact tests were also examined by coating with gold before being scanned in order to understand the failure mechanism of the composites under the presence of carbon black and coir filler. The morphology such as phase structure, dispersion, and adhesion of the components were investigated.

CHAPTER IV

RESULTS AND DISCUSSION

4.1 Characterization of Raw Materials

4.1.1 Morphological Studies of Coir Fiber, Coir Filler, and Carbon Black

Morphology of coir fiber, coir filler, and carbon black is illustrated by SEM micrographs in Figure 4.1, 4.2, and 4.3, respectively. For the morphology of the coir fiber, it was observed that some positions of fiber surface were non-smooth due to the appearance of several coir scales protruding from the fiber surface. In addition, small voids distributing around the fiber surface can be noticed. However, as shown in Figure 4.1 (b), smooth surface of the coir fiber without the coir scales or the protrusions can also be observed.

As presented in Figure 4.1 (c), the cross section of fractured surface of the coir fiber showed that its diameter was approximately 200 μm . At high magnification (Figure 4.1 (d)), the fractured surface of the coir fiber revealed that the coir fiber consisted of numerous fiber cells which had an oval cross section joining together in the coir fiber. As shown, the fiber cells had average diameter of approximately 10 μm with a relatively large lumen. In addition, the coir fiber also composed of middle lamellae (a pectin-rich layer acting as a glue to hold the fiber cells together) between the fiber cells. It has been reported that the middle lamellae and cell walls of the coir fiber have high content of lignin resulting in high stiffness and toughness properties of the coir fiber. [23]

The SEM micrographs of the coir filler are illustrated in Figure 4.2. As shown in Figure 4.2 (a), the ground coir fiber screened through a 50 mesh sieve with diameter less than 297 μm exhibited a variety of shapes and sizes. Some fiber particles exhibited a larva-like structure with an approximate length of 270 μm (Figure 4.2 (b)), while the others showed a particulate shape having all its dimension nearly equal with an approximate diameter of 130 μm (Figure 4.2 (d)). However, the majority of the coir filler seemed to have its diameter less than 50 μm . Higher magnifications of both particles (Figure 4.2 (c) and (e)) showed the rifts surrounding the surfaces of both particles and the coir scales protruding from their surfaces. These results indicated that vibrational

forces applying from the attritor during preparation can break up and reduce the coir fiber into the particles having different shapes and sizes.

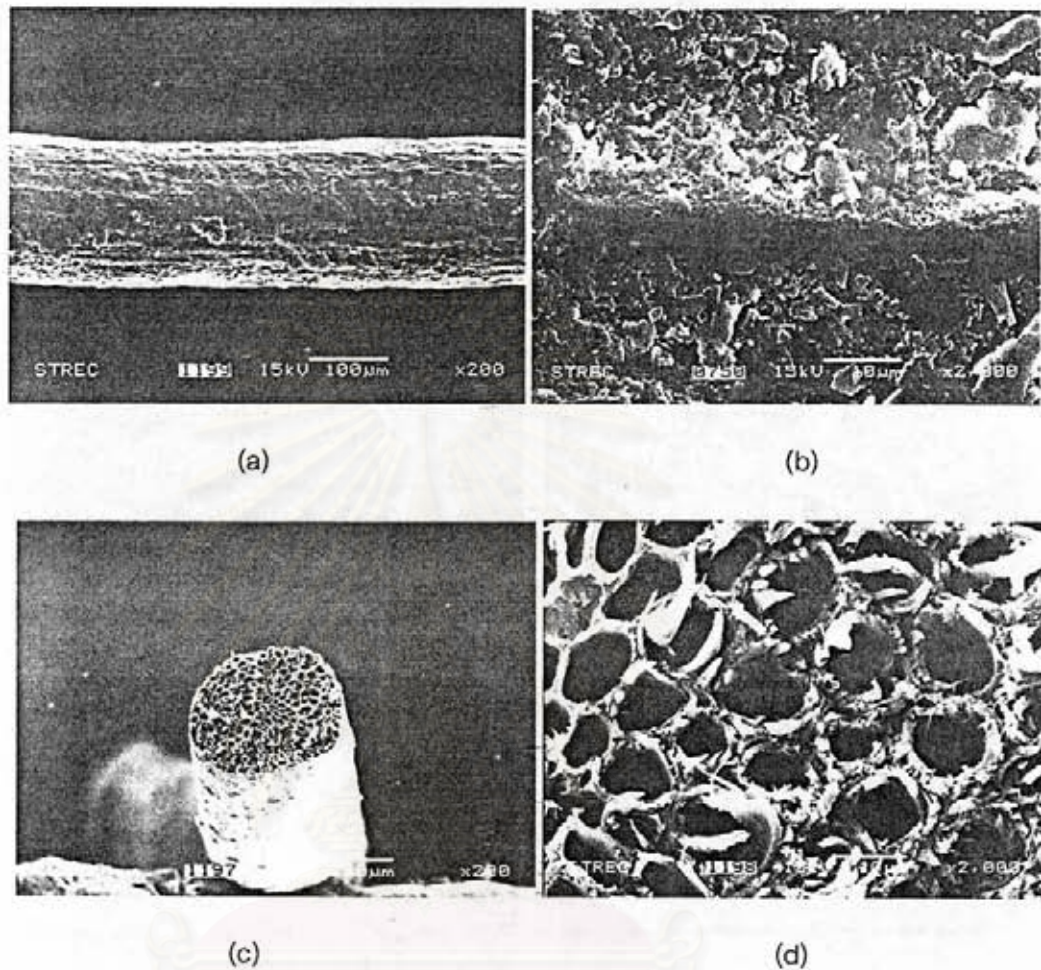


Figure 4.1 SEM micrographs of (a) lengthwise section of coir fiber at low magnification (magnification : 200 x, scale bar 100 μm); (b) lengthwise section of coir fiber at high magnification (magnification : 2,000 x, scale bar 10 μm); (c) fractured surface of coir fiber at low magnification (magnification : 200 x, scale bar 100 μm); and (d) fractured surface of coir fiber at high magnification (magnification : 2,000 x, scale bar 10 μm).

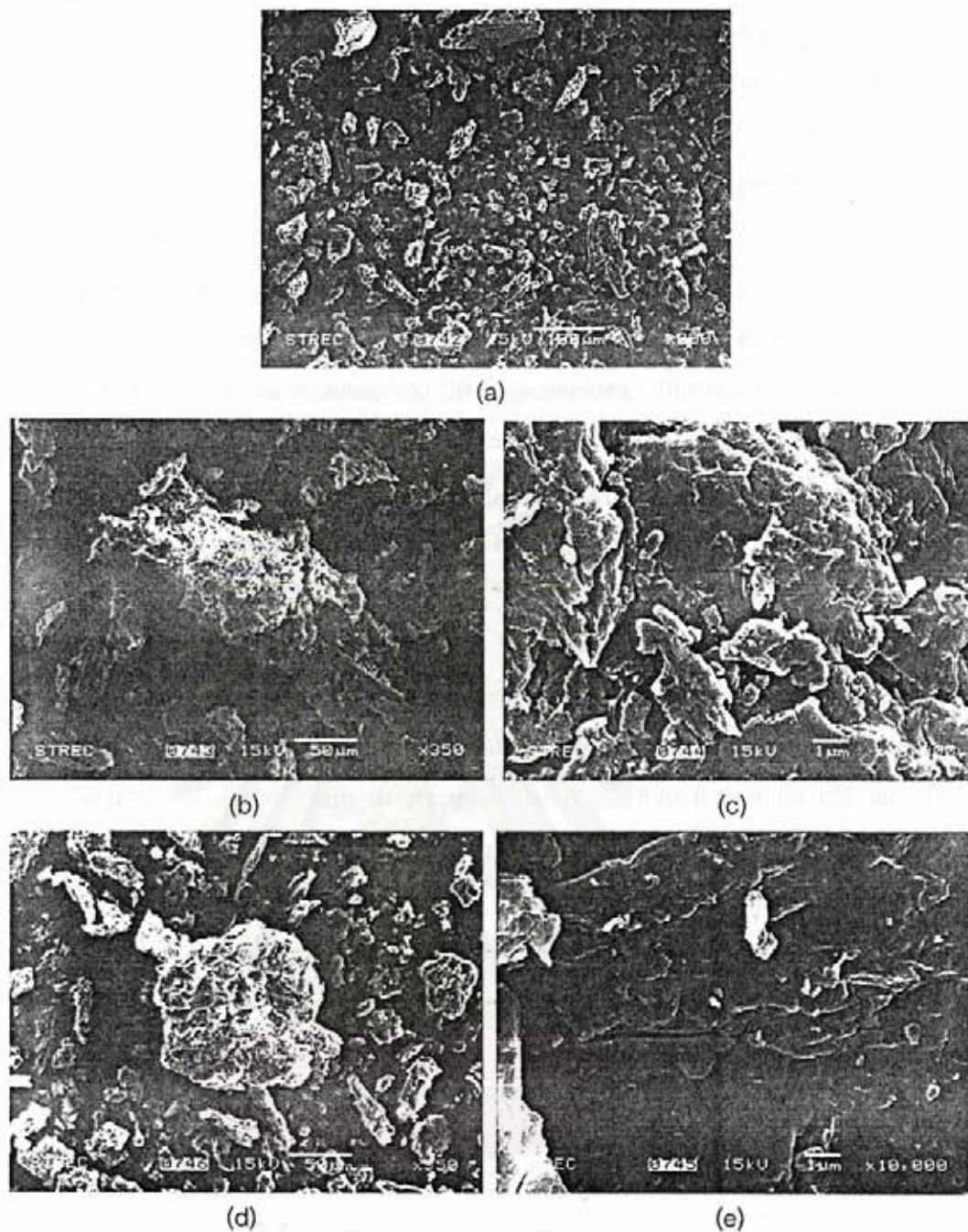
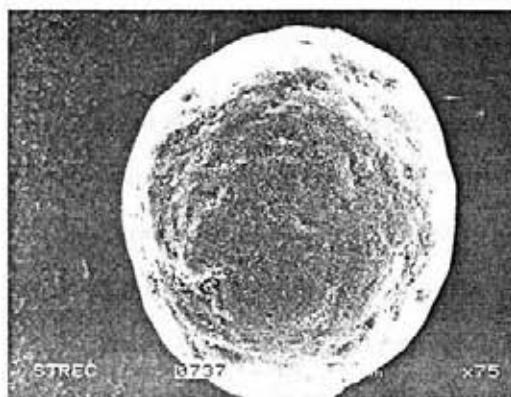
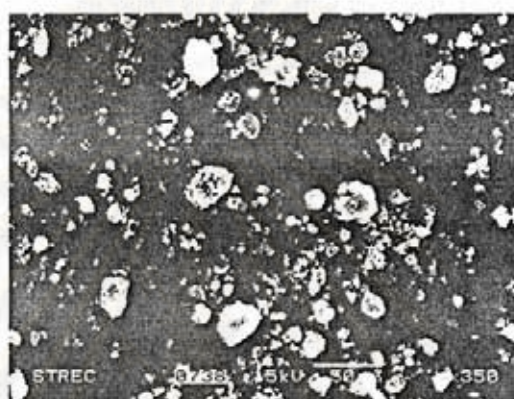


Figure 4.2 SEM micrographs of (a) coir filler (magnification : 200 x, scale bar 100 μm); (b) a lava-like structure of fiber particle (magnification : 350 x, scale bar 50 μm); (c) surface of the lava-like structure particle (magnification : 10,000 x, scale bar 1 μm); (d) a particulate shape of fiber particle (magnification : 350 x, scale bar 50 μm); and (e) surface of the particulate particle (magnification : 10,000 x, scale bar 1 μm).

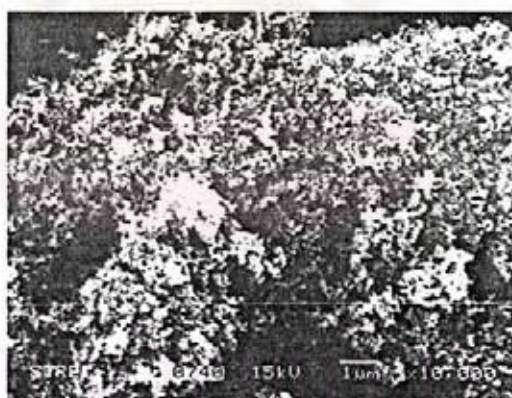
In view of morphology of carbon black, carbon black pellet with its diameter of approximately 1 mm (before premixing in a ball mill) is shown in Figure 4.3 (a). It was noted that size of carbon black pellets generally fall between 0.1-1 mm to facilitate the ease of handling and to reduce the creation of dust. [31] After premixing in a ball mill, however, the SEM micrograph of carbon black presented in Figure 4.3 (b) showed that the agglomerate structure of carbon black creating from cluster of the carbon black aggregates was occurred. This indicated that premixing of carbon black in a ball mill can break up carbon black pellets into CB agglomerates. This result can be explained that the carbon black pellets were reduced into the aggregates during mixing; however, strong electrical forces maintaining the bond between the aggregates promoted the formation of the agglomerates (adhering of hundred to thousands of the aggregates). [31] Typically, the size of CB agglomerates was on a scale of 1-100 μm or larger than 100 μm and that of the CB aggregates was between 85-500 nm. [31] As illustrated in Figure 4.3 (c), higher magnification of the CB agglomerates revealed that the CB agglomerate was created from a great number of aggregates consisting of extremely small CB particles with the diameter of approximately less than 0.1 μm (or 100 nm). This result is in good agreement with J. Donnet and coworkers that the size of CB particles generally falls in a range of 15-300 nm. [32] For particle size distributions, the low angle laser light scattering (LALLS) technique was used to measure the size distributions of both coir filler and carbon black and the results were presented in the following section.



(a)



(b)



(c)

Figure 4.3 SEM micrographs of (a) carbon black pellet (magnification : 75 x, scale bar 200 μm); (b) carbon black agglomerates at low magnification (magnification : 350 x, scale bar 50 μm); and (c) carbon black agglomerates at high magnification (magnification : 10,000 x, scale bar 1 μm).

4.1.2 Particle Size Distribution of Coir Filler and Carbon Black

As noted earlier, particle size distributions of the coir filler and carbon black were determined by LALLS technique which can measure particle size in a range of 0.05–3,480 μm [30]. Analysis result of the particle size distribution through this technique indicated that the particle size of the coir filler distributed between 0.05–500 μm and had an average diameter of 58.50 μm (as seen in Appendix A). As presented in Figure 4.4, it revealed that the particle of coir filler with diameter less than 50 μm showed the highest volume percentage (~ 68.38%) as compared with the particles of coir filler with diameter larger than 50 μm . For the particles of the coir filler with diameter of larger than 297 μm , it can be suggested that these particles may be a hard segment of fiber with thin and long shape which can not be ground into a small particle by the attritor; as a result, these thin and long particles can pass through a 50 mesh sieve with diameter less than 297 μm and found in a very low volume percentage. When the light was projected through lengthwise section of the hard segment suspending in the medium, the detector detected light intensity that scattered from the lengthwise section of the hard segment and calculated light intensity with other factors as diameter using Mie theory; similarly, if the hard segment showed its cross section to the light projecting through it, the detector also detected light intensity that scattered from the cross section of the hard segment and calculated light intensity with other factors as diameter.

In case of carbon black, after premixing, the carbon black was brought to measure the particle size distribution by LALLS technique without sieving. It was found that the particle size of carbon black distributed in a range of 0.2–400 μm and had an average diameter of 15.62 μm (as seen in Appendix A). As demonstrated in Figure 4.4, similar to the coir filler, the particle of carbon black with diameter less than 50 μm exhibited the highest volume percentage in comparison with the particles of carbon black having diameter larger than 50 μm . These results revealed that most of the carbon black (after premixing) was in the form of agglomerate structure.

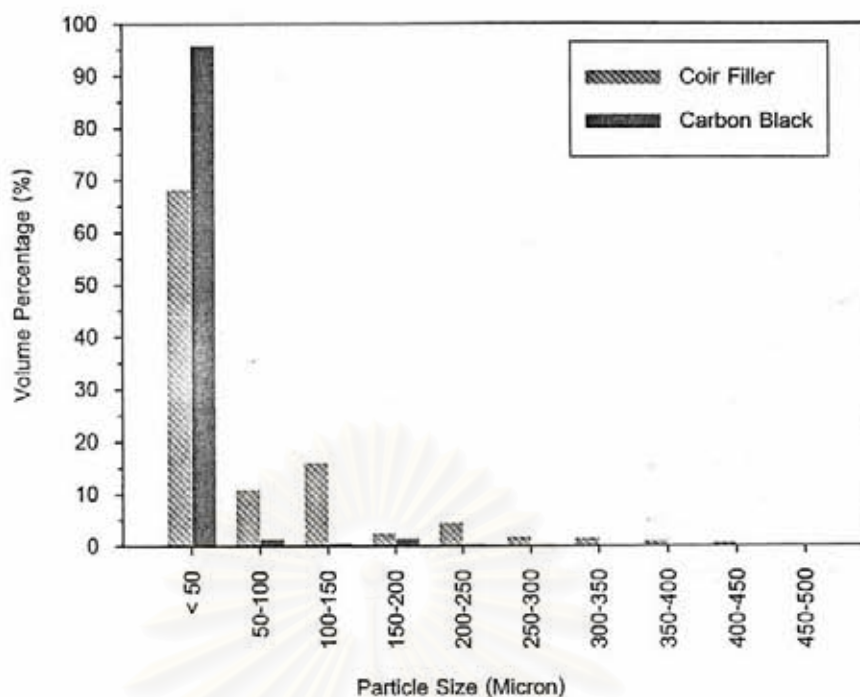


Figure 4.4 Volume percentages of coir filler and carbon black.

4.1.3 Thermal Properties of Coir Filler

To approach suitable processing temperature in mixing processes of coir filler/HIPS and coir filler/HIPS/CB composites, it was necessary to determine the degradation temperature of coir filler by TGA technique. Weight loss of coir filler as a function of temperature (TGA thermogram) and its derivative thermogram were shown in Figure 4.5.

As presented in Figure 4.5, the TGA thermogram exhibited two steps of weight loss as a function of temperature. The first step of weight loss occurred below 100°C was due to the gradual evaporation of moisture and the second step of weight loss displayed approximately at 260-360°C was a result of the thermal degradation of three major components of coir filler namely alpha-cellulose, hemi-cellulose, and lignin. It has been reported that thermal decomposition of lignocellulosic filler was in the range of 150-500°C as a consequence of thermal degradation of hemi-cellulose between 150 and 350°C, decomposition of alpha-cellulose between 275 and 350°C, and mass loss of

lignin between 250 and 500°C. [33] Therefore, with regard to the thermal decomposition of coir filler, it can be concluded that the second step of weight loss of coir filler between 260-360°C was attributed to the thermal decomposition of alpha-cellulose, hemicellulose, and lignin. These results can be confirmed by considering the derivative curve of the TGA thermogram. It can be seen that the degradation temperature of coir filler in the range of 260-360°C showed two peaks of weight decrease at approximately 290°C and 330°C, respectively. Therefore, weight decrease of coir filler at 290°C might represent the decomposition of alpha-cellulose and/or hemicellulose and weight decrease of coir filler at 330°C might be associated with the degradation of lignin. With a further rise in temperature to 800°C, the coir filler continuously degraded and showed charring reaction until the end of the experimental leaving remained char residue.

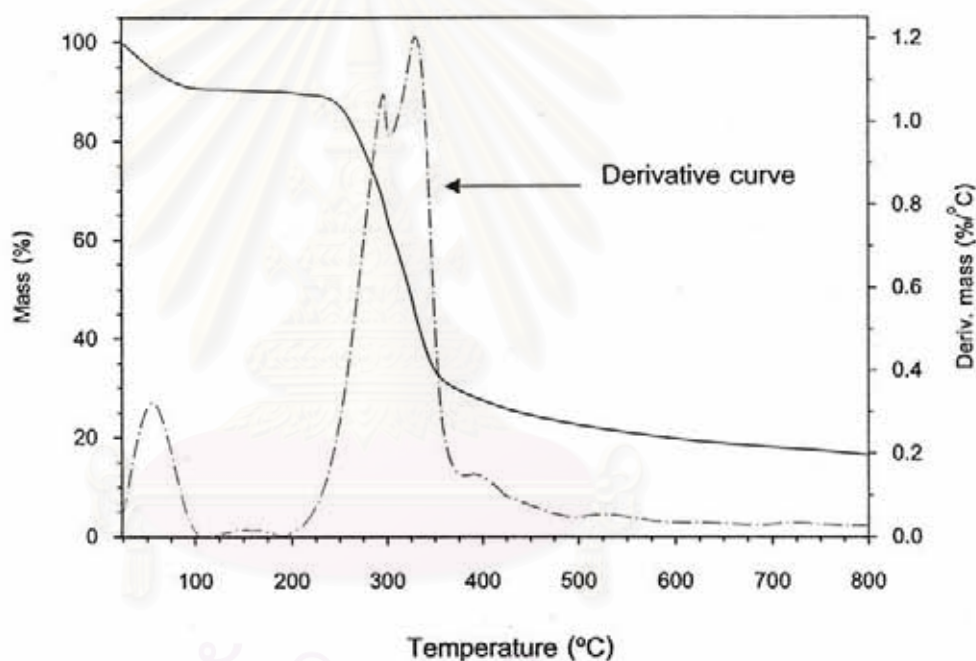


Figure 4.5 TGA thermogram of coir filler.

4.2 Surface Resistivity and Morphology of the Composites

4.2.1 Surface Resistivity of the Composites

4.2.1.1 Effect of CB Content

Logarithm of surface resistivity of the composites as a function of CB and coir filler contents was presented in Figure 4.7 (a) and (b), respectively. As shown in Figure 4.7 (a), pure HIPS had the surface resistivity value of $\sim 10^{16}$ ohm/square which can be classified as an insulating material having the resistivity greater than 10^{12} ohm/square. However, it can be seen that the incorporation of CB in the HIPS matrix resulted in the alteration of the surface resistivity of the composites. Although at low CB loading of 1 and 3 phr both composites showed surface resistivity values of $\sim 10^{16}$ ohm/square which were still in the insulating range. This result indicated that the resistivity of the composites was not dependent on the low quantity of CB. However, when CB loading was increased to 5 phr, the surface resistivity of the composite was sharply decreased to 10^7 ohm/square which could be designated as a static dissipative composite having the surface resistivity in the range of 10^5 - 10^9 ohm/square. Based on this result, it can be stated that the rapid drop of the resistivity represented the drastic transition of the composite from insulator to conductor. In addition, this result suggested that HIPS/CB composite reached the percolation threshold at CB loading of ~ 5 phr. Above the critical content of CB, the surface resistivity values of the composites were slightly decreased when CB content increased.

The decrease in the resistivity of the composites with the addition of CB above 5 phr can be explained by the percolation theory. The conduction through the bulk of the compound was controlled by a number of paths (the aggregate chains). As the number of particles increased, the number of continuous chain or conductive path through the compound increased. The total resistance for any chain consisted of the sum of individual resistance at each point of contact. If the resistance at each point of contact remained constant, the resistivity of the composite followed the form

$$\rho = \rho_0(\phi - \phi_c)^{-t} \quad (4.1)$$

Where ρ is the resistivity of the composite, ρ_0 is a scale factor, ϕ is the volume fraction of filler, ϕ_c is the volume fraction of filler at the percolation point, and t is a geometric factor. The value t commonly is 1.6-2. [34]

From the equation, it can be described that the resistivity of the composite depended on the volume fraction of filler (ϕ). When the volume fraction of filler increased, the resistivity of the composite (ρ) was decreased. In other words, it can be stated that the electrical conductivity of the composite was increased with increasing the conductive filler loading (above the critical CB content). Accordingly, the resistivity of the composites was decreased at CB content greater than critical value (5 phr).

4.2.1.2 Effect of Coir Filler Content

Logarithm of surface resistivity of the composites as a function of coir filler content was shown in Figure 4.6 (b). For HIPS/coir filler composites, it can be seen that the surface resistivity values of all composites were $\sim 10^{15}$ ohm/square which were less than that of pure HIPS. However, the incorporation of coir filler in the HIPS matrix did not lead to a significant change in the surface resistivity of the composites. Their surface resistivity values were still in the range of an insulating material. The decrease in the surface resistivity values of the composites, compared with pure HIPS, may be due to the moisture containing in the coir filler.

Regarding to HIPS/CB/coir filler composites, the amount of CB adding into the composites was fixed at 5 phr whereas different contents of coir filler were varied. This is because CB loading of 5 phr was the lowest amount to promote conductive properties of HIPS/CB composite; it might be suitable to maintain a balance between cost effective, electrical conductivity, and mechanical properties of the composites. As seen in Figure 4.6 (b), it can be noticed that at low coir filler loading of 1 and 3 phr the surface resistivity values of the composites were within the same range to that of HIPS/5CB composite. When coir filler loading was increased to 5-9 phr, the surface resistivity of the composites tended to decrease slightly. At coir filler loading of 11-15 phr, the resistivity values of the composites were gradually increased.

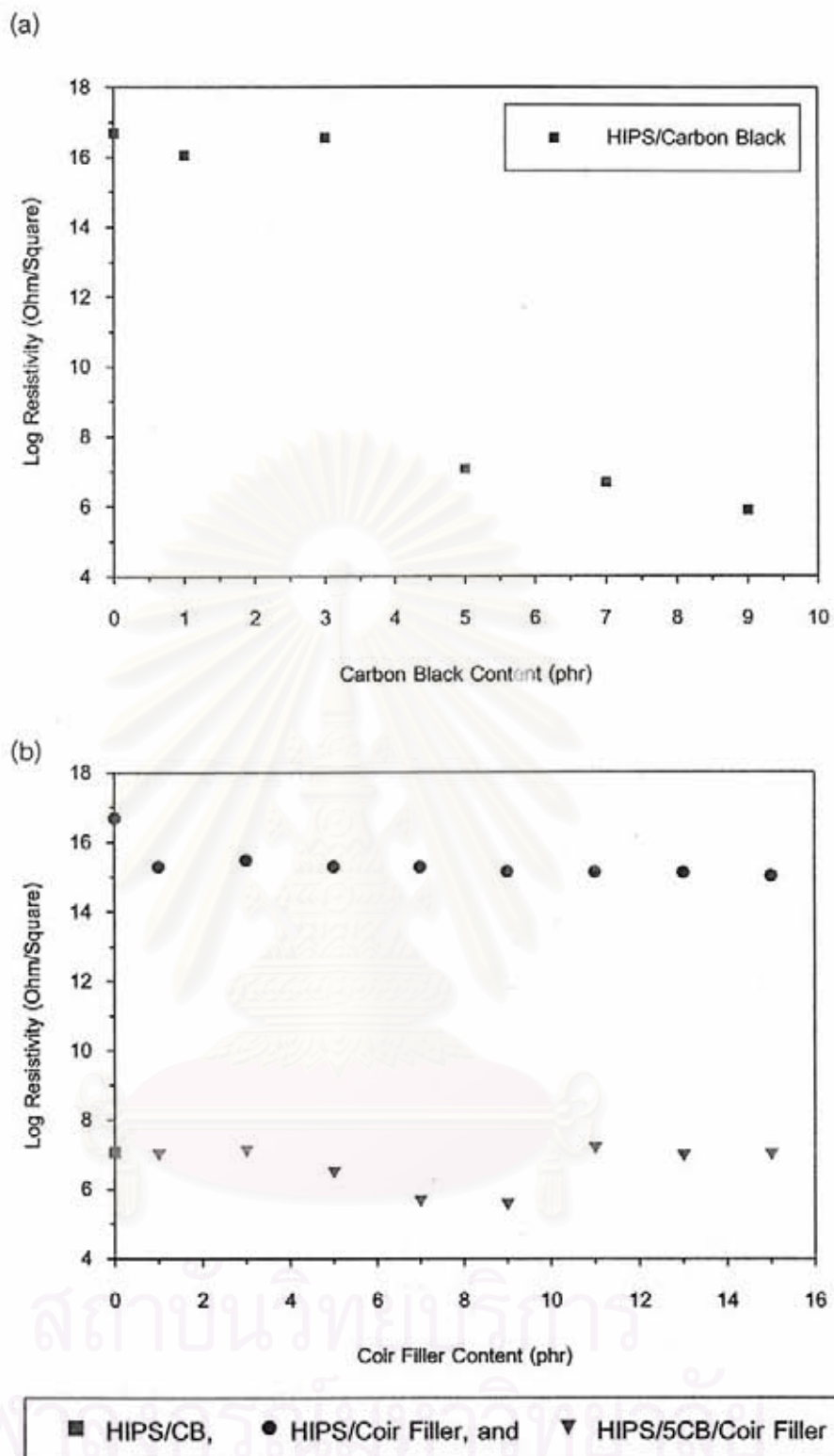


Figure 4.6 Logarithm of surface resistivity of (a) HIPS/CB composites as a function of CB content and (b) HIPS/5CB, HIPS/coir filler, and HIPS/5CB/coir filler composites as a function of coir filler content.

These results can be explained that for HIPS/coir filler composites, despite the fact that coir filler was an insulating filler [35], the addition of insulating coir filler did not increase the surface resistivity of the insulating composites. In case of HIPS/CB/coir filler composites, the conductive properties of the three-phase composites resulted from the presence of the conductive CB while the addition of insulating coir filler did not change the conductive composites into the insulator. In addition, the incorporation of coir filler loading, in particular at 5-9 phr, tended to increase the electrical conductivity of the three-phase composites gradually.

4.2.2 Morphology of the Composites

It has been established that electrical conductivity of CB-filled single polymer composites depended on several factors such as CB contents, polymer properties, and processing parameters. These factors also affected on morphology of the conductive composites. [5,10] Accordingly, in this work morphology of the conductive composites was taken in order to study their electrical conductivity.

4.2.2.1 Effect of CB Content

SEM micrographs of freeze-fractured surfaces of pure HIPS and HIPS/CB composites are illustrated in Figure 4.7 (a-b) and (c-f), respectively. As shown in Figure 4.7 (b), smooth surface of pure HIPS was observed at high magnification. In addition, it can be seen that polybutadiene rubber phase was randomly distributed as dark circles on the fractured surface. These results are in good agreement with the literature [35].

In case of HIPS/CB composites, at low magnification HIPS/3CB composite (Figure 4.7 (c)) showed numerous white spots distributing in the matrix. As illustrated in Figure 4.7 (d), higher magnification revealed that these white spots represented the CB aggregates and/or the CB particles dispersing uniformly in the HIPS matrix. Some CB agglomerates can also be observed. This result suggested that high mixing efficiency of low mixing speed (20 rpm) was a significant factor that led to break up and reduce CB agglomerates into the CB aggregates and/or the CB particles. Since low CB loading of 3 phr was incorporated in the matrix, the distance between CB was far apart. As a result, the electrical conductive path was discontinuous due to a very less amount and

hence disabled to facilitate the electrical conduction through the matrix. Accordingly, the surface resistivity of this composite was still in the insulating range.

In contrast, for HIPS/5CB composite, white spots can no longer be observed in the matrix (Figure 4.7 (e)). As presented in Figure 4.7 (f), it can be seen that surface of HIPS predominantly exhibited feature of network pattern. In addition, it can also be noticed that the rubber phase (dark circles) was free from the network. These results suggested that the network structure was created from linkage of the CB aggregate chains in the matrix. However, CB can not penetrate in to the rubber phase to form network structure due to the high viscosity of the rubber phase. Accordingly, when CB loading reached 5 phr, the sharp drop of the surface resistivity and the drastic transition of the composite from insulator to conductor were obtained. The gradual enhancement of the electrical conductivity of the composites at CB content greater than critical value (5 phr) might be resulted from the increment of the CB aggregate chains to form more conductive bridges in the HIPS matrix.

4.2.2.2 Effect of Coir Filler Content

In system of CB-containing multiphase composite, it was demonstrated that suitable level of polarity of the polymer disperse phase was one of the key factors that led to enhance the electrical conductivity of the multiphase system. The suitable polarity of the disperse phase can induce CB to locate at the interface between the continuous phase and the disperse phase or within the polymer disperse phase; hence, CB had less opportunity to distribute uniformly in the continuous phase of the multiphase composite. As a result, the electrical conductivity of CB-filled multiphase composite was increased. [6] In this study, effects of the polarity of coir filler, coir filler content, and coir filler distribution on the electrical conductivity of HIPS/5CB/coir filler composites were investigated through morphology of the multiphase composites.

จุฬาลงกรณ์มหาวิทยาลัย

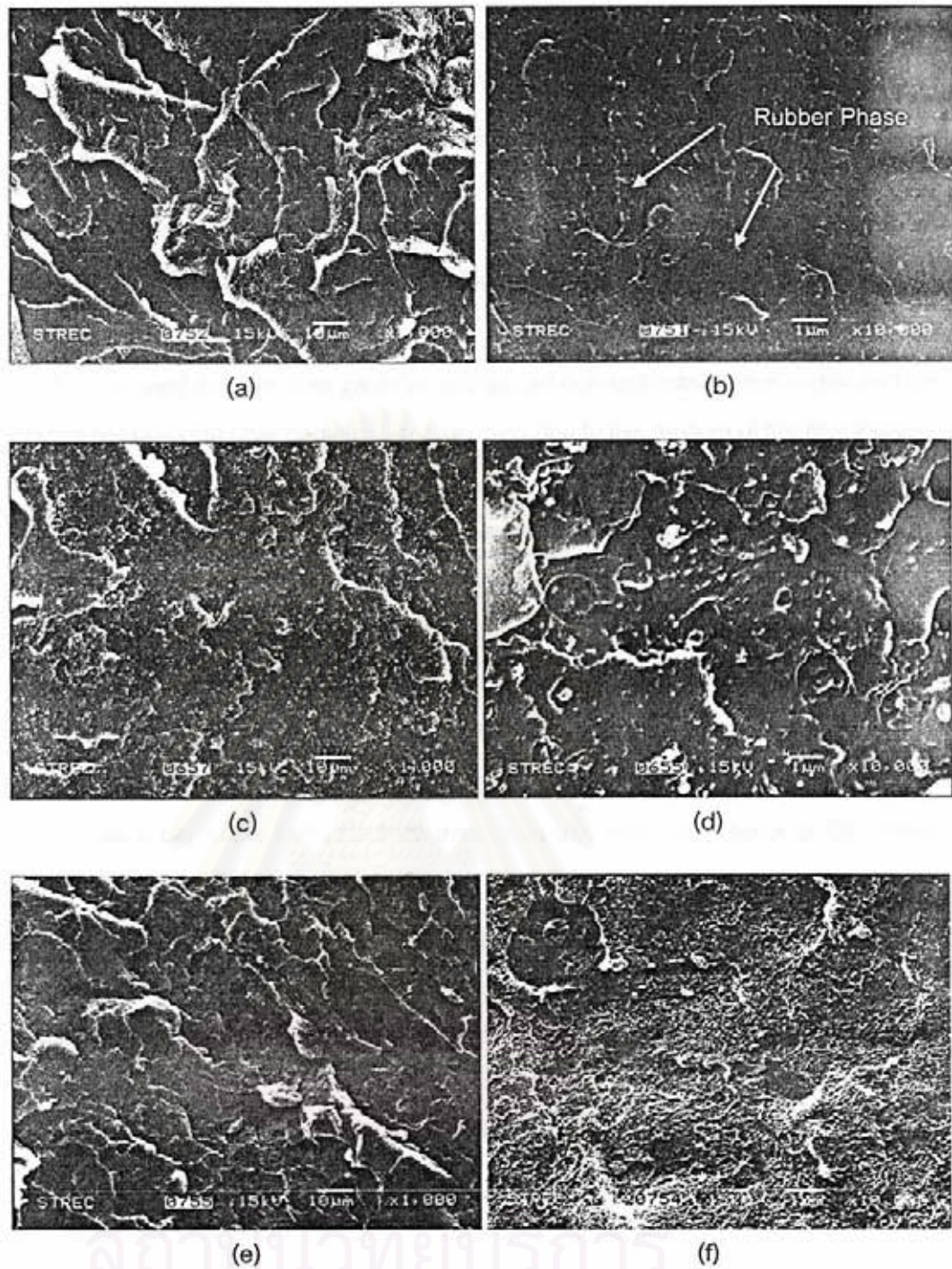
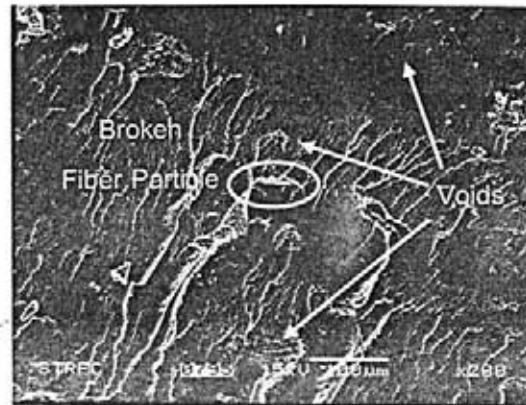


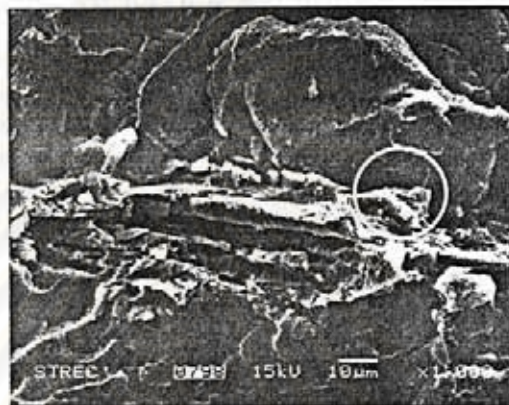
Figure 4.7 SEM micrographs of (a) HIPS at low magnification (magnification : 1,000 x, scale bar 10 μm); (b) HIPS at high magnification (magnification : 10,000 x, scale bar 1 μm); (c) HIPS/3CB composite at low magnification; (d) HIPS/3CB composite at high magnification; (e) HIPS/5CB composite at low magnification; and (f) HIPS/5CB composite at high magnification.

SEM micrographs of the conductive composite with coir filler loading of 3 phr were presented in Figure 4.8 (a-c). As shown in Figure 4.8 (a), it can be seen that most of the fiber particles were pulled out of the matrix, leaving voids with the diameter of less than 50 μm within the matrix during freeze-fracture of the specimen in liquid nitrogen due to poor adhesion between the fiber particles and the matrix. However, the little amount of the broken fiber particles with approximately diameter of larger than 50 μm can be observed. Based on this result, the voids representing the occupation of the fiber particles revealed that the fiber particles distributed non-uniformly in the matrix and the distance between the fiber particles was very high due to low amount of the filler loading. One of the fiber particles that remained in the matrix was shown in Figure 4.8 (b). It can be observed that the fiber particle was ruptured whereas surface of the matrix was similar to that of HIPS/5CB composite. At high magnification (Figure 4.8 (c)), it can be seen that the unbreakable part of the fiber particle was slightly covered with some of very thin and short chains of CB. This result can be explained that the fiber particle had better affinity with CB as compared with HIPS because CB was still held on surface of the fiber particle. In addition, it can also be explained that the polarity of the fiber particle was a key factor that promoted these very thin and short chains of CB. When the CB agglomerates were induced to cluster on the fiber particle due to the polarity of the fiber particle, this polarity of the fiber particle might broke up and reduce the agglomerates into primary aggregates. However, strong electrical forces between the CB particles can promote the flocculation or the linkage of the primary aggregate chains in network pattern within the matrix. As a result, the resistivity of HIPS/5CB/3coir filler composite was closed to HIPS/5CB composite and still in a static dissipative range.

สถาบันวิทยบริการ
จุฬาลงกรณ์มหาวิทยาลัย



(a)



(b)



(c)

Figure 4.8 SEM micrographs of (a) HIPS/5CB/3coir filler composite (magnification : 200 x, scale bar 100 μm); (b) fiber particle at low magnification (magnification : 1,000 x, scale bar 10 μm); and (c) fiber particle at high magnification (magnification : 10,000 x, scale bar 1 μm).

Figure 4.9 (a-d) demonstrated morphology of HIPS/5CB/5coir filler composites. As illustrated in Figure 4.9 (a), both the fiber particles with an approximate diameter of larger than 50 μm and the voids representing the fiber particles with an approximate diameter of less than 50 μm were observed in the matrix. These voids seemed to distribute uniformly throughout the matrix whereas the fiber particles tended to accumulate and have less amount compared with the voids. As shown in Figure 4.9 (b), it was observed that the unbreakable part of the fiber particle with an approximate diameter of 100 μm was covered with many tiny white spots. Higher magnification of the SEM micrograph (Figure 4.9 (c)) revealed that the many tiny white spots were the numerous CB particles that accumulated on the fiber surface. It can be seen that some of the particles were in the form of network structure whereas the others came to flocculate in the agglomerate structure. Similarly, high magnification of the other position (Figure 4.9 (d)) also revealed that the rough surfaces of this fiber particle predominantly showed the network pattern of the primary aggregate chains. For surface of the matrix, similar to HIPS/5CB/3coir filler it can be suggested that the CB aggregates and/or agglomerates that left from the induction of the fiber particles might come to flocculate and link together in the network structure within the matrix. Based on these results, it can be confirmed that coir filler had good affinity with CB. In addition, it can be suggested that the polarity of filler was in the suitable level as the fiber particles can promote the primary aggregate chains without uniformly dispersion of the CB particles.

To describe the gradual enhancement of the electrical conductivity of this composite, it can be explained that the relatively uniform distribution of the voids with an approximate diameter of less than 50 μm and the accumulation of the fiber particles with an approximate diameter of larger than 50 μm in the matrix might promote the enhancement of the electrical conductivity of this composite. The relatively uniform distribution of the smaller fiber particles resulted in more uniform of the electrical conductivity of the composite as compared with HIPS/5CB and HIPS/5CB/3coir filler composites. In addition, the accumulation of the larger fiber particles might cause the increment of the continuity of the conductive bridges that also led to the enhancement of the electrical conductivity of the composite. Furthermore, these results can also be implied that the incorporation of coir filler loading of 5 phr might promote more primary

aggregate chains due to its suitable polarity in comparison with HIPS/5CB composite. Higher amount of the aggregate chains might lead to slight enhancement of the electrical conductivity of the composite.

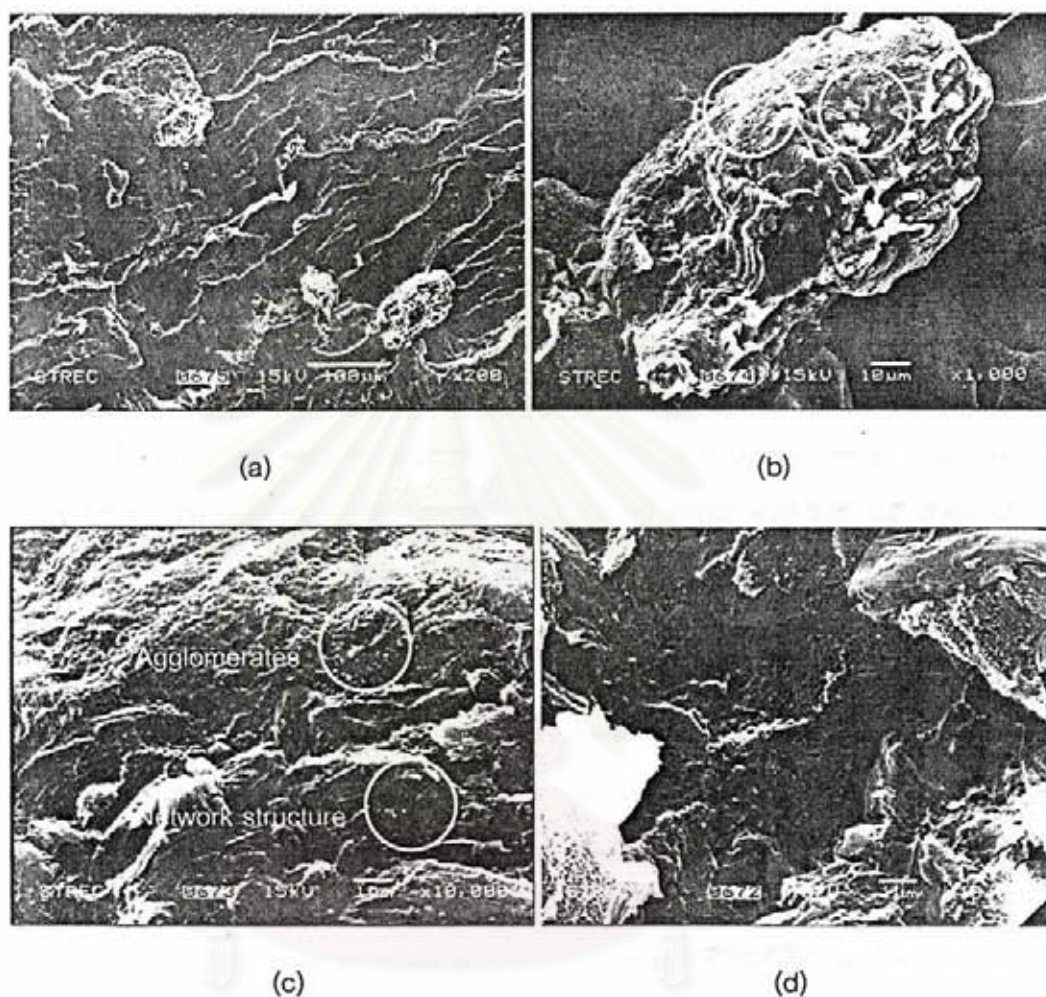


Figure 4.9 SEM micrographs of (a) HIPS/5CB/5coir filler composite (magnification : 200 x, scale bar 100 μm); (b) fiber particle at low magnification (magnification : 1,000 x, scale bar 10 μm); and (c,d) fiber particle at high magnification (magnification : 10,000 x, scale bar 1 μm).

Figure 4.10 (a-e) illustrated morphology of HIPS/5CB/9coir filler composite. As shown in Figure 4.10 (a), it was observed that both the amount of the fiber particles with an approximate diameter of larger than 50 μm and the voids representing the fiber particles with an approximate diameter of less than 50 μm were higher than the former composite. For distribution of the fiber particles, similar to HIPS/5CB/5coir filler composite it can be seen that the fiber particles tended to accumulate whereas the small voids tended to distribute uniformly in the matrix. As presented in Figure 4.10 (b), the accumulated fiber particles were shown to clarify the distribution or dispersion of CB on their surfaces. Higher magnification of these fiber particles (Figure 4.10 (c)) presented some crowds of the large CB agglomerates adhered on the surfaces of the two fiber particles and each crowd seemed to link together. To confirm the existence of the CB network on the fiber particle, the fiber particle located in another area of the matrix was presented in Figure 4.10 (d). At high magnification (Figure 4.10 (e)), it was clearly observed that the CB network appeared on the surface of fiber particle. Regarding to the electrical conductivity of this composite, it can be suggested that higher amount of the coir filler, characteristic of the filler distribution, and suitable polarity of the filler might result in the highest electrical conductivity of this composite.

The slight decrement of the electrical conductivity of the composites with coir filler loading higher than 9 phr might be due to the excess amount of coir filler which may require higher amount of CB (> 5 phr) to accumulate or cover all over every fiber particles. As a result, some fiber particles that had less amount of CB (the un-effective CB) on their surfaces exhibited as the insulating areas in the matrix. Accordingly, the surface resistivity of these composites was higher than HIPS/5CB/9coir filler composite. However, the resistivity values of these composites were still in a static dissipative range.

สถาบันวิทยบริการ
จุฬาลงกรณ์มหาวิทยาลัย

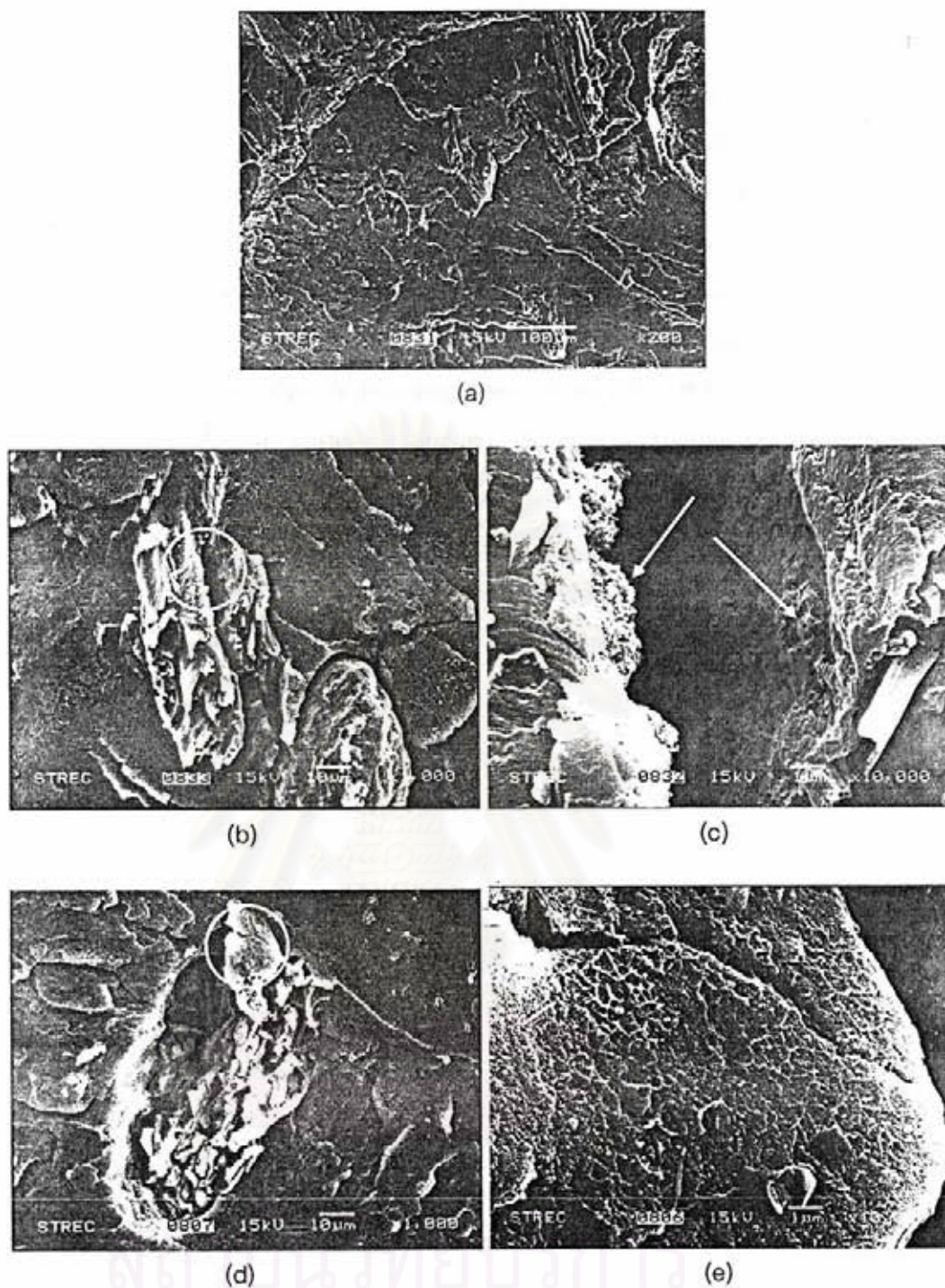


Figure 4.10 SEM micrographs of (a) HIPS/5CB/9coir filler composite (magnification : 200 x, scale bar 100 μm); (b,d) fiber particle at low magnification (magnification : 1,000 x, scale bar 10 μm); and (c,e) fiber particle at high magnification (magnification : 10,000 x, scale bar 1 μm).

In conclusion, these results can be concluded that the polarity of coir filler promoted two characteristics of CB distributions on the filler surface or at the interface of the composite namely the CB agglomerates and the primary aggregate chains which led to enhance the electrical conductivity of the composites. In addition, quantity and distribution of the fiber particles also influenced on the electrical conductivity of the composites. For HIPS/5CB composite, network structure was created within the matrix, whereas network structure of HIPS/5CB/coir filler composites was generated on surface of the fiber particles (interface of the composites) and/or within the matrix. Accordingly, the resistivity values of HIPS/5CB/coir filler and HIPS/5CB composites were not too much difference and still in the static dissipative range.



สถาบันวิทยบริการ
จุฬาลงกรณ์มหาวิทยาลัย



4.3 Mechanical Properties of the Composites

4.3.1 Notched Izod Impact Strength of the Composites

The impact toughness of the composites was determined through notched Izod impact tests. In other words, the energy required for crack propagation was measured through the notched Izod specimens. The plots of the notched Izod impact strength of the composites versus carbon black and coir filler contents were shown in Figure 4.12 and 4.13, respectively.

4.3.1.1 Effect of Carbon Black (CB) Content

– For HIPS/CB composites, as presented in Figure 4.11, it was observed that the impact strengths of the composites were decreased when the content of CB increased. Based on these results, it can be explained that the presence of CB in the matrix reduced the energy absorbing capabilities and the toughness of the composites. In addition, it can be suggested that the changes in the impact strength with different CB content might be related to the morphology of the composites. At low CB loading of 3 phr, the presence of the CB aggregates/agglomerates in the matrix might facilitate crack propagation that led to the reduction in the impact energy of the notched Izod specimen. When CB loading increased to 5 phr (at the critical CB content), the more reduction of the impact strength of the composite might be associated with the formation of conductive network in the matrix. It was expected that the critical crack propagation and unstable crack growth in such this system were conducted easier and faster than in the virgin polymer or in the composites where the continuous network of CB had not been formed. Further reduction in the impact strength of the composites with the addition of CB loading beyond the percolation region might be associated with the increment of the conductive paths.

จุฬาลงกรณ์มหาวิทยาลัย

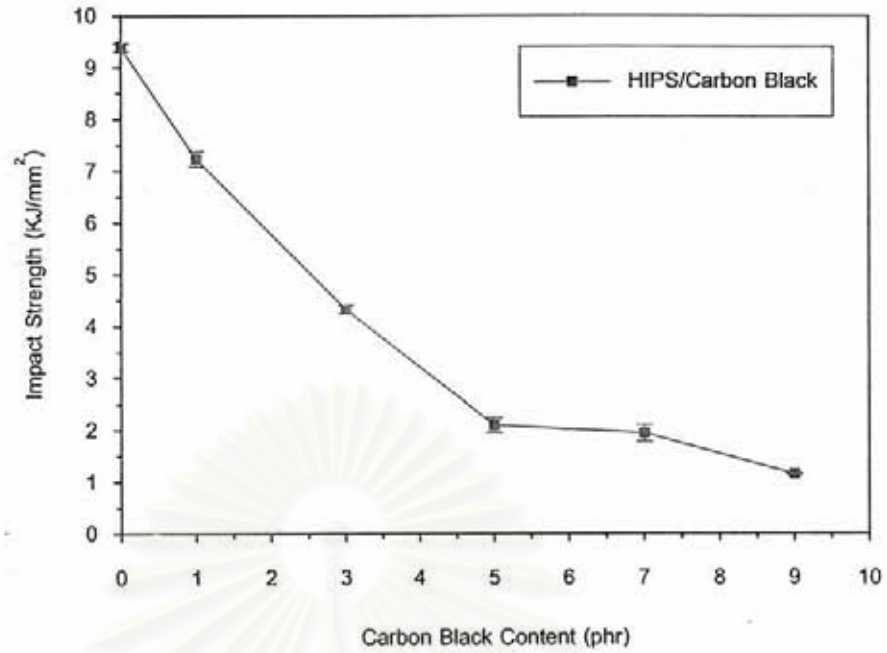


Figure 4.11 Notched Izod impact strength of HIPS/CB composites as a function of CB content.

4.3.1.2 Effect of Coir Filler Content

The impact strength of HIPS/coir filler and HIPS/5CB/coir filler composites were presented in Figure 4.12. For HIPS/coir filler composites, similar to HIPS/CB composites the impact strengths of the composites were decreased when the quantity of coir filler increased. This result can be explained that poor adhesion between the interface of the hydrophilic coir filler and the hydrophobic HIPS might ease crack propagation that led to the reduction in the impact energy of the composites. In addition, some agglomerates of the fiber particles appearing in the matrix might create regions of stress concentration that required less energy to elongate the crack propagation. Accordingly, larger amount of the filler promoted higher weak interface regions and higher stress concentration. Thus, the impact strengths of the composites were reduced with the increasing of the filler loading. However, in comparison to the composites filled with coir filler and CB, the higher impact strengths of the composites filled with coir filler were observed even for

higher content of coir filler. These indicated that the coir filler-filled composites required higher work of fracture such as debonding and pull-out. In addition, it has been reported that larger filler particles had higher critical crack propagation energy as compared with the smaller particles due to the increment of fracture surface area. [41] Toughening mechanisms of the coir filler-filled composites were investigated through their morphology. Figure 4.13 (a,b) and (c,d) showed the SEM micrographs of the composites with coir filler loading of 7 and 15 phr broken under impact tests, respectively.

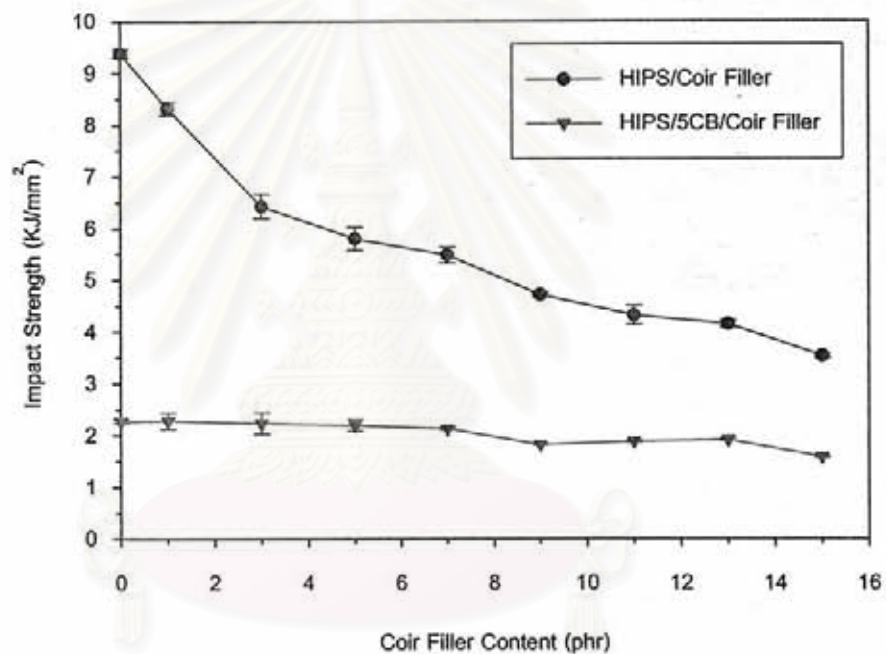
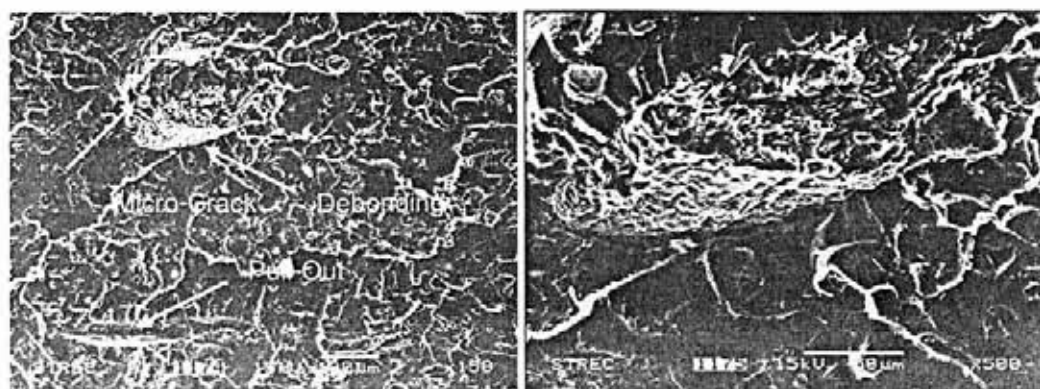
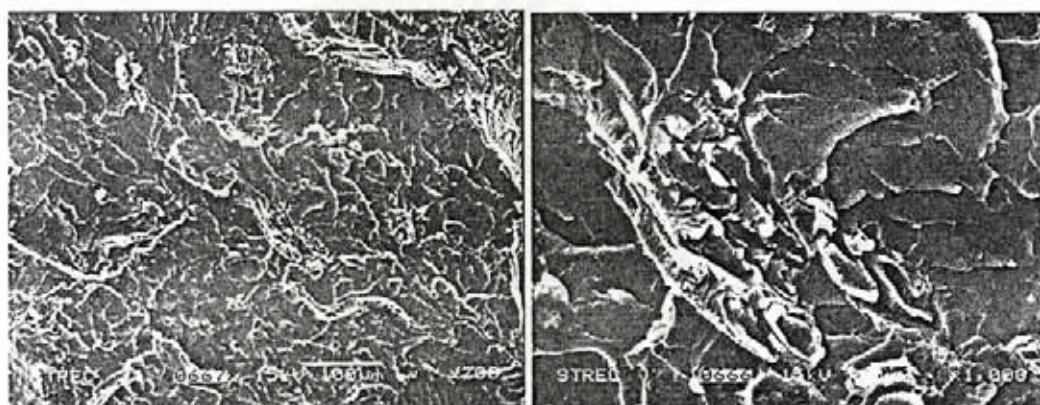


Figure 4.12 Notched Izod impact strength of the composites as a function of coir filler content.



(a)

(b)



(c)

(d)

Figure 4.13 SEM micrographs of (a) crack growth region of HIPS/7coir filler composite (magnification : 150 x, scale bar 100 μm); (b) micro-cracks and debonding of HIPS/7coir filler composite (magnification : 500 x, scale bar 10 μm); (c) crack growth region of HIPS/15coir filler composite (magnification : 200 x, scale bar 100 μm); and (d) micro-cracks of HIPS/15coir filler composite (magnification : 1,000 x, scale bar 10 μm) under impact loading.

สถาบันวิทยบริการ
จุฬาลงกรณ์มหาวิทยาลัย

As presented in Figure 4.13 (a), several mechanisms such as debonding, micro-cracks, fiber particle fracture, and fiber pull-out can be observed. At higher magnification (Figure 4.13 (b)), it can be seen that micro-cracks and debonding were generated around the fiber surface. These results can be explained that when the growing crack encountered the fiber particle, it tended to travel along the weak interface of the fiber particle and the matrix. After that, the fiber particle was broken at its weakest point and debonded. Finally, the fiber particle was pulled out of the matrix. In case of the micro-cracks, it had been pointed out by H. S. Yang and coworkers [42] that poor interfacial bonding induced micro-spaces between the fiber particle and the matrix. The micro-spaces caused the occurrence of numerous micro-cracks around the fiber particle.

Similarly, as illustrated in Figure 4.13 (c), the impact fracture surface of the composites with coir filler loading of 15 phr also showed debonding, micro-cracks, fiber fracture, and fiber pull-out. Higher magnification (Figure 4.13 (d)) revealed that micro-cracks were generated around the fiber particles. However, the amount of cracks in the matrix with coir filler loading of 15 phr seemed to be higher than the composite with coir filler loading of 7 phr.

With respect to HIPS/5CB/coir filler composites, it was observed that the incorporation of both CB and coir filler resulted in the rapid drop of the impact strengths of the composite as compared with pure HIPS and HIPS/coir filler composites. However, it can be seen that the impact strengths of the three-phase composites were closed to HIPS/5CB composites. These results can be suggested that the presence of CB might predominantly influence on the impact strengths of the three-phase composites. As described in section 4.2, it was indicated that the CB particles of the three-phase composites were in the form of network and agglomerates and located at the surfaces of fiber particles and within the matrix. Based on this result, it can be suggested that the presence of the CB particles (network and agglomerates) at the interface of the composites might facilitate and enhance the debonding of the weak interface between the fiber particles and the matrix. In addition, similar to HIPS/5CB composite the CB network located within the matrix might facilitate the ease of the critical crack

propagation and unstable crack growth. Consequently, the impact strengths of the three-phase composites were significantly less than pure HIPS and HIPS/coir filler composites and closed to HIPS/5CB composite. As seen in Figure 4.14, it can be seen that the growing cracks moved pass the CB agglomerates located at the interface between the fiber particle and the matrix and traveled along the weak interface of the three-phase composites with coir filler loading of 7 phr. In addition, it can also be seen that the cracks propagated through the interface between the matrix and CB (located within the matrix).

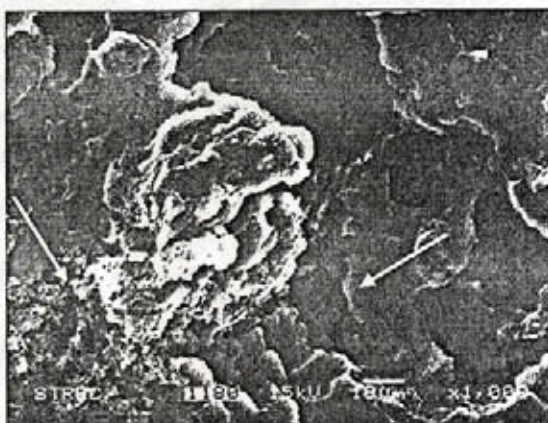


Figure 4.14 Crack growth region of HIPS/5carbon black/7coir filler composite under impact loading.

For pure HIPS, as presented in Figure 4.15, growing cracks and micro-voids obtained from debonding and/or cavitation of the rubber particle (formation of a hole within the rubber particle core to release hydrostatic stress) under impact loading were clearly observed. This result indicated that the HIPS specimen was brittle under impact loading because toughening mechanisms of toughened polymer such as crazing and/or micro-shear yielding can not be observed. This result is in good agreement with P. Antich and coworkers [43] that impact fracture surface of the HIPS specimen showed crack growth region with debonding of the elastomeric particles which indicated the brittleness of HIPS under impact loading.

Finally, it can be suggested that the greater reduction of the impact toughness of all composites as compared with pure HIPS might resulted from the combined effects of the matrix brittleness and the others that were described above.

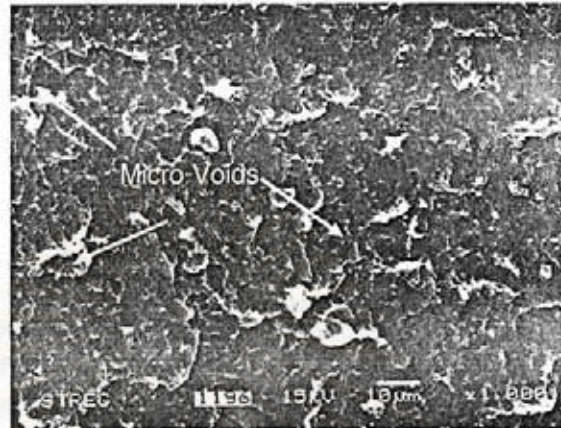


Figure 4.15 Crack growth region of pure HIPS under impact loading.

สถาบันวิทยบริการ
จุฬาลงกรณ์มหาวิทยาลัย

4.3.2 Tensile Properties of the Composites

The tensile properties indicate behavior of materials under applied tension forces. Tensile testing provides useful data such as tensile yield strength, tensile strength at maximum, tensile strength at break (ultimate tensile strength), tensile modulus (Young's modulus), and elongation at yield and break. In addition, stress-strain or load-extension curve can be used to define mechanical behaviors of the materials such as ductility and brittleness. Accordingly, the stress-strain behavior and tensile properties of the composites such as tensile strength at maximum, tensile modulus, and elongation at break were presented in this section.

4.3.2.1 Stress-Strain Behavior

The load-extension curves of pure HIPS and the composites were shown in Figure 4.16. For pure HIPS, the shape of load-extension curve indicated ductile behavior of the material due to the presence of yield point and extensive plastic deformation until failure. Initial slope of the ductile-HIPS curve was presented in the region of elastic deformation and the yield point was reached at about 430 N. After reaching the yield point, the stress or load dropped where shear-banding and/or crazing were formed. After that, the shear-bands and stress whitening were propagated through the entire gauge section of the specimen with a constant load. Subsequently, the stress or load gradually increased in strain-hardening region. Finally, load dropped and the specimen fractured.

In case of HIPS/5CB and HIPS/5coir filler composites, from the load-extension curve it can be suggested that both composites fractured during neck formation. As pointed out by J. Li and coworkers [39] that fracture of the specimen during neck formation indicated quasi-brittle behavior of the material. Accordingly, these composites exhibited quasi-brittle characteristic. In comparison, it can be seen that the initial slope of the composite filled with CB was less than the composite filled with coir filler. This result indicated that the modulus of HIPS/coir filler composite was higher than HIPS/CB composite. However, as compared with pure HIPS, it was found that both

composites had lower areas under the curves whereas the initial slopes were higher. This result indicated that the addition of rigid filler reduced toughness of polymer whereas stiffness was enhanced.

For the three-phase composite, from the load-extension curve it can be suggested that the three-phase composite failed after the maximum load (during formation of shear-bands). Fracture of the specimen prior to neck formation indicated quasi-brittle behavior of the three-phase composite. In comparison, it was clearly observed that the load-extension curve of the three-phase composite showed the initial slope closed to the composite filled with coir filler whereas area under the curve was lowest. This indicated that the inclusion of CB and coir filler enhanced stiffness of the three-phase composite whereas toughness was reduced as compared with the others.

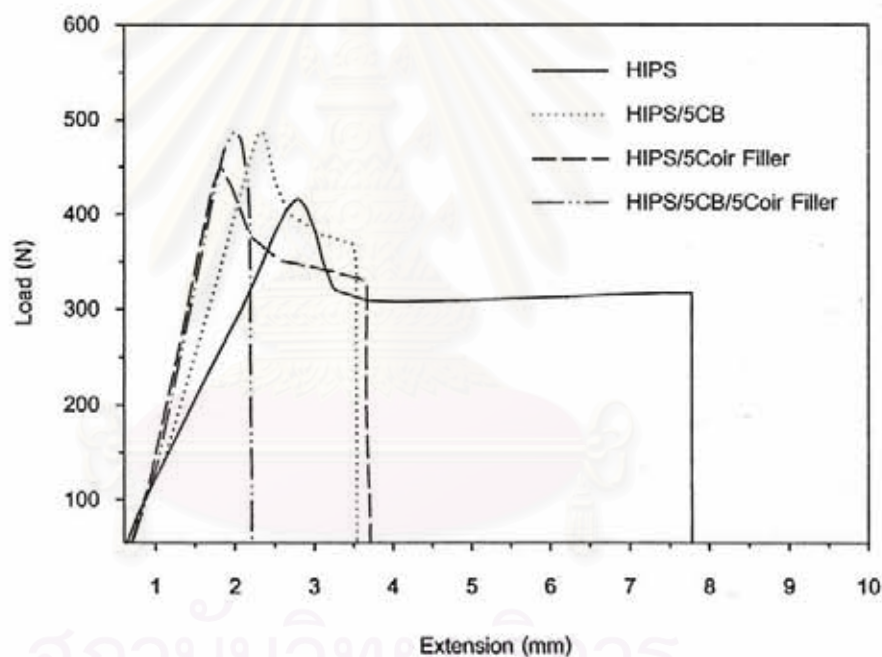


Figure 4.16 Load-extension curve of the composites.

สถาบันวิทยบริการ
จุฬาลงกรณ์มหาวิทยาลัย

4.3.2.2 Effect of Carbon Black Content

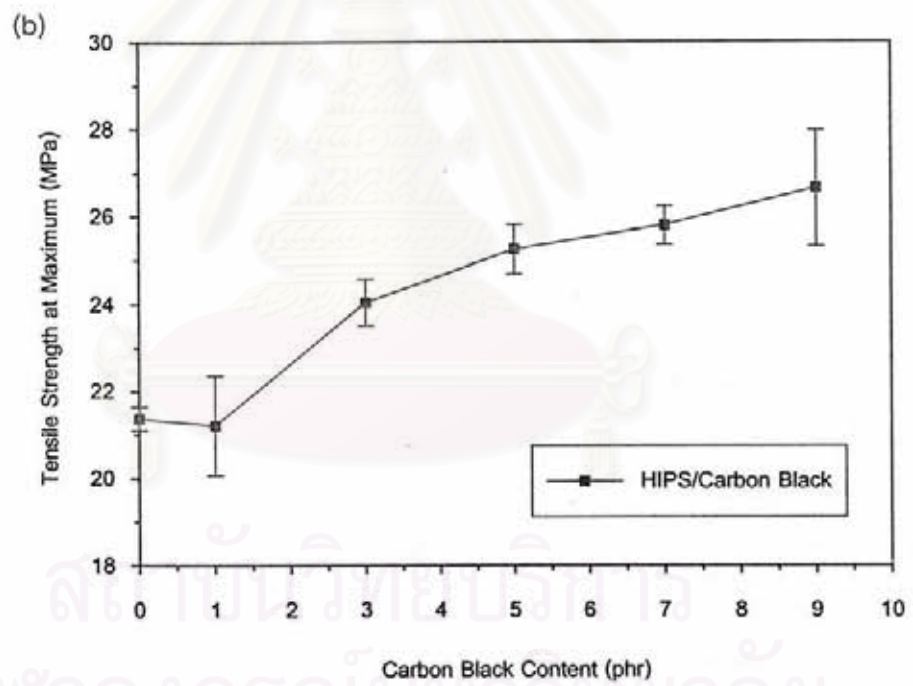
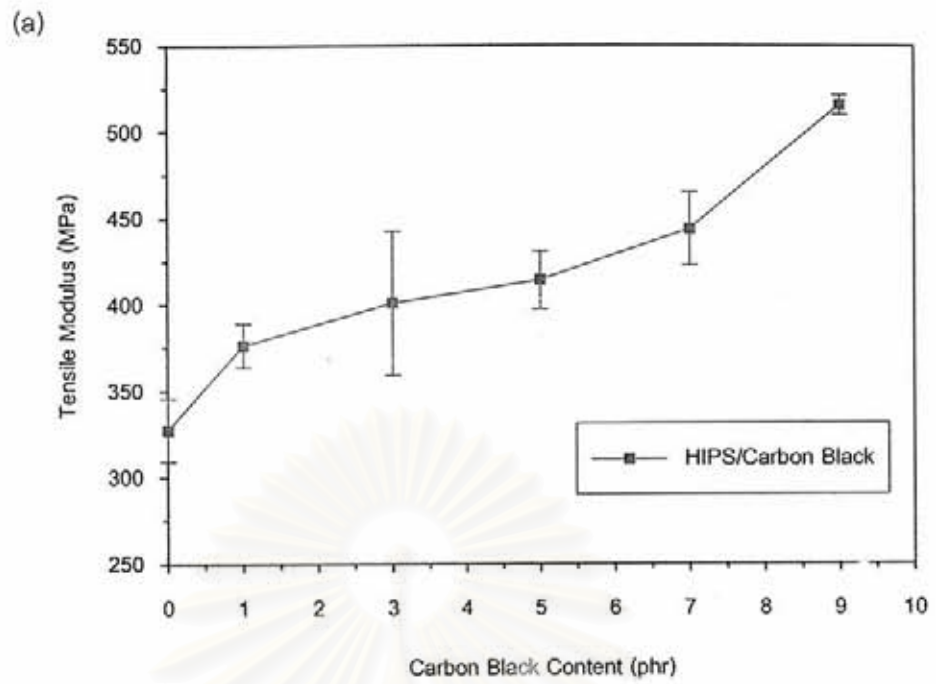
Figure 4.17 (a), (b), and (c) showed the effects of CB content on tensile modulus, tensile strength, and elongation at break of the composites, respectively. As presented in Figure 4.17 (a), it was observed that tensile modulus of the composites was increased when the amount of CB increased. This indicated that CB was able to impart greater stiffness of the composites. In addition, these results can be explained through Kerner's equation, which assumes good adhesion between the polymer and the rigid-spherical filler particle. [44]

$$E_c / E_m = 1 + [15\phi_f(1-\nu_m)/\phi_m(8-10\nu_m)] \quad (4.2)$$

Where E_c and E_m are the modulus of composite and unfilled polymer, ϕ_f and ϕ_m are the volume fractions of filler and polymer, and ν_m is the Poisson's ratio of polymer. From this equation, it can be described that the modulus of the composite depended on the filler volume fraction. When the volume fraction of the filler increased, the modulus of the composite was increased.

As shown in Figure 4.17 (b), similar to tensile modulus it was observed that the tensile strength of the composites tended to increased with increasing CB loading. However, it can be seen the gradual reduction in tensile strength of the composite with CB loading of 1 phr. This result might be attributed to debonding of the filler particles from the matrix under applied tension forces due to the dilution of the matrix. The enhancement in tensile strength of the composite at higher CB loading (3-9 phr) might be associated with the reinforcing effect of the CB filler. In other words, it can be said that the dislocation of matrix phase was sufficiently impeded at higher content of CB; as a result, the stress was more uniformly distributed in the composite under applied tension forces.

As shown in Figure 4.17 (c), it was obvious that elongation at break of the composites was decreased when the content of CB increased. This result might be associated with the impediment effect of CB to reduce the deformability of the matrix (at higher CB loading).



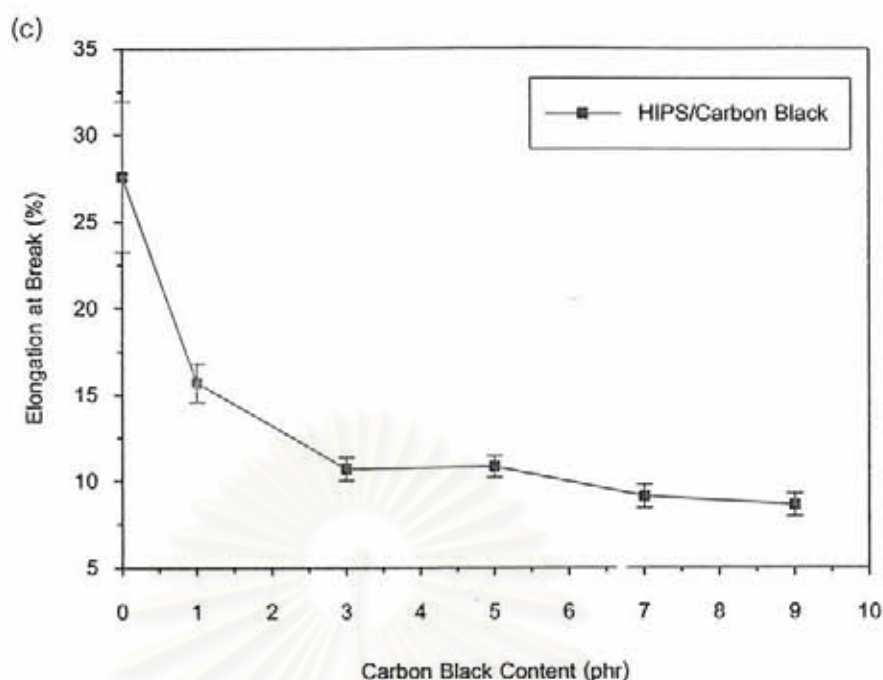
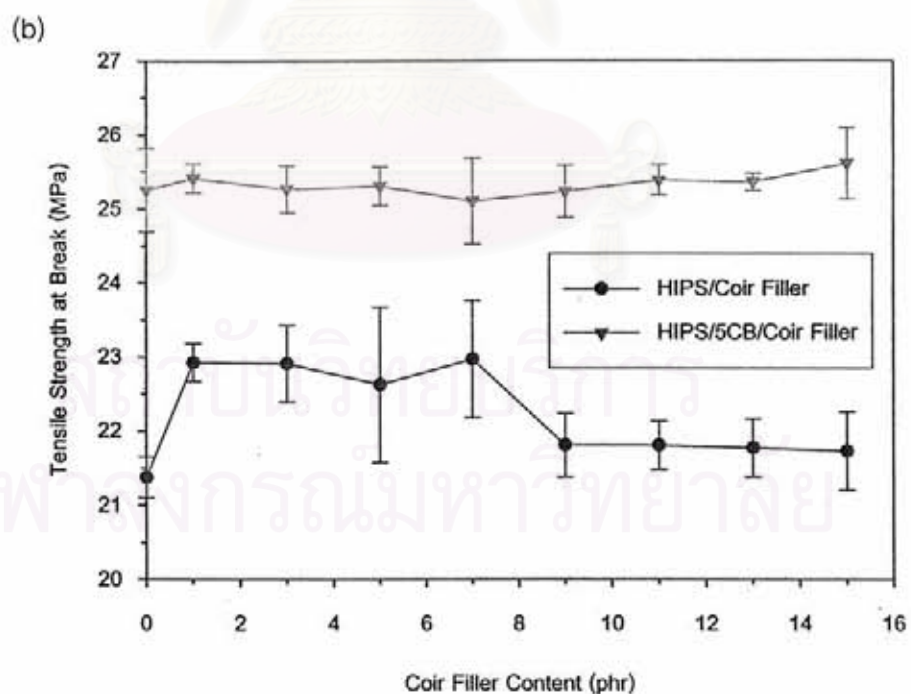
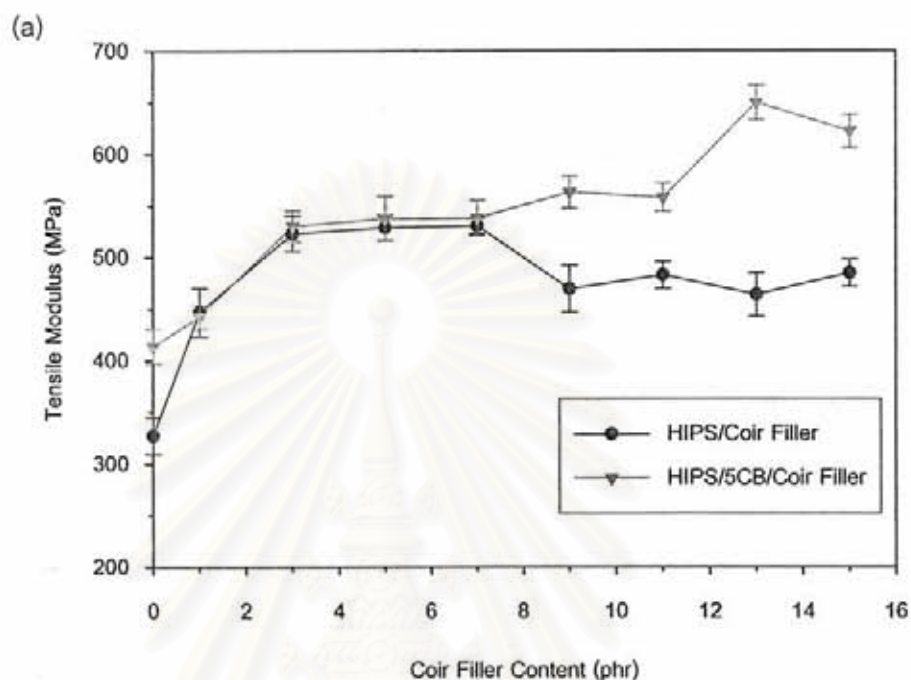


Figure 4.17 The effect of CB content on (a) tensile modulus, (b) tensile strength, and (c) elongation at break of HIPS/CB composites.

4.3.2.3 Effect of Coir Filler Content

Figure 4.18 (a), (b), and (c) showed the effects of coir filler content on tensile modulus, tensile strength, and elongation at break of the composites, respectively. As presented in Figure 4.18 (a) and (b), for HIPS/coir filler composites it can be seen that both tensile modulus and tensile strength of the composites tended to increase significantly when the content of coir filler was in the range of 1-7 phr. At higher content of coir filler (9-15 phr), both tensile modulus and tensile strength of the composites were slightly dropped. However, the greater tensile modulus and tensile strength of the composites as compared with pure HIPS were observed. These results indicated the ability of coir filler to impart greater stiffness to the composites. The reduction in tensile modulus of the composites with the addition of coir filler at higher filler loading (9-15 phr) might be associated with the presence of larger or more numerous defects such as

voids, cracks, and/or stress concentrations due to poor distribution of the fiber particles and the appearance of higher end effects as a result of relatively low aspect ratio of the fiber particle.



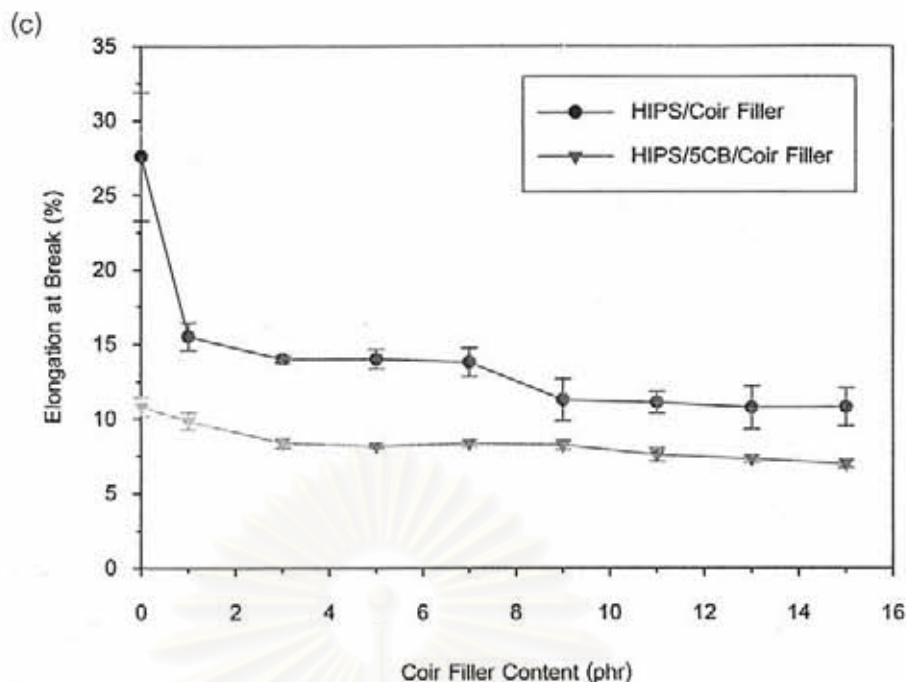


Figure 4.18 The effect of coir filler content on (a) tensile modulus, (b) tensile strength, and (c) elongation at break of the composites.

As presented in Figure 4.18 (c), it was clearly observed that elongation at break of the HIPS/coir filler composites was decreased as the content of coir filler increased. This result might be associated with the restriction effect of coir filler to reduce the deformability of the matrix (at higher coir filler loading).

For HIPS/5CB/coir filler composites, as seen in Figure 4.18 (a), it can be obviously seen that tensile modulus of the three phase composites was increased when the content of coir filler increased. This result might be attributed to the reinforcing effects of coir filler and CB.

As shown in Figure 4.18 (b), it can be seen that the addition of coir filler maintained tensile strength of the three-phase composites which closed to the HIPS/5CB composite.

In comparison, it can be seen that both tensile modulus and tensile strength of the three-phase composites were higher than pure HIPS and HIPS/coir filler composites. In addition, as compared with HIPS/5CB composite, the higher tensile modulus of the three-phase composite was observed, while tensile strength of those composite was not too much difference. These results can be confirmed the reinforcing effects of CB and coir filler. In other words, it can be suggested that the inclusion of CB and coir filler might efficiency promote the uniform distribution of stress in the three-phase composites.

As illustrated in Figure 4.18 (c), the small reduction in the elongation at break of the three phase composites with increasing coir filler content can be noticed. This result might be due to the greater restraint effect of coir filler (at higher coir filler loading) and the impediment effect of CB to reduce the deformability of the matrix efficiently. In comparison, it can be seen that the elongation at break of the three-phase composites was less than those of pure HIPS, HIPS/coir filler composites, and HIPS/5CB composites. This result can be confirmed the effects of the inclusion of the two fillers to sufficiently inhibit the movement of matrix phase even at the low filler content (CB and 1 phr of coir filler).

4.3.3 Flexural Properties of the Composites

4.3.3.1 Effect of Carbon Black Content

The changes in flexural modulus and flexural strength of the composites with respect to CB content were shown in Figure 4.19 (a) and (b), respectively. It can be seen that both flexural modulus and flexural strength of the composites were increased when the amount of CB increased. In comparison, the flexural modulus and flexural strength of HIPS/9CB composite were increased 25.71% and 25.53%, respectively as compared with pure HIPS. These results can be explained that the presence of CB produced higher energy absorption for a given displacement of the samples in three point bending and also improved the stiffness of the composites. Such behaviors in the flexural strength and flexural modulus of these composites were similar to CB-filled thermoplastic resin composites. [40]

4.3.3.2 Effect of Coir Filler Content

Figure 4.20 (a) and (b) showed the effects of coir filler loading on the flexural modulus and flexural strength of the composites, respectively. For HIPS/coir filler composites, it can be seen that both flexural modulus and flexural strength of the composites with coir filler loading of 1-7 phr were higher than those of pure HIPS. However, when coir filler loading was increased to 9-15 phr, both flexural modulus and flexural strength of the composites decreased. Similar to tensile properties, the reduction in both flexural modulus and flexural strength of these composites might be associated with the less uniform distribution of the filler (at higher filler loading) and the presence of larger defects such as voids, cracks, or stress concentration spots. Nevertheless, it can be seen that the flexural modulus of these composites was still higher than that of pure HIPS. These results indicated that the addition of coir filler enhanced the stiffness of the composites. In particular, with the suitable amount of coir filler (i.e., up to 7 phr), the coir filler acted as effective reinforcing agent.

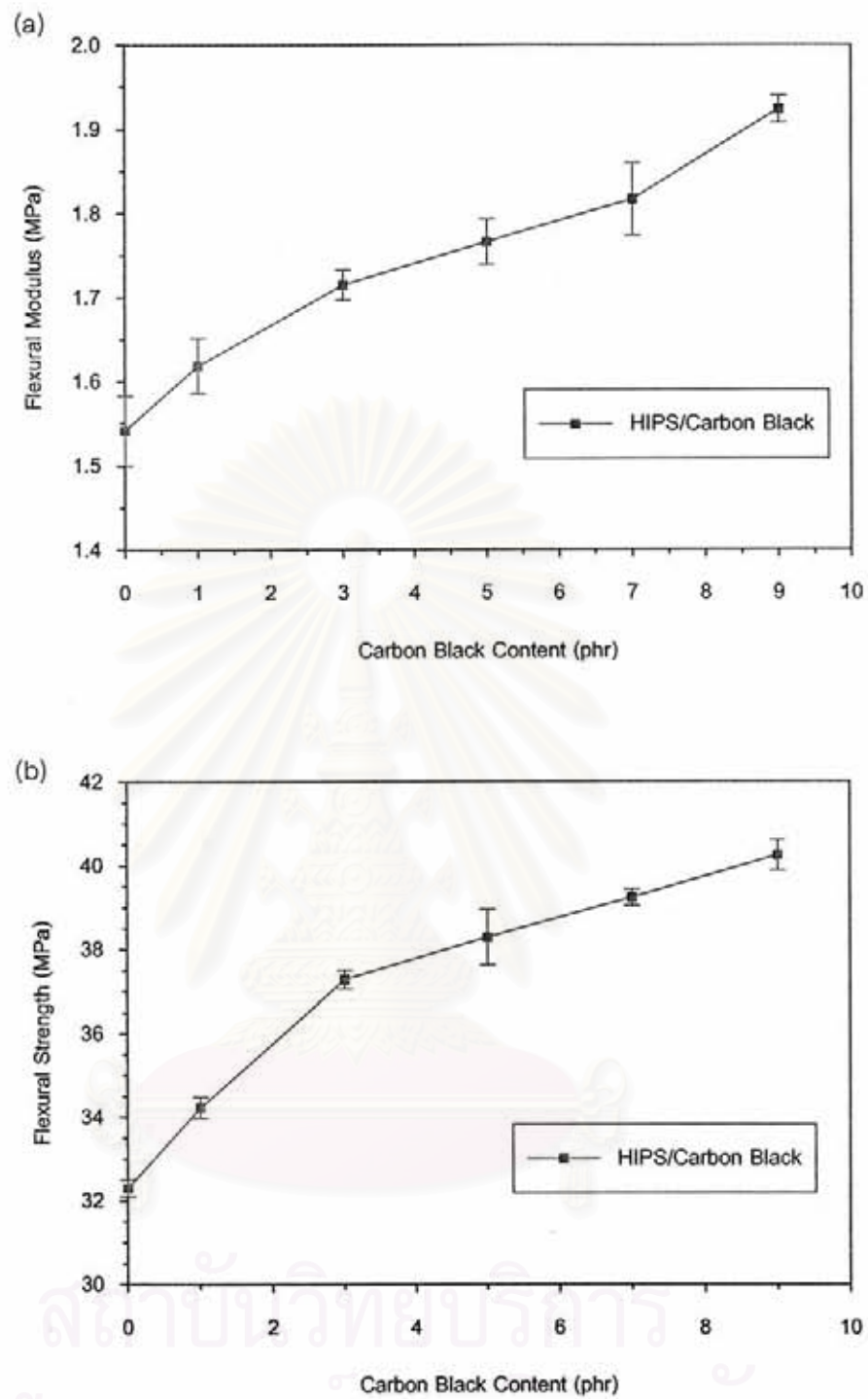


Figure 4.19 Flexural modulus (a) and flexural strength (b) of HIPS/CB composites.

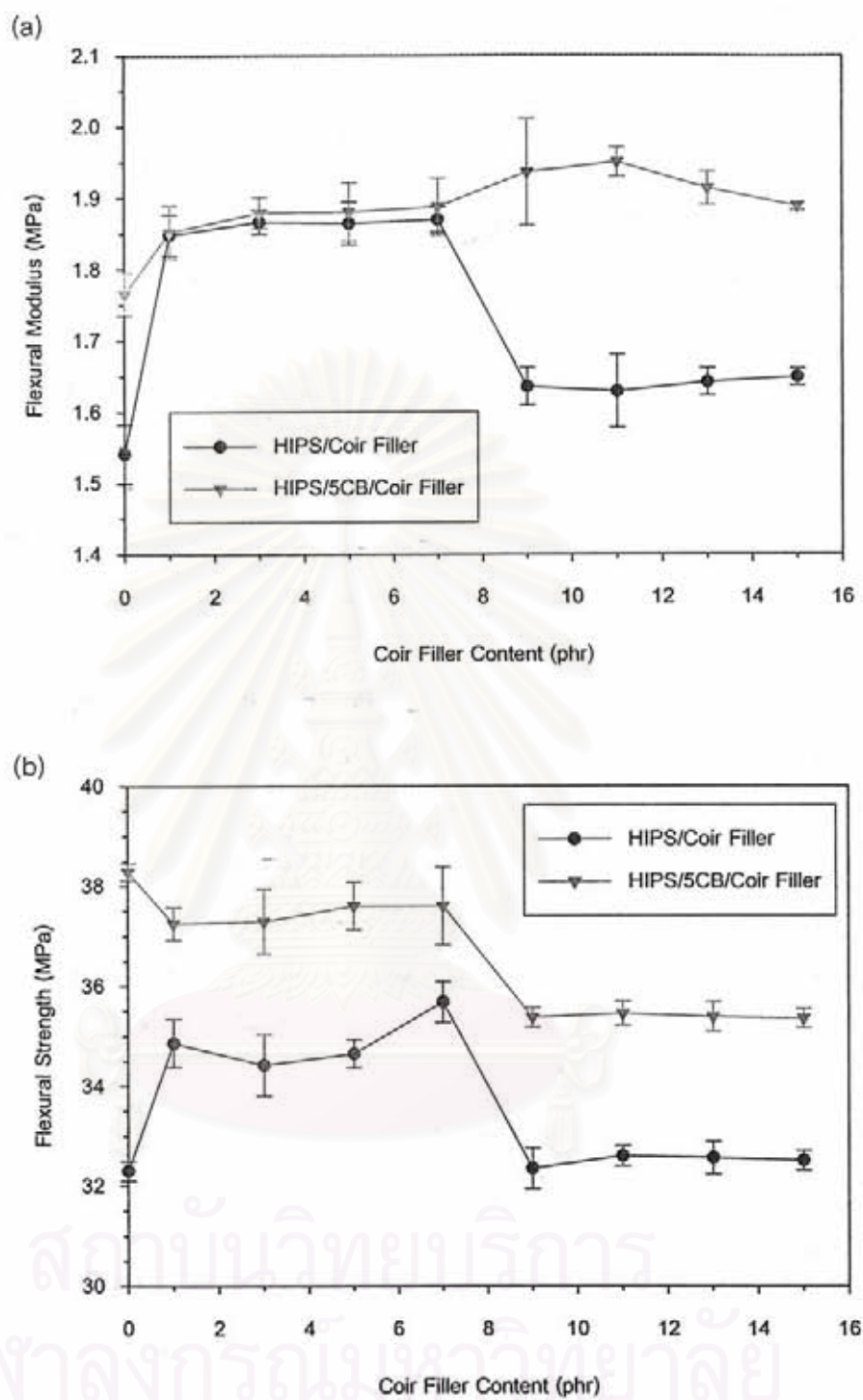


Figure 4.20 Flexural modulus (a) and flexural strength (b) of the composites as a function of coir filler content.

As compared with HIPS/CB composites, the addition of CB enhanced both flexural modulus and flexural strength of the composites whereas the addition of coir filler reduced both flexural modulus and flexural strength of the composites (at higher coir filler loading). This result might be associated with the effect of filler particle size. Because CB had smaller particle size, distribution of small CB particle in the polymer matrix was better than coir filler which had relatively larger particle size. The larger particle size of coir filler resulted in poor distribution of coir filler (at higher coir filler loading) in the matrix.

In case of the three phase composites, it can be seen that the flexural modulus of the composites were increased when the coir filler content increased. This indicated that the addition of coir filler and CB enhanced the stiffness of the three-phase composites. On the contrary, as shown in Figure 4.20 (b), it was observed that flexural strength of the three-phase composites tended to decreased when the content of coir filler increased. As pointed out by Sato and coworkers [41] for glass fiber reinforced nylon 6,6, when load was applied in three-point bending tests, cracks were formed at the fiber ends first, then along the interface, and then in the matrix. Accordingly, the above result can be suggested that the increment of coir filler generated and facilitated more numerous of cracks resulting in more reduction in flexural strength of the three-phase composites with higher coir filler loading.

In comparison, it can be seen that both flexural modulus and flexural strength of the three-phase composites were higher than pure HIPS and coir filler filled-composites. This result indicated that for three-point bending tests the inclusion of CB and coir filler in three-phase composites resulted in more stiffness and strength.

CHAPTER V

CONCLUSIONS AND RECOMMENDATIONS



5.1 Conclusions

In this work, the use of coir fiber as a filler in high impact polystyrene/carbon black composites can maintain the electrical conductivity of the three-phase composites in the static dissipative range which was suitable for using in electronic packaging applications such as intimate packaging. In addition, the coir fiber can also improve mechanical properties of the three-phase composites namely tensile modulus, tensile strength, and flexural modulus. However, poor impact strength was obtained when coir filler was incorporated in the three-phase composites. The electrical properties and mechanical properties of the composites are summarized as follows:

1. For HIPS/CB composites, the composite reached the percolation threshold at CB loading of ~5 phr. At the percolation threshold, network structure of CB was formed within the HIPS matrix and the surface resistivity of the composite was sharply decreased to 10^7 ohm/square which can be designated as a static dissipative composite having the surface resistivity in the range of 10^5 - 10^9 ohm/square.

2. In case of HIPS/coir filler composites, the addition of insulating coir filler did not increase the surface resistivity of the composites. The gradual decrease in the resistivity of the composites might be associated with moisture absorption of the hydrophilic coir filler.

3. For the three-phase composites, the conductive properties of the composites resulted from the presence of the conductive CB while the addition of insulating coir filler did not change the conductive composites into the insulators due to the polarity effect of coir filler. The polarity of coir filler can induce CB to cluster and form network structure (CB agglomerates and primary aggregate chains) on the fiber surface. As a result, the coir filler did not exhibit as an insulating area in the matrix. Thus, the electrical conductivity of the composites still remained in the static dissipative range. In addition, the incorporation of coir filler loading, in particular at 5-9 phr, tended to increase the

electrical conductivity of the three-phase composites gradually due to the quantity and distribution of coir filler in this range and the polarity effect of coir filler to promote CB agglomerates and primary aggregate chains.

4. For impact strength, in comparison to pure HIPS the greater reduction in the impact toughness of HIPS/CB composites might resulted from the effect of CB to facilitate the ease of crack propagation. The reduction in the impact strength of HIPS/coir filler composites might be associated with weak interface of coir filler and HIPS and poor distribution of coir filler (at higher filler loading). Finally, the greater reduction in impact strength of the three-phase composites might be attributed to the effects of CB and coir filler to promote the ease of crack propagation. However, the reduction in impact toughness of all composites also included the effect of matrix brittleness.

5. For tensile properties, the HIPS/CB composites showed higher tensile modulus and tensile strength whereas elongation at break of the composites was lower than pure HIPS due to the impediment effect of CB. In case of HIPS/coir filler composites, the composites exhibited higher tensile modulus and higher tensile strength (except at coir filler loading of 9-15 phr) whereas elongation at break of the composites were lower than pure HIPS due to the restriction effect of coir filler. Finally, the inclusion of CB and coir filler promoted the greater enhancement in tensile modulus and tensile strength of the three-phase composites.

6. For flexural properties, both flexural modulus and flexural strength of the HIPS/CB composites are higher than pure HIPS. In case of HIPS/coir filler composites, both flexural modulus and flexural strength of the composites with coir filler loading of 1-7 phr were higher than pure HIPS. However, both flexural modulus and flexural strength of the composites with higher coir filler loading (9-15 phr) were decreased due to poor distribution of the filler. For the three-phase composites, similar to HIPS/CB composites both flexural modulus and flexural strength of the composites are higher than pure HIPS.

7. In conclusion, the HIPS/CB (5phr)/coir filler (9 phr) composite showed suitable mechanical properties and had the lowest resistivity.

5.2 Recommendations

In the next section, effect of coir fiber (in form of continuous fiber) on the percolation threshold of the three-phase composites should be investigated. Each formula of HIPS/coir fiber composites should be varied with different contents of CB (such as 1-9 phr) to observe the percolation threshold of each formula. If any of them reaches the lower percolation threshold as compared with the percolation threshold of HIPS/CB composites, it is not only to reduce the critical CB content, but also to decrease the reduction in impact strength of the three-phase composites. In addition, the higher screw speed should be used to optimize between energy consumption and cost effective.



สถาบันวิทยบริการ
จุฬาลงกรณ์มหาวิทยาลัย

REFERENCES



- [1.] Fundamentals of electrostatic discharge[Online]. 2001. Available from:
<http://www.denclare.com> [2005, July 5]
- [2.] William M., and George, W.W. Conductive plastic. In J.M. Magolis (ed.),
Conductive Polymers and Plastics Handbook, pp.120-121. New York: Chapman and
Hall, 1989.
- [3.] Gamboa, K.M.N.; Ferreira, A.J.B.; Camago, S.S.; and Soares, B.G. Electrical
conductivity of polystyrene/styrene-butadiene block copolymer blends containing
carbon black. Polymer Bulletin 38 (1997): 95-100.
- [4.] Massao, S.; Kazuya, S.; Shigeo A.; Keizo, M.; and Hideaki N. Dispersion of fillers and E
electrical conductivity of polymer blends filled with carbon black. Polymer Bulletin
25(1991): 265-271.
- [5.] Breuer O.; Tchoudakov, R.; Narkis, M.; and Siegmann, A. Segregated structures in
carbon black-containing immiscible polymer blends: HIPS/LLDPE systems. Journal
of Applied Polymer Science 64 (1997): 1097-1106.
- [6.] Ying, L.; Shifeng, W.; Yong, Z.; and Yinxi, Z. Electrical properties and morphology of
polypropylene/epoxy/glass Fiber composites filled with carbon black. Journal of
Applied Polymer Science 98 (2005): 1142-1149.
- [7.] Phiboonkulsamrit, S.; Thavarangkul, N.; and Chinsirikul, W. Development of carbon
black (CB)/high impact polystyrene conductive compound: using twin screw
extruder technique for electronic packaging applications. The Third Thailand
Materials Science and Technology Conference, pp. 131-133. Bangkok, Thailand,
Aug. 10-11, 2004. Bangkok: Miracle Grand Convention Hotel.
- [8.] Breuer O.; Tchoudakov, R.; and Narkis, M. Electrical properties of structured
HIPS/gamma-irradiated UHMWPE/carbon black blends. Polymer Engineering and
Science 40 (2000): 1015-1024.
- [9.] Feller, J.F. Conductive polymer composites: influence of extrusion conditions on positive
temperature coefficient effect of poly(butylenes terephthalate)/poly(olefin)-carbon
black blends. Journal of Applied Polymer Science 91 (2003): 2151-2157.

- [10.] Breuer O.; Tchoudakov, R.; Narkis, M.; and Siegmann, A. The interrelation between morphology, resistivity, and flow properties of carbon black-containing HIPS/EVA blends. *Journal of Applied Polymer Science* 73 (1999): 1655-1668.
- [11.] Lee, S.M.; Cho, D., Park, W.H.; Lee, S.G.; Han, S.O.; and Drzal, L.T. Novel silk/poly(butylenes succinate) biocomposites: the effect of short fibre content on their mechanical properties. *Composites Science and Technology* (2004): 1-11.
- [12.] Lu, X.; Zhange, M.Q.; Rong, M.Z.; Shi, G.; and Yang, G.C. Self-reinforced melt processable composites of sisal. *Composites Science and Technology* 63 (2003): 177-186.
- [13.] Mutjé, P.; Vallejos, M.E.; Gironès, J.; Vilaseca, F.; López, A.; López, J.P.; and Méndez, J.A. Effect of maleated polypropylene as coupling agent for polypropylene composites reinforced with hemp strands. *Journal of Applied Polymer Science* 102 (2006): 833-840.
- [14.] Abad, M.; Noguera, P.; Phuchades, R.; Maquirira, A.; and Noguera, V. Physico-chemical properties of some coconut coir dusts for use as a peat substitute for containerised ornamental plants. *Bioresource Technology* 82 (2002): 241-245.
- [15.] Tchoudakov, R.; Breuer, O.; and Narkis, M.; Conductive polymer blends with low carbon black loading: polypropylene/polyamide. *Polymer Engineering and Science* 36 (1996): 1336-1346.
- [16.] Shinohara, Y.; Kishimoto, H.; and Amemiya, Y. Real-time observation of filler aggregate structure[Online]. 2006. Available from: <http://www.spring8.or.jp/pdf> [2005, July 5]
- [17.] Shear Rate[Online]. 2006. Available from: [http:// www.composite.about.com](http://www.composite.about.com) [2005, July 5]
- [18.] Ying, L.; Shifeng, W.; Yong, Z.; and Yinxi, Z. Carbon black filled immiscible polypropylene/epoxy blends. *Journal of Applied Polymer Science* 99 (2005): 461-471.
- [19.] ESD protective packaging[Online]. 2006. Available from: http://www.static-sol.com/ESD_Guide/technical/packaging.htm [2005, July 5]
- [20.] The macrogalleria - polystyrene[Online]. 2006. Available from: <http://www.pslc.ws/macrogcss/styrene.html> [2005, July 5]

- [21.] STYRON 486M - Dow - polystyrene, high impact plastic[Online]. 2006. Available from: <http://www.ides.com/grades/ds/E50677.htm> [2005, July 5]
- [22.] Sudhakaran, M.; and Vasudev, R. Applications of coir in agricultural textiles[Online]. 2001. Available from: <http://www.coir-india.com> [2005, July 5]
- [23.] DAM, J.E.G.; Oever, M.J.A.; Teunissen, W.; Keijzers, R.P.; and Peralta, G. Process for production of high density/high performance biderless boards from whole coconut husk part:1 lignin as intrinsic thermosetting binder resin, Industrial Crops and Products, 19 (2004): 207-216.
- [24.] Properties of carbon[Online]. 2006. Available from: <http://www.dendritics.com/scales/el-carbon.asp> [2006, July 9]
- [25.] Carbon: world of earth science[Online]. 2006. Available from: <http://www.science.enotes.com/earth-science/carbon> [2006, July 9]
- [26.] Ball mill[Online]. 2006. Available from: <http://www.en.wikipedia.org> [2006, July 9]
- [27.] Twin screw extruder[Online]. 2006. Available from: <http://www.ift.confex.com/ift/2005/boa.htm> [2006, July 9]
- [28.] Compression molding[Online]. 2006. Available from: http://www.plastics-car.com/s_plasticscar/sec_inner.asp [2006, July 9]
- [29.] Surface resistivity measurement[Online]. 2006. Available from: <http://www.www.keithley.com> [2006, July 9]
- [30.] Low Angle Laser Light Scattering (LALLS)[Online]. 2006. Available from: <http://www.thaiscience.com> [2006, July 30]
- [31.] Carbon black pellets[Online]. 2006. Available from: <http://www.cabot-corp.com> [2006, July 30]
- [32.] Carbon black particle[Online]. 2006. Available from: <http://www.cabot-corp.com> [2006, July 30]
- [33.] Yang, H.S.; Wolcott, M.P.; Kim, H.S.; and Kim, H.J. Thermal properties of lignocellulosic filler-thermoplastic polymer bio-composites. Journal of Thermal Analysis and Calorimetry 82 (2005): 157-160.

- [34.] Sau, K.P.; Chaki, T.K.; and Khastgir, D. Electrical and mechanical properties of conducting carbon black filled composites based on rubber and rubber blends. Journal of Applied Polymer Science 71 (1999): 887-895.
- [35.] Tchoudakov, R.; Breuer, O.; and Narkis, M. Conductive polymer blends with low carbon black loading: high impact polystyrene/thermoplastic elastomer (styrene-isoprene-styrene). Polymer Engineering and Science 37 (1997): 1928-1935.
- [36.] Stark, N.M. Effects of wood fiber characteristics on mechanical properties of wood/polypropylene composites. Wood and Fiber Science 35 (2003): 167-174.
- [37.] Yang, H.S.; Kim, H.J.; Son, J.; Park, H.J.; Lee, B.J.; Hwang, T.S. Rice husk flour filled polypropylene composites; mechanical and morphological study. Composite Structures 63 (2004): 305-312.
- [38.] Antich, P.; Vazquez, A.; Mondragon, I.; and Bernal, C. Mechanical behavior of high impact polystyrene reinforced with short sisal fibers. Composites: Part A 37 (2006): 139-150.
- [39.] Li, J.X.; Silverstein, M.; Hiltner, A.; and Baer, E. The ductile-to-quasi-brittle transition of particulate-filled thermoplastic polyester. Journal of Applied Polymer Science 52 (1994): 255-267.
- [40.] Chiu, H.T.; and Chiu, W.M. Influence of mechanical properties in carbon black (CB) filled isotactic polypropylene (iPP) and propylene-ethylene block copolymer. Journal of Applied Polymer Science 61 (1996): 607-612.



APPENDICES

สถาบันวิทยบริการ
จุฬาลงกรณ์มหาวิทยาลัย

Appendix A : Particle Size Distribution

Table A1 Particle Size Distribution of Coir Fiber

Size_Low – Size_High (μm)	In %			Mean
	No.1	No.2	No.3	
0.05-0.06	2.74	2.79	2.93	2.82
0.06-0.07	4.96	4.86	5.15	4.99
0.07-0.08	6.22	6.11	6.33	6.22
0.08-0.09	6.43	6.33	6.38	6.38
0.09-0.11	5.67	5.60	5.44	5.57
0.11-0.13	4.31	4.27	4.02	4.20
0.13-0.15	2.86	2.85	2.60	2.77
0.15-0.17	1.69	1.69	1.51	1.63
0.17-0.20	0.92	0.92	0.83	0.89
0.20-0.23	0.47	0.48	0.43	0.46
0.23-0.27	0.25	0.25	0.22	0.24
0.27-0.31	0.14	0.14	0.14	0.14
0.31-0.36	0.09	0.09	0.09	0.09
0.36-0.42	0.06	0.07	0.08	0.07
0.42-0.49	0.05	0.05	0.05	0.05
0.49-0.58	0.05	0.05	0.05	0.05
0.58-0.67	0.05	0.05	0.05	0.05
0.67-0.78	0.06	0.06	0.06	0.06
0.78-0.91	0.09	0.09	0.12	0.10
0.91-1.06	0.14	0.14	0.17	0.15
1.06-1.24	0.20	0.20	0.23	0.21
1.24-1.44	0.23	0.23	0.26	0.24
1.44-1.68	0.25	0.25	0.25	0.25

Appendix A : Particle Size Distribution

Table A1 Particle Size Distribution of Coir Fiber (Contd)

Size_Low – Size_High (μm)	In %			Mean
	No.1	No.2	No.3	
1.68-1.95	0.30	0.30	0.33	0.31
1.95-2.28	0.35	0.36	0.40	0.37
2.28-2.65	0.40	0.41	0.42	0.41
2.65-3.09	0.48	0.49	0.53	0.50
3.09-3.60	0.57	0.57	0.63	0.59
3.60-4.19	0.67	0.68	0.75	0.70
4.19-4.88	0.80	0.82	0.87	0.83
4.88-5.69	0.95	0.96	1.03	0.98
5.69-6.63	1.09	1.10	1.17	1.12
6.63-7.72	1.21	1.21	1.30	1.24
7.72-9.00	1.31	1.31	1.37	1.33
9.00-10.48	1.39	1.39	1.45	1.41
10.48-12.21	1.46	1.46	1.52	1.48
12.21-14.22	1.52	1.53	1.57	1.54
14.22-16.57	1.58	1.59	1.60	1.59
16.57-19.31	1.65	1.65	1.68	1.66
19.31-22.49	1.72	1.73	1.74	1.73
22.49-26.20	1.81	1.81	1.87	1.83
26.20-30.53	1.92	1.92	1.98	1.94
30.53-35.56	2.04	2.04	2.13	2.07
35.56-41.43	2.18	2.18	2.30	2.22
41.43-48.27	2.33	2.34	2.47	2.38
48.27-56.23	2.49	2.48	2.62	2.53

Appendix A : Particle Size Distribution

Table A1 Particle Size Distribution of Coir Fiber (Contd)

Size_Low – Size_High (μm)	In %			Mean
	No.1	No.2	No.3	
56.23-65.51	2.61	2.63	2.74	2.66
65.51-76.32	2.74	2.72	2.79	2.75
76.32-88.91	2.82	2.79	2.82	2.81
88.91-103.58	2.87	2.85	2.80	2.84
103.58-120.67	2.89	2.89	2.80	2.86
120.67-140.58	2.83	2.84	2.67	2.78
140.58-163.77	2.73	2.75	2.53	2.67
163.77-190.80	2.59	2.62	2.38	2.53
190.80-222.28	2.43	2.47	1.94	2.37
222.28-258.95	2.20	2.25	2.00	2.15
258.95-301.68	1.89	1.95	1.74	1.86
301.68-351.46	1.49	1.56	1.42	1.49
351.46-409.45	1.02	1.09	1.04	1.05
409.45-477.01	0.56	0.56	0.74	0.62
477.01-500.00	0.09	0.09	0.36	0.18
Mean Diameter	58.18	59.67	57.65	58.50

จุฬาลงกรณ์มหาวิทยาลัย

Appendix A : Particle Size Distribution

Table A2 Particle Size Distribution of Carbon Black

Size_Low – Size_High (μm)	In %			Mean
	No.1	No.2	No.3	
0.05-0.06	0.00	0.00	0.00	0.00
0.06-0.07	0.00	0.00	0.00	0.00
0.07-0.08	0.00	0.00	0.00	0.00
0.08-0.09	0.00	0.00	0.00	0.00
0.09-0.11	0.00	0.00	0.00	0.00
0.11-0.13	0.00	0.00	0.00	0.00
0.13-0.15	0.00	0.00	0.00	0.00
0.15-0.17	0.00	0.00	0.00	0.00
0.17-0.20	0.00	0.00	0.00	0.00
0.20-0.23	0.00	0.00	0.00	0.00
0.23-0.27	0.06	0.04	0.05	0.05
0.27-0.31	0.19	0.15	0.17	0.17
0.31-0.36	0.31	0.27	0.29	0.29
0.36-0.42	0.46	0.41	0.44	0.44
0.42-0.49	0.59	0.55	0.58	0.57
0.49-0.58	0.75	0.68	0.73	0.72
0.58-0.67	0.90	0.80	0.88	0.86
0.67-0.78	0.95	0.88	0.98	0.56
0.78-0.91	0.96	0.91	1.05	0.97
0.91-1.06	1.03	0.95	1.14	0.62
1.06-1.24	1.09	0.98	1.22	1.10
1.24-1.44	1.14	1.02	1.31	1.57

Appendix A : Particle Size Distribution

Table A2 Particle Size Distribution of Carbon Black (Contd)

Size_Low – Size_High (μm)	In %			Mean
	No.1	No.2	No.3	
1.44-1.68	1.23	1.10	1.43	0.75
1.68-1.95	1.37	1.22	1.59	1.39
1.95-2.28	1.58	1.43	1.82	0.97
2.28-2.65	1.90	1.75	2.14	1.93
2.65-3.09	2.34	2.20	2.55	2.36
3.09-3.60	2.90	2.79	3.07	2.92
3.60-4.19	3.57	3.48	3.67	3.57
4.19-4.88	4.32	4.26	4.32	4.30
4.88-5.69	5.07	5.04	4.96	5.02
5.69-6.63	5.77	5.77	5.54	5.69
6.63-7.72	6.32	6.36	5.99	6.22
7.72-9.00	6.67	6.76	6.28	6.57
9.00-10.48	6.80	6.93	6.39	6.71
10.48-12.21	6.74	6.92	6.34	6.67
12.21-14.22	6.56	6.78	6.19	6.51
14.22-16.57	5.89	6.10	5.62	5.87
16.57-19.31	5.09	5.27	4.91	5.09
19.31-22.49	4.23	4.36	4.13	4.24
22.49-26.20	3.39	3.47	3.35	3.40
26.20-30.53	2.61	2.65	2.61	2.62
30.53-35.56	1.94	1.95	1.95	1.95
35.56-41.43	1.39	1.38	1.39	1.39
41.43-48.27	0.95	0.93	0.95	0.94

Appendix A : Particle Size Distribution

Table A2 Particie Size Distribution of Carbon Black (Contd)

Size_Low – Size_High (μm)	In %			Mean
	No.1	No.2	No.3	
48.27-56.23	0.61	0.60	0.61	0.61
56.23-65.51	0.37	0.37	0.38	0.37
65-51-76.32	0.22	0.21	0.23	0.22
76.32-88.91	0.13	0.13	0.16	0.14
88.91-103.58	0.10	0.09	0.14	0.11
103.58-120.67	0.11	0.10	0.16	0.12
120.67-140.58	0.14	0.13	0.22	0.16
140.58-163.77	0.18	0.19	0.29	0.22
163.77-190.80	0.23	0.27	0.37	0.29
190.80-222.28	0.28	0.34	0.43	0.35
222.28-258.95	0.28	0.37	0.43	0.36
258.95-301.68	0.22	0.34	0.36	0.31
301.68-351.46	0.09	0.21	0.19	0.16
351.46-409.45	0.00	0.08	0.02	0.05
409.45-477.01	0.00	0.00	0.00	0.00
477.01-500.00	0.00	0.00	0.00	0.00
Mean Diameter	14.48	16.06	16.33	15.62

Appendix B : Surface Resistivity

Table B1 Surface Resistivity (Ohm/Square) of the Composites

Surface Resistivity							
Sample	Trial Number					Mean	Log Resistivity
	1	2	3	4	5		
HIPS	5.14×10^{16}	5.00×10^{16}	5.05×10^{16}	4.93×10^{16}	4.93×10^{16}	5.01×10^{16}	16.70
HIPS/1CB	1.11×10^{16}	1.23×10^{16}	1.32×10^{16}	1.05×10^{16}	1.05×10^{16}	1.15×10^{16}	16.06
HIPS/3CB	3.59×10^{16}	3.37×10^{16}	3.57×10^{16}	3.37×10^{16}	3.68×10^{16}	3.52×10^{16}	16.55
HIPS/5CB	1.16×10^7	1.20×10^7	1.19×10^7	1.25×10^7	1.19×10^7	1.20×10^7	7.08
HIPS/7CB	4.58×10^6	4.54×10^6	4.90×10^6	5.05×10^6	4.93×10^6	4.80×10^6	6.68
HIPS/9CB	8.91×10^5	7.68×10^5	7.39×10^5	6.88×10^5	7.84×10^5	7.74×10^5	5.89
HIPS/1coir filler	2.00×10^{15}	1.95×10^{15}	2.09×10^{15}	1.99×10^{15}	1.97×10^{15}	2.00×10^{15}	15.30
HIPS/3coir filler	2.62×10^{15}	2.49×10^{15}	2.51×10^{15}	2.55×10^{15}	2.68×10^{15}	2.57×10^{15}	15.49
HIPS/5coir filler	2.02×10^{15}	1.98×10^{15}	2.01×10^{15}	1.99×10^{15}	2.06×10^{15}	2.01×10^{15}	15.30
HIPS/7coir filler	1.87×10^{15}	1.91×10^{15}	1.87×10^{15}	1.91×10^{15}	1.93×10^{15}	1.90×10^{15}	15.28
HIPS/9coir filler	1.43×10^{15}	1.40×10^{15}	1.43×10^{15}	1.40×10^{15}	1.39×10^{15}	1.41×10^{15}	15.15
HIPS/11coir filler	1.32×10^{15}	1.35×10^{15}	1.33×10^{15}	1.34×10^{15}	1.30×10^{15}	1.33×10^{15}	15.12
HIPS/13coir filler	1.34×10^{15}	1.37×10^{15}	1.28×10^{15}	1.34×10^{15}	1.35×10^{15}	1.34×10^{15}	15.13
HIPS/15coir filler	1.02×10^{15}	1.07×10^{15}	1.06×10^{15}	1.05×10^{15}	9.97×10^{14}	1.04×10^{15}	15.02
HIPS/5CB/1CF	1.22×10^7	1.17×10^7	9.83×10^6	1.15×10^7	1.02×10^7	1.11×10^7	7.05
HIPS/5CB/3CF	1.31×10^7	1.33×10^7	1.58×10^7	1.59×10^7	1.42×10^7	1.45×10^7	7.16
HIPS/5CB/5CF	3.46×10^6	3.48×10^6	3.29×10^6	3.70×10^6	3.43×10^6	3.47×10^6	6.54
HIPS/5CB/7CF	4.82×10^5	5.28×10^5	5.21×10^5	5.67×10^5	5.42×10^5	5.28×10^5	5.72

Appendix B : Surface Resistivity

Table B1 Surface Resistivity (Ohm/Square) of the Composites (Contd)

Surface Resistivity							
Sample	Trial Number					Mean	Log Resistivity
	1	2	3	4	5		
HIPS/5CB/9CF	4.17×10^5	3.89×10^5	4.01×10^5	4.29×10^5	4.36×10^5	4.15×10^5	5.62
HIPS/5CB/11CF	1.84×10^7	1.52×10^7	1.56×10^7	2.00×10^7	1.55×10^7	1.69×10^7	7.23
HIPS/5CB/13CF	1.30×10^7	9.99×10^6	1.29×10^7	1.16×10^7	9.71×10^6	1.11×10^7	7.05
HIPS/5CB/15CF	9.64×10^6	1.11×10^7	9.01×10^6	1.17×10^7	1.01×10^7	1.03×10^7	7.01

สถาบันวิทยบริการ
จุฬาลงกรณ์มหาวิทยาลัย

Appendix C : Mechanical Properties

Table C1 Impact Strength (KJ/mm²) of the Composites

Impact Strength							
Sample	Trial Number					Mean	SD
	1	2	3	4	5		
HIPS	9.3	9.5	9.3	9.3	9.5	9.39	0.08
HIPS/1CB	7.3	7.2	7.4	7.2	7.1	7.24	0.15
HIPS/3CB	4.3	4.4	4.4	4.5	4.4	4.40	0.08
HIPS/5CB	2.2	2.3	2.3	2.3	2.3	2.28	0.04
HIPS/7CB	2.0	2.0	1.7	1.7	2.0	1.94	0.16
HIPS/9CB	1.2	1.1	1.1	1.1	1.2	1.14	0.05
HIPS/1coir filler	8.6	8.6	8.6	8.5	8.4	8.54	0.09
HIPS/3coir filler	6.5	6.1	6.4	6.0	6.4	6.28	0.22
HIPS/5coir filler	5.7	6.0	5.6	6.1	5.6	5.80	0.23
HIPS/7coir filler	5.4	5.6	5.3	5.5	5.7	5.50	0.16
HIPS/9coir filler	4.7	4.7	4.7	4.7	4.7	4.72	0.04
HIPS/11coir filler	4.3	4.4	4.3	4.3	4.3	4.32	0.04
HIPS/13coir filler	4.2	4.1	4.2	4.1	4.1	4.14	0.05
HIPS/15coir filler	3.6	3.5	3.6	3.6	3.6	3.58	0.04
HIPS/5CB/1CF	2.4	2.4	2.4	2.3	2.4	2.38	0.04
HIPS/5CB/3CF	2.2	1.9	2.4	2.4	2.2	2.22	0.20
HIPS/5CB/5CF	2.2	2.3	2.3	2.3	2.0	2.22	0.13
HIPS/5CB/7CF	2.2	2.2	2.2	2.1	2.2	2.18	0.04

Appendix C : Mechanical Properties

Table C1 Impact Strength (KJ/mm³) of the Composites (Contd)

Impact Strength							
Sample	Trial Number					Mean	SD
	1	2	3	4	5		
HIPS/5CB/9CF	1.8	1.8	1.8	1.8	1.8	1.80	0.00
HIPS/5CB/11CF	1.9	1.9	1.9	1.9	1.9	1.90	0.00
HIPS/5CB/13CF	1.9	1.9	1.9	1.8	1.9	1.88	0.04
HIPS/5CB/15CF	1.6	1.6	1.6	1.6	1.6	1.60	0.00

สถาบันวิทยบริการ
จุฬาลงกรณ์มหาวิทยาลัย

Appendix C : Mechanical Properties

Table C2 Tensile Modulus (MPa) of the Composites

Tensile Modulus							
Sample	Trial Number					Mean	SD
	1	2	3	4	5		
HIPS	316.41	327.57	322.31	313.87	358.82	327.80	18.14
HIPS/1CB	389.49	384.50	356.45	378.25	374.39	376.62	12.67
HIPS/3CB	392.33	436.53	430.14	352.16	457.93	401.22	41.81
HIPS/5CB	414.31	413.63	408.33	440.95	394.69	414.38	16.81
HIPS/7CB	439.13	416.59	449.93	437.39	474.59	443.52	21.15
HIPS/9CB	509.48	512.20	516.12	514.37	524.69	515.37	5.77
HIPS/1coir filler	428.71	422.86	482.23	453.04	449.67	447.30	23.46
HIPS/3coir filler	533.47	539.11	505.46	504.28	535.03	523.47	17.10
HIPS/5coir filler	520.14	535.73	545.47	514.68	531.06	529.42	12.28
HIPS/7coir filler	523.87	533.12	534.21	521.79	540.62	530.72	7.79
HIPS/9coir filler	437.19	497.20	481.64	458.95	472.77	469.55	22.81
HIPS/11coir filler	494.95	488.83	491.66	463.54	475.15	482.82	13.15
HIPS/13coir filler	478.33	467.35	427.08	469.74	477.24	463.95	21.14
HIPS/15coir filler	494.76	493.26	488.04	485.78	462.19	484.81	13.17
HIPS/5CB/1CF	441.10	454.73	424.69	449.66	444.38	442.91	11.43
HIPS/5CB/3CF	534.58	510.04	541.35	546.69	521.31	530.80	14.99
HIPS/5CB/5CF	515.29	559.35	543.34	557.18	515.22	538.08	21.72
HIPS/5CB/7CF	514.13	527.91	550.43	557.08	542.31	538.37	17.38

Appendix C : Mechanical Properties

Table C2 Tensile Modulus (MPa) of the Composites (Contd)

Tensile Modulus							
Sample	Trial Number					Mean	SD
	1	2	3	4	5		
HIPS/5CB/9CF	573.00	565.03	567.92	536.40	575.09	563.49	15.66
HIPS/5CB/11CF	552.76	577.46	565.04	554.72	541.04	558.02	13.73
HIPS/5CB/13CF	645.40	656.78	657.84	666.77	623.49	650.05	16.68
HIPS/5CB/15CF	621.33	632.06	621.26	598.35	642.08	622.29	16.28

สถาบันวิทยบริการ
จุฬาลงกรณ์มหาวิทยาลัย

Appendix C : Mechanical Properties

Table C3 Tensile Strength at Maximum (MPa) of the Composites

Tensile Strength at Maximum							
Sample	Trial Number					Mean	SD
	1	2	3	4	5		
HIPS	22.60	21.62	21.62	21.49	21.00	21.38	0.28
HIPS/1CB	22.16	20.29	22.78	20.66	20.34	21.23	1.15
HIPS/3CB	23.50	24.92	23.93	23.77	24.17	24.06	0.54
HIPS/5CB	25.02	25.62	26.04	25.00	24.63	25.26	0.56
HIPS/7CB	26.03	26.29	25.95	25.17	25.56	25.80	0.44
HIPS/9CB	26.24	28.91	25.40	26.32	26.40	26.65	1.32
HIPS/1coir filler	22.80	23.07	23.11	23.13	22.54	22.93	0.25
HIPS/3coir filler	22.91	23.10	23.66	22.28	22.62	22.91	0.52
HIPS/5coir filler	24.32	22.77	21.58	22.47	22.00	22.63	1.05
HIPS/7coir filler	22.72	22.84	23.76	23.71	21.84	22.97	0.79
HIPS/9coir filler	21.09	22.20	22.00	21.79	21.99	21.81	0.43
HIPS/11coir filler	21.48	22.15	22.12	21.48	21.83	21.81	0.33
HIPS/13coir filler	21.27	21.70	22.22	21.56	22.12	21.78	0.39
HIPS/15coir filler	21.40	21.03	22.21	21.75	22.27	21.73	0.53
HIPS/5CB/1CF	25.44	25.26	25.23	25.46	25.71	25.42	0.19
HIPS/5CB/3CF	25.64	24.98	24.89	25.44	25.40	25.27	0.32
HIPS/5CB/5CF	25.32	25.54	25.56	25.22	24.92	25.31	0.26
HIPS/5CB/7CF	25.51	25.79	25.08	24.88	24.29	25.11	0.58

Appendix C : Mechanical Properties

Table C3 Tensile Strength at Maximum (MPa) of the Composites (Contd)

Tensile Strength at Maximum							
Sample	Trial Number					Mean	SD
	1	2	3	4	5		
HIPS/5CB/9CF	25.03	25.22	25.08	25.04	25.86	25.24	0.35
HIPS/5CB/11CF	25.49	25.53	25.23	25.12	25.59	25.39	0.20
HIPS/5CB/13CF	25.35	25.33	25.49	25.20	25.47	25.37	0.12
HIPS/5CB/15CF	25.98	25.80	25.90	25.62	24.79	25.62	0.48

สถาบันวิทยบริการ
จุฬาลงกรณ์มหาวิทยาลัย

Appendix C : Mechanical Properties

Table C4 Elongation at Break (%) of the Composites

Elongation at Break							
Sample	Trial Number					Mean	SD
	1	2	3	4	5		
HIPS	30.346	26.869	23.326	24.027	33.570	27.628	4.32
HIPS/1CB	15.771	13.892	15.741	16.786	16.409	15.720	1.11
HIPS/3CB	11.212	10.039	10.573	10.158	11.599	10.716	0.67
HIPS/5CB	10.817	10.737	10.383	11.898	10.397	10.846	0.62
HIPS/7CB	7.999	9.404	9.058	9.795	9.367	9.124	0.67
HIPS/9CB	7.999	9.288	9.175	7.877	8.802	8.628	0.66
HIPS/1coir filler	17.130	15.104	14.861	15.592	15.042	15.546	0.93
HIPS/3coir filler	13.816	13.946	14.166	13.708	14.208	14.012	0.22
HIPS/5coir filler	13.875	13.833	13.746	15.295	14.400	14.030	0.65
HIPS/7coir filler	14.965	13.061	14.081	14.328	12.578	13.803	0.97
HIPS/9coir filler	12.544	11.326	10.938	9.125	12.491	11.285	1.40
HIPS/11coir filler	11.894	10.057	11.566	10.812	11.137	11.093	0.71
HIPS/13coir filler	11.812	12.506	8.860	10.053	10.506	10.747	1.44
HIPS/15coir filler	10.714	11.613	8.687	10.931	11.922	10.773	1.27
HIPS/5CB/1CF	9.600	10.200	9.202	10.727	9.669	9.879	0.59
HIPS/5CB/3CF	8.114	8.127	8.247	8.727	8.856	8.414	0.35
HIPS/5CB/5CF	8.059	8.166	8.295	8.289	8.112	8.184	0.11
HIPS/5CB/7CF	8.399	8.027	8.494	8.371	8.570	8.372	0.21

Appendix C : Mechanical Properties

Table C4 Elongation at Break (%) of the Composites (Contd)

Elongation at Break							
Sample	Trial Number					Mean	SD
	1	2	3	4	5		
HIPS/5CB/9CF	8.269	7.517	8.560	8.213	8.587	8.276	0.34
HIPS/5CB/11CF	7.845	7.224	7.880	7.988	6.985	7.584	0.45
HIPS/5CB/13CF	7.420	7.476	7.061	7.533	7.102	7.318	0.22
HIPS/5CB/15CF	6.540	7.199	6.984	7.077	7.197	6.999	0.27

สถาบันวิทยบริการ
จุฬาลงกรณ์มหาวิทยาลัย

Appendix C : Mechanical Properties

Table C5 Flexural Modulus (MPa) of the Composites

Flexural Modulus							
Sample	Trial Number					Mean	SD
	1	2	3	4	5		
HIPS	1.574	1.556	1.471	1.557	1.562	1.542	0.04
HIPS/1CB	1.649	1.654	1.609	1.574	1.609	1.619	0.03
HIPS/3CB	1.693	1.705	1.714	1.723	1.704	1.715	0.02
HIPS/5CB	1.773	1.791	1.744	1.791	1.740	1.766	0.02
HIPS/7CB	1.840	1.852	1.813	1.831	1.744	1.816	0.04
HIPS/9CB	1.921	1.909	1.927	1.911	1.949	1.923	0.02
HIPS/1coir filler	1.833	1.826	1.833	1.895	1.860	1.849	0.02
HIPS/3coir filler	1.843	1.875	1.860	1.868	1.887	1.867	0.02
HIPS/5coir filler	1.893	1.900	1.843	1.855	1.833	1.865	0.02
HIPS/7coir filler	1.860	1.843	1.884	1.872	1.879	1.870	0.03
HIPS/9coir filler	1.662	1.643	1.651	1.630	1.593	1.636	0.03
HIPS/11coir filler	1.654	1.672	1.672	1.583	1.565	1.629	0.05
HIPS/13coir filler	1.661	1.651	1.651	1.634	1.612	1.642	0.02
HIPS/15coir filler	1.664	1.650	1.637	1.657	1.637	1.649	0.01
HIPS/5CB/1CF	1.857	1.841	1.868	1.832	1.862	1.852	0.02
HIPS/5CB/3CF	1.887	1.881	1.843	1.899	1.892	1.880	0.02
HIPS/5CB/5CF	1.877	1.892	1.816	1.892	1.929	1.885	0.03
HIPS/5CB/7CF	1.898	1.871	1.852	1.871	1.952	1.848	0.04

Appendix C : Mechanical Properties

Table C5 Flexural Modulus (MPa) of the Composites (Contd)

Flexural Modulus							
Sample	Trial Number					Mean	SD
	1	2	3	4	5		
HIPS/5CB/9CF	1.926	1.889	1.894	1.905	2.067	1.936	0.07
HIPS/5CB/11CF	1.945	1.980	1.929	1.944	1.968	1.950	0.02
HIPS/5CB/13CF	1.941	1.887	1.883	1.911	1.911	1.913	0.02
HIPS/5CB/15CF	1.880	1.891	1.886	1.886	1.895	1.888	0.01

สถาบันวิทยบริการ
จุฬาลงกรณ์มหาวิทยาลัย

Appendix C : Mechanical Properties

Table C6 Flexural Strength (MPa) of the Composites

Flexural Strength							
Sample	Trial Number					Mean	SD
	1	2	3	4	5		
HIPS	32.29	32.39	32.00	32.54	32.34	32.31	0.20
HIPS/1CB	34.81	34.77	34.86	35.38	34.90	34.24	0.25
HIPS/3CB	37.00	37.51	37.49	37.29	37.15	37.29	0.22
HIPS/5CB	37.53	37.64	38.76	38.94	38.60	38.29	0.66
HIPS/7CB	39.12	39.28	39.01	39.53	39.19	39.23	0.20
HIPS/9CB	41.07	40.36	40.70	40.10	40.57	40.56	0.36
HIPS/1coir filler	33.85	34.83	34.97	34.45	34.07	34.87	0.48
HIPS/3coir filler	33.85	34.83	34.97	34.45	33.55	34.43	0.62
HIPS/5coir filler	34.69	34.29	34.78	35.02	34.54	34.66	0.28
HIPS/7coir filler	36.00	36.13	35.13	35.46	35.73	35.69	0.41
HIPS/9coir filler	32.11	32.89	32.67	31.91	32.23	32.36	0.41
HIPS/11coir filler	32.77	32.67	32.65	32.49	32.48	32.61	0.20
HIPS/13coir filler	32.23	32.99	32.27	32.58	32.46	32.57	0.33
HIPS/15coir filler	32.44	32.59	32.83	32.30	32.46	32.52	0.20
HIPS/5CB/1CF	36.94	37.41	37.34	37.68	36.91	37.26	0.33
HIPS/5CB/3CF	38.29	37.33	37.34	36.55	36.99	37.30	0.64
HIPS/5CB/5CF	36.92	37.98	37.40	38.10	37.60	37.61	0.47
HIPS/5CB/7CF	36.81	38.71	37.09	37.34	38.10	37.61	0.78

Appendix C : Mechanical Properties

Table C6 Flexural Strength (MPa) of the Composites (Contd)

Flexural Strength							
Sample	Trial Number					Mean	SD
	1	2	3	4	5		
HIPS/5CB/9CF	35.66	35.43	35.54	35.23	35.15	35.38	0.20
HIPS/5CB/11CF	35.64	35.70	35.22	35.54	35.19	35.46	0.24
HIPS/5CB/13CF	35.23	35.53	35.18	35.15	35.84	35.39	0.30
HIPS/5CB/15CF	35.32	35.69	35.21	35.37	35.21	35.36	0.20

สถาบันวิทยบริการ
จุฬาลงกรณ์มหาวิทยาลัย

BIOGRAPHY

Miss Wachraporn Polsaen was born in Nakornrachasima, Thailand, on December 5,1980. She received the Bachelor of Engineering degree majority in Polymer Engineering, Faculty of Engineering, Suranaree University in 2003. Afterwards, she persued her post graduate degree at the Department of Material Science in 2004. She completed the programme and obtained her Master degree in Applied Polymer Science and Textile Technology in October 2006.



สถาบันวิทยบริการ
จุฬาลงกรณ์มหาวิทยาลัย